INFORMATION TO USERS

This manuscript has been reproduced from the microfilm master. UMI films the text directly from the original or copy submitted. Thus, some thesis and dissertation copies are in typewriter face, while others may be from any type of computer printer.

The quality of this reproduction is dependent upon the quality of the copy submitted. Broken or indistinct print, colored or poor quality illustrations and photographs, print bleedthrough, substandard margins, and improper alignment can adversely affect reproduction.

In the unlikely event that the author did not send UMI a complete manuscript and there are missing pages, these will be noted. Also, if unauthorized copyright material had to be removed, a note will indicate the deletion.

Oversize materials (e.g., maps, drawings, charts) are reproduced by sectioning the original, beginning at the upper left-hand corner and continuing from left to right in equal sections with small overlaps.

Photographs included in the original manuscript have been reproduced xerographically in this copy. Higher quality 6" x 9" black and white photographic prints are available for any photographs or illustrations appearing in this copy for an additional charge. Contact UMI directly to order.

Bell & Howell Information and Learning
300 North Zeeb Road, Ann Arbor, MI 48106-1346 USA
800-521-0600

The Adaptation Of Solenoid Actuated Injectors

For Use With Dimethyl Ether Fuel In Diesel Engines

Babak Torab

A Thesis
in
The Department
of
Mechanical Engineering

Presented in Partial Fulfillment of the Requirements
for the Degree of Master of Applied Science at
Concordia University
Montreal, Quebec, Canada

September 1999

ABSTRACT

The Adaptation Of Solenoid Actuated Injectors For Use With Dimethyl Ether Fuel In Diesel Engines

Babak Torab, M.A.Sc.

Dimethyl ether (DME) is an alternative fuel which, of late, has shown tremendous potential in reducing the pollution emissions of automobiles. Simultaneously, electronic actuated fuel injectors, with the use of solenoids, have repeatedly demonstrated superior performance with respect to needle movement control. This thesis, in order to combine the advantages of both electronic actuation and DME fuel, presents an adaptation of the novel use of solenoid operated fuel injectors with DME. The thesis also sets to reduce injector nozzle seat wear, by reducing the bouncing of the injector needle at the bottom of its stroke. The injector design presented incorporates a lengthened elastic rod, a new driving circuit for the solenoid, and incorporates them into a common rail system. The thesis also presents, for the first time in the literature, a methodology for measuring the force acting on the nozzle seat in injector closing. Through modeling, simulation and testing, an injector compatible with DME fuel was designed, where injector needle movement was properly controlled, and nozzle seat force reduced. As such, an important step has been taken in developing technology allowing DME to be a more common alternative fuel in automobiles.

DEDICATION

This thesis is written in memory of my aunt, Mehrie Zargham, and in memory of my supervisor, Dr. Tadeusz Krepec, whose assistance, love and support gave me the opportunity to a new and better life.

ACKNOWLEDGEMENTS

The author would like to thank the following people, without whose contribution, support, and help, this thesis would not have been possible.

Dr. H. Hong and Dr. T. Krepec for their suggestion of this research project, their guidance, knowledge, continuous encouragement, and ideas.

My cousin, Reza Zargham, for his editorial work.

Gilles Huard and Eric Lambert for their technical assistance with the driving circuit.

The employees of the machine shop of Concordia University, led by Paul Scheiwiller, for their help in building the injector.

Andrea Heser for helping gather and consolidate past research.

My family, including Leili Baggi, Roy Zangabouri, Don Sohrab, Effi and Alba for their love and unwavering support.

This project was supported by CANMET, Natural Resources Canada, to whom the author is also grateful.

TABLE OF CONTENTS

LIST OF FIGURES

LIST OF TABLES

TABLE PAGE

NOMENCLATURE

d	- seat diameter of the nozzle orifice (m)
d_o	- outside diameter of the metal rods (m)
d_i	- inside diameter of the metal rods (m)
d_r	- material damping of the metal rods (kg/s)
d_t	- material damping of the seat (kg/s)
d_p	- material damping of the stop (kg/s)
fd_n	- viscous damping force due to the needle motion (N)
fd_c	- viscous damping force due to the core motion (N)
g	- acceleration due to gravity (9.806 m/s^2)
h	- air-gap between the solenoid magnetic pole and the moving core (m)
k_p	- spring stiffness of the stop (kN/mm)
k_r	- spring stiffness of the metal rods (kN/mm)
k_s	- stiffness of the injector return spring (kN/mm)
k_t	- spring stiffness of the seat (kN/mm)
l	- lenght of the metal rods (m)
m_c	- mass of solenoid core (kg)
m_n	- mass of injector needle (kg)
x_c	- core displacement (m)
x_n	- needle displacement (m)
$\dot{x}_c$	- core velocity (m/s)
$\dot{x}_n$	- needle velocity (m/s)

$\ddot{x}_c$ - core acceleration (m/s^2)

$\ddot{x}_n$ - needle acceleration (m/s^2)

H_{MAX} - maximum needle displacement (0.635 mm)

A_1 - pole end effective area (m^2)

A_m - effective needle area (m^2)

E - modulus elasticity of the metal rods (MPa)

F_P - pressure force acting on the injector needle (N)

F_R - needle reaction force (N)

F_S - electromagnetic pulling force (N)

G_{MAX} - maximum air-gap (m)

K_{PR} - spring preload (N)

P - pressure inside the injector above the effective area (MPa)

P_e - pressure below the effective area (MPa)

$W(\varphi,h)_{mag}$ - stored magnetic energy (J)

θ - angle of the needle conical tip (^{0})

φ - magnetic flux (Wb)

μ_0 - permeability of free space ($4\pi\times10^{-7}$ Wb/A-m)

CHAPTER 1

INTRODUCTION

Over the last half century, the use of automobiles has increased exponentially, and their presence has become a constant and pervasive aspect of most societies around the globe. Traditionally powered by fossil fuels, the predominance of automobiles as the main transportation tool in the world has led to an increase in air pollution. In response, the research and development work in vehicular internal combustion engines, in recent years, has been performed in two fundamental directions:

1. towards fuel economy
2. towards overall pollution reduction

Recent research work in the United States, financed by the Partnership for a New Generation of Vehicles (PNGV) consortium, has concluded that the new generation of small, high speed, directly injected and turbo-charged diesel engines, can become the most efficient power source for the new breed of hybrid electric vehicles (HEVs) [1]. The use of such engines has the goal to obtain economies of up to 80 miles per gallon for the mid-size car, and to reduce threefold the harmful exhaust gas emissions, including the carbon dioxide emissions responsible for the greenhouse effect [2]. The high speed direct injection diesel engine provides a substantially higher thermal efficiency as compared to traditional spark-ignited gasoline, or even indirect injection diesel engines. As a result of these and other benefits, the Audi car company now manufactures 44% of its Western Europe output with a direct injection diesel engine as opposed to 0% in 1989. The company predicts this type of engine to comprise 82% of its automobile production by the year 2003 [3].

There are still, however, several problems regarding the pollution caused by a diesel engine, which can hinder their mass development. The first two of these include an excessive mass of solid particulates (soot) in the exhaust gases of these engines, and an unacceptable amount of nitrogen oxides (NOx), the substances found to be contributing factors in causing cancer. Another important cause of direct injection related pollution, is the post-injection phenomenon, which aggravates the emissions of the aforementioned toxins.

One possible solution to make the diesel engines cleaner, would be the use of dimethyl ether (DME) as fuel. DME is currently in limited use, and is really only present in industry for chemical processes. Its benefits, however, have yet to be well recognized on a broader base through large scale production from natural gas. Research in the use of this fuel has identified it as having excellent possibilities for solving the E^3 equation; that is to say, that the fuel is effective in meeting energy, economic and environmental goals. For a country whose richness in natural gas is well recognized, interesting possibilities present themselves for Canada with regards to the mass use of DME.

DME remains in a gaseous state in atmospheric conditions. However, at 5 bar pressure, it changes to a liquid state and can be stored in the same manner as propane or butane in the fuel tank. When injected directly into the combustion chamber of a diesel engine, it produces only a very short ignition delay which is due to its high cetane number of 60, thus reducing the content of NOx pollutants emitted in the injection process. Furthermore, the short ignition delay results in a quiet combustion and, consequently, a reduction in engine noise. Since DME changes to a gaseous state during injection, it

produces almost no solid particulates and, when combined with its reduced NOx emissions, can be thus considered as an ideal fuel for modern high speed diesel engines.

Solenoid operated fuel injectors have been used almost exclusively in spark ignition engines, mainly for the manifold injection of gasoline, natural gas and propane. In diesel engines requiring direct fuel injection, solenoids are being used in unit injectors and distributor type fuel injection pumps. In this capacity, they served mainly to control the fuel injection process by spilling the excess of fuel back to the tank, while the fuel injection process was performed directly, either through mechanic or hydraulic means. If solenoids were to be utilized in the fuel injection process as well, significant gains could be made by more accurately controlling the amount of fuel discharged into the engine, and by minimizing both the opening and closing delays of the injector.

The aim of this thesis is to reap the benefits that can be derived from the unique combination of direct injection diesel engines, the use of DME as fuel, and the expansion of solenoids into the direct injection process. The proposed design incorporates all three of these goals. A secondary contribution that is also presented in this thesis, is the introduction of a method for the measurement of nozzle needle seat force. Seat force is caused by the high kinetic energy released by the injector needle on the nozzle seat as it closes. This, in turn, results in the bouncing of the injector needle, increasing the injector seat wear, and is the principal cause of undesired post-injection. Since incorporating solenoids in the direct injection system can aid in the reduction of post-injection, measuring this seat force is of primary importance in proving, in a practical application, the benefits of using an electronically controlled fuel injection system. In the existing

literature, there is no standard for measuring this seat force, and this thesis is the first to present such a standard.

There are certain complications that arise when attempting to integrate an electronically controlled fuel injection system using solenoids into a direct injection process. Foremost among these is the tendency for solenoids to overheat due to the proximity of the combustion chamber, resulting in a loss of solenoid force. This loss of force is further exacerbated by the fact that even a higher force is needed to overcome the excess fuel pressure existing in diesel engines, as compared to the low pressure system in spark-ignition engines. In the design of this thesis' injector, the first major modification is that the length of the rod has been increased. As such, the solenoid is further distanced from the heat in the combustion chamber. The second step involves using a common rail system as opposed to unit injectors, and placing the solenoid within the rail. Since the common rail has a continuous flow of fuel, the fuel serves to cool the solenoid. As such, the electronically controlled fuel injection system can function effectively, even in the increased pressure and temperature environment of the diesel engine.

As already mentioned, post-injection remains a persistent cause of pollution. Post-injection, a result of the spring-loaded injector rod, occurs when the injector needle starts to bounce, discharging residual fuel into the combustion chamber. In order to reduce post-injection, the injector in this thesis is designed with an elastic rod, which can distribute the kinetic energy impact over time, reducing the needle spring back amplitude. The resulting decrease in the bouncing of the injector needle leads to a significant decrease in the fuel post-injection as well.

There are also some complications that arise with using DME as an automotive fuel. For DME to be stored in a car's fuel tank, it needs to remain in liquid form under pressure. Then, to be injected into the combustion chamber, its pressure has to be increased to over 100 bar. This high pressure prevents it from boiling in the increased temperature of the common rail and injector. As such, any injector body design needs to be able to withstand the high pressure to which it will be exposed.

This thesis is structured in the following manner. Following this introduction is a literature review in Chapter 2, highlighting the major works and contributions to the field over the last ten years. Chapter 3 presents the research concept and chronology, while Chapter 4 outlines an analysis of DME injection, and design configurations. This chapter reviews the characteristics of DME fuel, giving a thorough evaluation of the potential problems associated with using solenoid operated injectors for direct injection of DME in diesel engines, as well as the alternative solutions aimed at solving these problems. The section concludes with the proposed alternative design concepts of the injection system. Chapter 5 presents the selected injection system design. This chapter gives a detailed, technical analysis of the benefits of solenoid use, the direct and common rail injection systems, the use of elastic rods, as well as the necessity for, and design of, a new solenoid driving circuit. It also presents the technical specifications of the designed injector. Chapter 6 covers the modeling of the injection process, the computer simulation, and the results. Chapter 7 presents the injector test setup and conditions, observations, and results. In this chapter, a comparison is also found between the testing results with those expected and predicted by the simulation of the previous chapter. Chapter 8 concludes the project, gives recommendations, and suggests possible areas for further research.

The principal conclusion of this thesis is that while significant gains have been made in the areas of pollution reduction and fuel economy, further progress can be made by using DME as fuel, and incorporating the control benefits of electronic fuel injection systems with solenoids. Combined with the use of a common rail, and lengthened elastic rod in the injector design, such improvements hope to further improve the cause of environmental responsiveness in the automobile industry.

The design of this thesis has been presented at the 1998 FutureCar competition in June 1998, and the design modifications for incorporation into the Volkswagon diesel engine were presented at the 1999 FutureCar competition in June 1999, Detroit, Michigan.

CHAPTER 2

LITERATURE SURVEY

This thesis begins with a review of the existing literature and the evolution of direct fuel injection systems for high speed diesel engines. Although a significant amount of accomplishments exist over the course of the last quarter century, there is undoubtedly a concentration of significant developments in the last ten years. Thanks to the increasingly stringent regulations regarding emission standards in this period, the technology has been spurred towards continuous landmark achievements. Given the quantity and revolutionary nature of these breakthroughs, it seems a reasonable first approximation to assume that a survey of the literature confined to the last ten years would give a fairly thorough representation of the progress made in the field. Furthermore, given the principal position of DME in this thesis, as well as the fuel's recent rise to notoriety, it seems further appropriate to confine the literature review to a ten-year period. As such, this chapter investigates the major developments that have occurred in the direct injection system technology, for high speed diesel engines supplied by gaseous fuels, in the period 1988-1998.

In 1988, Wakerell [4] published a report on the research conducted at the Southwest Research Institute in San Antonio, Texas. This research was focused on the direct injection of natural gas into a cylinder of a dual fuel diesel engine for a locomotive. The natural gas injector was designed through the modification of a diesel injector. To "lift" the needle, a special, hydraulically operated, piston was added, activated by a diesel injection pump driven by the engine. The natural gas was supplied at 345 bar pressure through the enlarged orifices of the nozzle. The gas injector was installed in place of the

diesel injector, and a small pencil-injector was used to inject the diesel fuel pilot dose. However, this injection system did not provide a stable engine operation at the part load condition (below notch 3). The explanation provided was that the pilot injector was incorrectly positioned.

Also in 1988, Michael Karpuk of TDA Inc., along with Scott Cowley of the Colorado School of Mines [5], published a report investigating on board DME generation to assist the cold starting in a methanol engine. Since methanol-fueled engines have difficulty starting at ambient temperatures below 10°C, due mainly to the methanol's low vapor pressure and high heat of vaporization, the study explored the potential gains of incorporating DME as an ignition aid. Since DME has a high vapor pressure and wide flammability limits, it can be a superior fuel for cold starting methanol engines. The study found that on board DME generation would be an attractive method of cold starting methanol fueled engines, and designed an electrically headed methanol dehydration reactor to produce DME on board methanol-fueled vehicles.

In 1989, Krepec et al.[6], at Concordia University, published the first results on a new, electronically controlled fuel injection system. This system was initially developed for direct injection of hydrogen and was subsequently adapted for natural gas. This system consisted of solenoid operated injectors having the gas inflow throttled by a metering valve, actuated by a stepper motor under electronic control. Such a configuration was able to control effectively the gas injection time and the gas pressure in the injector. The main factor in the design was the ability to control both the shape of the gas discharge rate and the dose of the injected gas. This combination proved to be important for the development of an efficient diesel combustion process. The system was

tested at 100 bar gas inlet pressure and was able to inject different gas doses by either varying the metering valve position, or the time of the injector opening. The research found that the direct injection system performed considerably well in several different configurations and test conditions. One of its main recommendations involved designing the injector needle as pressure balanced to close the back of the injector to eliminate leakage along the needle. Further recommendations included using stronger and lighter solenoids, as well as further investigation into the potential of dispensing with the metering valve, rendering the injection system more cost effective.

Green and Wallace (1989) at the University of Toronto [7], explored electrically actuated injectors for gaseous fuels. Two different injectors were developed for injection of hydrogen and natural gas, both operated by solenoids. Since they were intended for different engines, these injectors were very different in design and application. Common to both designs, however, was the ability to control the duration of injector opening while maintaining a fixed gas supply pressure. In this case, the injector acted as an on-off switch, opening and closing as quickly as possible, with the fully open flow rate being controlled by the nozzle orifice size and the differential pressure across the orifice. Furthermore, both injectors were based on using a high energy multiple solenoid for direct electromagnetic actuation.

The first injector, for direct injection of hydrogen in a 4-stroke diesel engine, had a flat-type solenoid immersed in the gas, which operated the injector needle through a long pull-rod. The solenoid acted in one direction only and a spring was installed close to the needle tip to provide for the injector closing. The design was aimed at a high flow rate of

hydrogen due to the large volumetric dose to be injected during the full power engine operation.

The second injector was made for a 2-stroke Detroit diesel engine and its operation pressure was much lower, for it injected gas when the engine piston was close to its bottom dead center (BDC) position. It had a similar solenoid to its counterpart, though much shorter, since it was not installed in the engine cylinder head.

Both of the injectors developed had opening durations of 1.5 ms. To achieve this goal, a special circuit was developed for the solenoid driver to cut-off the current when the injector had to be closed, in order to reduce the closing time period as well. The hydrogen injector was able to achieve 100 psi pressure, and the natural gas injector supplied 20 psi into the intake ports of a two-stroke cycle diesel engine.

In a presentation to the Future Transportation Technology Conference in August 1989, Beck et al. [8] investigated the use of electronic fuel injection for diesel engines adapted for dual fuel applications. The approach taken was to apply liquid fuel injection technology to use with gaseous fuels. Since the pilot valve used was equally applicable to gas or liquids, the same solenoid valve readily served as a direct acting, pulse width modulated, gas injection valve. The system was completed by replacing the mechanical governor with a rack actuator. This permitted the electronic control unit to direct the mechanical fuel pump in either pilot diesel, or full diesel operating modes. The system has been successfully applied to the Mercedes OM-352 diesel engine, used worldwide to power trucks and buses. The study found that one could adequately control both the main and pilot fuel through the use of an electronically controlled rack, on a conventional gear-driven fuel injection pump. It also found that the selection of dual fuel systems for diesel

engines is greatly dependent upon application and exhaust emission considerations, and that direct discharge into the intake port of each cylinder, through electronic controls, proved to be a satisfactory strategy.

The 1990s brought further advancements in the literature. The first to note, from Sydney, Australia, was provided by E.J. Lom of Apace Research and K.H. Ly of AGL Gas Co. in 1990 [9]. The two scientists explored high pressure injection of natural gas in a two stroke diesel engine. Their research investigated three alternative methods of injecting gas into the engine cylinder - the post pilot injection, the early in-cylinder injection just after exhaust valve closure, and port injection through an air inlet port. In order to conduct their tests, they designed and built a simple, hydraulically actuated gas injector, comprising of a standard Bosch in-line diesel fuel injection pump. Diesel fuel was used as a hydraulic medium, and the quantity of gas injected was determined by the amount of diesel fuel and by- the gas supply pressure. The fundamental conclusion of the study was that the post-pilot in-cylinder injection system offered the best method for fueling the engine with gas, particularly with respect to reducing hydrocarbon (HC) emissions.

In 1990, N. J. Beck added to his previous work, with contribution from the Soviet government and corporate researchers. Beck et al. (1990) [10] developed an all-electronic, dual fuel injection system for diesel engines. They replaced the traditional, mechanical diesel injection system with an all-electronic, hydraulically actuated system, coupled with multi-point injection for the gas system. The injector operated upon the accumulator injector principle, consisting of four elements - the accumulator, pressure intensifier, nozzle tip, and solenoid valve. The latter was the interface from the injector to

the electronic controller, and the high pressure plunger of the injector intensifer was actuated when energized. This was found to discharge the required amount of fuel into the accumulator, with a resulting pressure rise that was proportional to the area ratio of the intensifier pistons. Upon the solenoid being de-energized, the low pressure piston and high pressure plunger reacted. This created a pressure imbalance, which would lift the needle, opening the nozzle tip orifice. Injection occurred until the pressure in the accumulator fell to the needle valve closing pressure, preset by the spring force. The basic conclusion relevant to the actual injector was that timing and fuel quantity can be controlled electronically.

Still in 1990, Green, Cockshutt and King [11] followed the 1988 work of Karpuk and Cowley (discussed above), in examining DME as a methanol ignition improver. In their study, they supplied gaseous DME to the intake air stream of a four stroke engine that was operating on directly injected methanol. They were able to determine the amount of DME required to achieve a stable operation over the load/speed range of the engine, without the use of a glow plug. The technique was to introduce a small amount of DME into the intake air. The mixture of air and DME would begin a slow combustion early in the stroke. The remaining air in the charge would be heated by this combustion, and the injected methanol could be ignited. They found that the onset of combustion was very gentle, with the initial pressure rise being barely noticeable, and that HC emissions were reduced by as much as a factor of 10.

At this point, it became clear that, in order to meet future emission regulations for low particulate and NOx levels, both the engine combustion system and, particularly, the injection equipment, would have to be improved. Research conducted at Bosch in 1991,

by Lauvin et al. [12] was centered around electronically controlled high pressure unit injector systems for diesel engines. Of significant concern, with regards to the injection equipment, was the high injection pressure and the variable injection timing as a function of engine speed, load and temperature. They concluded that high injection pressure was found to be the primary requirement for reducing black smoke. Injection pressures were increased to 150 MPa at rated speed for engines with displacements of 2 liters per cylinder. The injector developed consisted of a plunger-type pumping element, a high pressure solenoid valve, and an injection nozzle, all combined in one unit. The solenoid valve and the nozzle were connected to either side of the pumping equipment chamber, which was formed by the plunger and the cylinder. The electromagnetically controlled valve, which opened and closed the path between the high pressure chamber and the fill bore, was the primary determinant of the function of the unit injector. The project was able to design a system that could generate high injection pressures, achieve variable injection timing, and provide cylinder cut-off as a new function.

To reciprocate, Karpuk et al. [13] built further upon the Bosch work later in 1991. Again their research was centered around investigating the use of DME in improving the ignition of methanol-fueled diesel engines. This study found great reductions of particulate emissions during operation on methanol-DME. NOx emissions were also reduced, and CO emissions were found to be negligible. The basic conclusion was that DME was an effective ignition-enhancer over the engine's entire operating range, without excessive maximum cycle pressure. Ignition timing was also found to be controllable by adjusting the concentration of DME in the inlet air, and that ignition delays for methanol-DME were much shorter than those for diesel fuel.

1991 also saw developments in the work of electronic fuel injection systems. Japanese researchers Miyaki, Fujisawa, et al [14], at Nippondenso Co., developed a new electronically controlled fuel injection system for diesel engines. The system used a high pressure common rail, with fully electronic and flexible control in fuel quantity and injection timing, as well as an adjustable injection rate shape. A fundamental merit of the common rail system was found to be its high degree of freedom of control. The system also had superior packageability and low drive torque loss, while achieving optimum injection pressure control. The common rail pressure was controlled by allowing the fuel discharge of the high pressure supply pump to vary with a pump control valve. By controlling the back pressure of the nozzle, the injection quantity and timing was also varied. This was accomplished by means of a three-way valve. The quantity was controlled by changing the pulse width, and injection timing was controlled by changing the timing of pulse. The three-way valve selectively would switch the fuel pressure of the nozzle back side of the injector between common-rail pressure and atmospheric pressure. It was not intended to directly control the fuel flow rate. As such, it acted, not as a flow rate controller, but as a pressure switching valve.

A 1992 study was performed by Slodwske, et al. of Navistar International Transportation Co. and Amoco Oil Co. [15], in order to assess the effects of fuel cetane number on exhaust emissions from a heavy duty diesel engine, with respect to 1994 emission requirements. The main contribution here was the conclusion that increasing the cetane number of fuel reduces all regulated diesel emissions species. In order to lower exhaust emissions, diesel engines were incorporating higher fuel injection pressures, retarded injection timing, more use of charge air intercooling, and electronic engine

controls. These changes were reviewed alongside the increased cetane number of the input fuels.

In 1992, Yang and Sorenson, at the Technical University of Denmark [16], published a study investigating direct digital control of the diesel fuel injection process. The authors were able to identify necessary modifications to the pump-pipe-injector system along the lines of mechanical simplicity, direct control capability, and reduced cost. In order to control simultaneously the injection timing, fuel quantity and hydraulic performance, a new solenoid control valve was designed. The system was analyzed on the basis of a comprehensive mechanical, magnetic, electrical, and hydraulic computer simulation. The authors also investigated the "new generation" of electronic diesel fuel control systems, classifying them into two categories: electronic common-rail systems and direct digitally controlled jerk pump systems. Both of these used a fast acting solenoid valve as interface between the hydro-mechanical injection equipment, and the microprocessor-based electronic control unit. This solenoid valve was able to perform direct simultaneous digital control of fuel quantity, injection timing, and injection rate. In the common rail system, the solenoid valve was used for hydraulic control of the needle valve movement. In the direct digitally controlled jerk pump system, the solenoid control valve functioned through spill control of the pumping fuel.

The Navistar International Transportation Corp. published a report by Hower et al. [17], on their new direct injection turbo-charged diesel engine in 1993. This new V-8 diesel engine had been designed for class 2 to class 8 trucks and buses. It incorporated several advanced technology features, including a hydraulically actuated, electronically controlled unit injector (HEUI). A unique fuel system developed by Caterpillar Inc. was

also incorporated into the design. This fuel system actuated the injectors with engine lubricating oil, and was electronically controlled for precise metering and timing of fuel injection. A Rexroth high pressure axial piston pump supplied the oil through oil manifolds on each bank, which served as accumulator volumes to the injectors. A solenoid-controlled poppet valve in each injector directed this high pressure oil to act on a piston, which was located over the fuel injection plunger. The oil pressure was multiplied by this arrangement to develop the desired fuel injection pressure. The high pressure fuel was then injected through a conventional multi-orifice nozzle. Injection pressure varied from 19 to 120 MPa, which was created by oil pressure varying from 3 to 19 MPa.

Still in 1993, Hong et al. [18] at Concordia University in Montreal, Canada, pursued the optimization of electronically controlled injectors. The goal was to develop solenoid operated injectors for diesel engines that could inject natural gas directly into the combustion chamber at high pressure. The new injectors had a similar size to the previous injectors, but had small and powerful solenoids located in the former spring chamber, while the spring was moved closer to the actual nozzle. The authors identified the limited commercial availability of solenoid actuators controlling the fuel injection process. They traced the cause to the requirement for the very fast operation of diesel injectors, when injecting a closely controlled dose of fuel during a very short time in the high pressure conditions of the engine combustion chamber. In order to increase the operating speed of solenoid operated injectors for direct injection of natural gas to the required doses, a special switching circuit was developed, and a multi-objective optimization method was applied in order to select the best design variables for the quick injector opening and closing. The solenoid used, a small Lisk L5, was placed in the former spring chamber of

the injector. The solenoid would lift the nozzle needle, which was connected to it by a rod. A spring located in the upper part of the central hole in the nozzle body assured the return of the needle. One highlight of the study was the revelation that both the opening and closing time of the injector could be reduced to below 1.0 ms. This made solenoid injectors' performance comparable to those of hydraulically operated injectors at moderate engine speeds. The authors also identified further possible improvements that they felt could be achieved with the use of more powerful solenoids, as well as improvements in matching the spring characteristic with the solenoid force. They also suggested modifying the needle seat design to reduce the unbalanced force on the needle that existed when the injector was closed.

Lakeview Associates' Roy Cuenca [19] in 1993 gave a thorough review of the evolution of diesel fuel injection equipment since the early 1970s. The objective: to present a review of new developments in fuel injection equipment for the heavy-duty, automotive diesel engine in North America in the past twenty years. The author's main claim was that the previous decade had witnessed more improvements and innovation in diesel fuel injection equipment than in the previous fifty years. He identified the driving force behind the diesel engine industry as the need to meet the challenges presented by emissions regulators, and that the main approaches could be classified as the reduction of one particular target – smoke, carbon monoxide, hydrocarbons, nitrogen oxides, or particulates. As fuel injection equipment played a direct role in about half of the solutions for emissions reduction, Cuenca identified it as one of the most important tools for achieving this goal of pollution reduction.

Kekedjian and Krepec of Concordia University [20] achieved further progress with new developments of solenoid operated gas injectors in 1994. As Krepec et al. had done in the previous year, this study attempted to overcome the slower and less repeatable dynamic response of solenoid operated injectors, as compared to hydraulic or mechanic diesel injectors. They also tackled the pestering problem of solenoid overheating, and the resulting loss of power which was considered detrimental for such injectors. Their new generation of injectors made use of a special inductive driving circuit for the solenoid to boost the opening of the injector needle by amplifying the supply voltage. The system also reduced the unbalanced pressure force acting on the injector needle when closed, by using a reversed differential angle in the conical needle seat. With this advancement, the injector was able to open at higher gas pressures, or to use a stronger return spring to accelerate its closing. Further highlights of the design included the use of a more powerful, but shorter solenoid which was attached to the upper cap, the fastening of electric wires with plastic seals, the direction of incoming gas around the solenoid to absorb heat, and a more elastic injector needle rod to reduce the needle bouncing. The study found, among other things, that the injector's opening required less than 0.7 ms to reach maximum flow from the nozzle, that there was lower heat released by the solenoid due to the short duration of high current (1.4 ms), and that the use of only 12 V of electric power supply was needed to generate 100 V across the solenoid coil.

Later in 1994, Guo, Murayama, et al. at Hokaido University [21], completed their 1992 works on improving the performance and emissions of a compression ignition, methanol engine, with DME. In this study, the possibility for further improvements in reducing the pilot doses of DME and emissions were investigated by optimizing the

methanol injection timing, DME injection timing, and the intake and exhaust throttling. The conclusion was that there was indeed a lower pilot dose of DME required upon the optimization of the injection timings. Though it was found that intake throttling had little effect on the reduction in the necessary pilot dose of DME, exhaust throttling was identified as being able to reduce the minimum amount of DME. Finally, the necessary level of DME was reduced to 5% of the total energy supply.

Yamaki et al. [22] of Mitsubishi Motors Corp., were studying the application of common rail fuel injection systems to a heavy duty diesel engine. Their study was focused on the parameters associated with injection timing, injection pressure and pilot injection. It also investigated the procedures for the optimization of these variables, using an electronically controlled common rail type fuel injection system, which they installed in an in-line 6 cylinder, 6.9 liter turbo-charged and inter-cooled DI diesel engine. One major conclusion was that not only high pressure injection, but also pilot injection, are effective for the reduction of smoke at high load, particularly at low speeds; and also that pilot injection could reduce NOx and HC emissions at low loads. By using an electronically controlled common rail type fuel injection system, the appropriate injection pressure was selected to reduce exhaust emissions and improve engine performance. The common rail type fuel injection system made high pressure injection (120 MPa) possible, injection timing and pressure independently variable and independent of the engine speed, and made pilot injection possible with quantity and timing also independently variable. The benefits of combining high pressure injection and pilot injection were identified. This combination was found to be effective for reducing NOx emissions and noise simultaneously, increasing

the low speed torque, and reducing smoke and acceleration time when the vehicle is started.

At Steyr Motorentechnik in 1994, Dolenc and Waras [23] studied a high pressure fuel system for high speed DI diesel engines with electronic control. The authors developed a two stage nozzle with the simple control of the cross section of the nozzle holes. In the first stage, prior to combustion, the nozzle needle would open a portion of the nozzle orifices. In the second stage, after the start of combustion, the nozzle needle opened the nozzle orifices completely. The high pressure sprays would inject the fuel into the already existing flame and, despite the high injection pressure, the fuel penetration was reduced. A double nozzle needle guide achieved the same uniform distribution of the fuel to the nozzle holes that occurred in the first stage with a limited needle lift. This double guided nozzle needle assured the durability and repeatability of the system. Since all electronic and electric components were placed outside of the engine, they were not exposed to the hot engine oil. The amount of injected fuel and the injection timing were controlled by the electronic system.

In mid summer of 1995, Sturman et al. [24] applied latching solenoid technology to fuel injection for specific fuels such as compressed and liquefied natural gas (CNG, LNG). The study provided a background of magnetic latching technology and addressed its application to an advanced, pressure balanced, gaseous fuel injector. The authors explained that the fundamental difficulty in designing a natural gas fuel injector lay in the low energy density of the fuel. A practical injector, offering compelling performance advantages, was possible by employing powerful solenoids and a pressure balanced valve design, while minimizing the mass of moving components. The latching solenoid design

incorporated a flat plate type armature. A continuous flux path was created between the armature and the pole, and a residual magnetic field would ensue. This latching force was able to hold the injector in the open position. The coil was de-energized once the solenoid was latched, and the injector would remain open. To close, a small reverse current pulse had to be applied to cancel the residual magnetism. When the field would collapse, the spring force would overcome the magnetic force, causing the injector to close. The result was compelling accuracy and repeatability, as compared to previous solenoid based injectors. Uniform opening and closing response times were independent of pressure and were achieved through a pressure balanced injector valve.

At the same time, Barkhimer and Wong of BKM Inc. [25] explored the application of digital, pulse-width-modulated sonic flow injectors for gaseous fuels. The injectors were composed of a solenoid coil and valve assembly, where the coil consisted of solenoid winding and electrical connection, and the valve was comprised of the valve body, which held the solenoid armature, ball poppet and seat. While de-energized, the supply pressure, assisted by a spring, would force the poppet on its seat, which prohibited gas flow. When the solenoid was energized, gas would pass through the valve seat and outlet port of the injector, while the ball poppet was lifted off the seat and held against the stop. The solenoid was a low resistance coil designed for rapid response, and was actuated by a current regulated driver. This driver limited the initial opening current to 4 amperes, then would fall and maintain at 1 ampere, in order to conserve energy for the duration of the energized time.

Yudanov of Invent Engineering in 1995 [26] investigated the development of the hydraulically actuated electronically controlled unit injector for diesel engines (HEUI).

The key design factors that determined the injection rate, pressure, energy efficiency, and accuracy of fuel delivery for such a system were identified, as well as their effect on performance parameters. The author compared two methods of fuel metering within an HEUI in terms of injection accuracy, reliability and controllability. The first method had a built-in small volume accumulator, and the second used a common external accumulator. The HEUI of the latter type had certain fundamental advantages over the former as they allowed for independent control of fuel delivery and injection pressure.

In 1995, an increased focus on the application of the above technologies to smaller engines was evidenced in the study performed by Yao-qing at the Wuxi Fuel Injection Equipment Research Institute [27]. Here, the author investigated the development of new-fashioned, low-inertia injectors for small-medium IDI diesel engines. The paper conducted a series of investigations on the optimization of the structure, the working process matching with engines, as well as the reliability and durability of these injectors. The highlights of the injectors' design lay in their reduced reciprocating mass of moving parts, small dead volume, simplified structure, lower manufacturing costs, excellent performance matching, and energy saving. The design was being increasingly applied in the Chinese market.

Whereas, in past research, DME was being used as an injector enhancer, 1995 saw a breakthrough in the notion of using DME as the primary source of fuel. Fleisch et al. [28] tested and evaluated medium-duty vehicle engines with DME blends at emissions levels that would surpass the California Ultra Low Emissions Vehicle (ULEV) regulation. This study reviewed the identification of truck and bus diesel engines as a significant source of nitrogen oxides (NOx), and particulate matter (PM). The ultimate conclusions

were that reducing the initial injection flow rate would lower NOx emissions without influencing fuel consumption. Furthermore, the authors found that increased air utilization would lower CO emissions and permit higher EGR rates with corresponding reductions in NOx emissions. The DME fueled diesel engine was able to meet California ULEV regulations while matching or bettering fuel economy and performance of the diesel baseline. With DME, the engine was able to provide very low emissions and completely smokeless operation with a maximum injection pressure of just 220 bar, and its application to direct injection diesel engines without major design modifications was also identified.

Austrian researchers Kapus and Ofner [29] were also studying DME as a primary source of fuel in 1995. They investigated the development of fuel injection equipment and combustion systems for DI diesels operated on DME. Due to its high cetane number, DME could lead to the combustion in a compression ignition engine without any ignition aid. The authors did identify some disadvantages of DME. Primary among these was the need to take significant measures to keep the fuel liquid in the tank and in the fuel injection system, given its low boiling point. Leakage into the environment would also have to be guarded against, given that DME immediately evaporates and could form an explosive mixture with air if concentrations of 3.4% vol. are exceeded. Furthermore, given its relatively low density and calorific value, DME operated engines would require increased injected fuel volume per stroke in order to achieve the same power output as with diesel fuel. This study was running concurrent to Sorenson et al. [30] who were also investigating the performance and emissions of a direct injection diesel engine fueled with DME. These researchers also found that DME gave very satisfactory combustion, performance and emissions, and that engine operation with thermal efficiency was

equivalent to that achieved with diesel fuels. The same general conclusions about reduced NOx and smoke emissions were also reached.

As the benefits of DME were becoming more well known, Hansen et al. [31] in 1995 sought to investigate the technologies for the large scale manufacture of DME from natural gas. The authors found that DME could be manufactured in large scale from syngas, using abundant resources such as natural gas, coal, and biomass. The plants used to manufacture DME would have a 4-8% lower investment cost to similar methanol plants, and a lower energy consumption of approximately 5% as compared to their methanol counterparts.

Stumpp and Ricco [32] in 1996 conducted a thorough examination of the use of a common rail in the fuel injection system for passenger car DI diesel engines. Their common rail allowed for a flexible fuel injection system, which permitted variation of fuel quantity, and injection pressure in the range of 150 to 1400 bar. It also allowed for free mapping of rate of injection and start of injection needed for DI diesel engines. The injectors were opened and closed by the electronic control unit at defined times. The injected fuel quantity was a function of the fuel pressure in the rail, the flow area of the injector, and the duration of injection. The study's conclusions regarding the advantages of a common rail system included reduced combustion noise resulting from a flexible pilot injection, and lower particulate emissions and large maximum engine torque, given the ability to handle injection pressure up to 1400 bar.

Hong et al. [33] in 1996 added to their contribution in the literature by exploring fuel delivery characteristics for solenoid operated diesel engine gaseous injectors. The study focused on the shape of the gas discharge rate versus time, since this could have a

substantial impact on the combustion process in the diesel engine. The shape of the gas discharge rate characteristic could be changed through the use of a throttling pintle nozzle or a double-spring configuration. The authors computer-simulated the gas delivery characteristics in order to assess the impact of three modes of fuel discharge rate control strategies. They concluded that the gas dose and its discharge rate could be shaped as required. It was found that the injected gas dose could be altered by varying the voltage pulse width, and/or the metering valve opening.

McCandless and Li of AVL Powertrain Engineering, Inc. [34] developed a novel fuel injection system for DME and other clean alternative fuels in 1997. The design was a common rail system specifically intended for direct injection of liquid DME in order to achieve low emissions of NOx and PM from diesel engines. The authors overcame technical challenges that made available diesel fuel injection equipment unsuitable for use with DME. These challenges included the unmanageability of internal system leakages with DME, and inappropriate injection pumping rates. The driving force behind the study was the belief that DME would soon become the "alternative fuel of choice" for diesel engines.

Also in 1997, Endo, Adachi, et al. [35] used a common rail fuel injection system in their engine design for Hino Motors. The design allowed a reduction in engine noise and vibration, and was able to also reduce the NOx emissions through the optimized control of injection characteristics. The rail provided a common gallery of fuel for each injector. Injection was achieved through electronic signals to a three way electromagnetic valve, where the initial timing and duration of electronic current determined the injection timing

and quantity. A small quantity of fuel given before the primary injection resulted in pilot injection, which was found to reduce the NOx emissions.

Yoda and Tsuda at Denso Corporation [36] published on the effects of injection nozzle improvements on a diesel engine in 1997. They found that a high flow velocity injection nozzle was more effective than conventional nozzles in atomizing the fuel spray and that the most effective method for achieving such nozzles was an enlargement of the chamfer at the spray hole inlet. Fuel spray atomization would aid in improving engine performance with lower NOx and PM emissions. Their tests of the high flow velocity nozzles concluded that they were indeed effective in reducing these emissions while also achieving higher engine output. Their results were obtained even without increasing the fuel pressure which would have aided the fuel spray atomization.

Finally in 1997, Arcoumanis et al. [37] investigated the application of a computer model to an in-line pump based injection system. Their model simulated the flow development in diesel injection systems and was applied to the pump connected to inclined multi-hole nozzles. The model was validated with the experimental data, which showed that pump and line pressure, as well as needle lift, injection rate, and quantity were all adequately predicted in the simulation. They finished by investigating the effect on the flow distribution inside the injection holes from the geometric details of the sac volume and holes.

In 1998, two important publications in the literature can be found, both with regards to common rail systems. The first, by Guerrassi and Dupraz [38] explored the common rail design for high speed direct injection diesel engines. The system included a new high pressure pump, a rail, and unit injectors which were able to accommodate a

rapid control valve within a 17 mm nozzle. It was possible to control the pressure range between 150 to 1600 bar at all engine operating conditions. In order to achieve a rapid control and reduce nozzle seat stress, the design included a low moving mass and small component dimensions. The former characteristic resulted in a reduced impact force acting on the nozzle seat when the needle would close.

The last paper to examine was published by Kato et al. at Mitsubishi Motors [39] in 1998. This paper investigated the improvement of engine performance through the use of a common rail system. Fuel consumption was improved by constraining the initial needle lift, which reduced the initial injection quantity, though black smoke was increased. When injection quantity was reduced through a reduction of the nozzle hole diameter, both consumption and black smoke were reduced at light loads. However, at medium and high loads, the injection period was lengthened, hampering overall performance. It was necessary to increase injection pressure in order to reduce the injection time. Two-way type injectors were found to greatly reduce leakage, as compared to their three-way counterparts, with commensurate reductions in drive losses and improved fuel consumption.

As shown in the literature survey, considerable advancements in the research on fuel injection systems have been made over the last ten years. Research was conducted in this area all around the world, from Austria to Japan, from Denmark to Canada, from the Soviet Union to the U.S.A. An overview was presented of the landmark contributions in electronic fuel injection technology using solenoids, alternative fuels including DME, and the incorporation of common-rail systems in the electronically controlled injection process.

The use of solenoids and an electronically controlled common rail fuel injection system have repeatedly shown improvements in injection control, reliability and accuracy. Solenoids allow for direct, simultaneous digital control of fuel quantity, injection rate and timing. Common rail systems provided for a high degree of freedom of injection pressure control. The use of DME began as a combustion enhancer for diesel engines, improving the ignition of the methanol fuel used. DME was able to accomplish this enhanced ignition due to its greater capability for auto-ignition, reflected in its higher cetane number. Here, its ability to reduce PM and NOx emissions was first discovered. Research then progressed towards establishing DME as the primary source of fuel in diesel engines, so as to further reap the rewards of its emissions characteristics, as well as observed improvements in engine performance.

The preceding chapter was intended to give a summary of landmark research conducted in the field of fuel injection, and the current state of engineering know-how in this field. The following chapters will show how this thesis hopes to draw on these advancements in order to propel technology ahead once again.

CHAPTER 3

RESEARCH CONCEPT AND CHRONOLOGY

Government regulations of engine emissions is continuously prompting researchers in the field of fuel injection to design systems which make engines more efficient, and environmentally friendly. Even without the prompting of regulators, engineers and scientists must continue to exercise social responsibility by striving towards the goal of clean air and energy conservation goals. It is in this vein, and with these ambitions, that this research was undertaken and conducted.

This work began by reviewing the major contributory works in recent literature on direct fuel injection systems. The discovery was made that solenoid actuated fuel injectors provided a significant increase in injection accuracy, reliability and control. This increased flexible control can be exercised over fuel quantity and injection timing, as well as an adjustable injection rate shape. Further research revealed that the use of DME would also provide unique opportunities in the reduction of NOx pollutants and PM emissions, with resultant near soot free, and ultra-clean combustion. Furthermore, the higher cetane number of DME results in a lower ignition delay and, therefore, greater engine power. As such, the environmental advantages of DME are combined with its ability to generate greater engine efficiency. As increasing research is beginning to indicate, the combination of these two fundamental building blocks of superior injection design - that is to say solenoid actuation and DME fuel use - would result in a fuel injection system of superior quality.

As such, the first step was to analyze the basic specifications and characteristics of DME fuel, as compared with the basic fuels for which traditional injectors had been

designed. This also involved an analysis of the problems that might be encountered in using DME fuel for direct injection in traditional systems. Upon reviewing the special attributes of DME, a model injector was identified upon which to affect necessary modifications. The next step was to therefore analyze the existing design of the electronically controlled injector for gaseous fuels developed at Concordia University, as well as its solenoid driving circuit. The intended modifications were aimed at adapting the system design for direct injection of DME in a targeted diesel engine. The fuel discharge process was analyzed, based on the technical data and characteristics of the diesel engine proposed for the demonstration project, in order to determine the specific design parameters of solenoid actuated injectors. The injectors were tested for needle movement characteristics, seat force, and pressure tolerance of the driving circuit. At this point, the discovery was made that the existing driving circuit was not powerful enough to withstand the 200 bar pressure necessary in the injection of DME fuel, and that a new driving circuit would need to be developed. Then, a technical specification of the solenoid operated injector was established for direct injection of DME, as the basis for the prototype injector's design.

The third stage was the design of the prototype injectors, and their ensuing computer simulation. The existing mathematical model was modified and computer simulated to predict the solenoid injector's behaviour under varying test conditions. The simulation results were to be used later for corrections to the design before the subsequent manufacture of the prototypes. The new driving circuit and corresponding computer program needed were developed at this point.

The test program was then developed and conducted and the facilities for solenoid injectors testing were designed. The test program included typical fuel injector tests, as well as special tests devised specifically for solenoid operation with DME fuel. These include needle lift, dynamic response tests and, for the first time in the literature, a test to measure the needle seat force was initiated and directed. The test results were used to validate the mathematical model of the injectors, and to prepare both design and model for optimization.

The final stage was the reporting of the research and its results, and is manifested in the form of this thesis. Further preparations are underway to incorporate the design in comprehensive complete engine tests within a non-laboratory environment.

CHAPTER 4

DME INJECTION AND CONFIGURATIONS

As discussed in the previous section, the second stage in this research, after reviewing existing literature, involved analyzing the existing design of the electronically controlled injectors for gaseous fuels. The aim was to modify the design of these injectors to adapt them for the direct injection of DME in a targeted diesel engine. To accomplish this, it is first necessary to analyze the basic specifications and characteristics of DME fuel and contrast them with the basic fuels for which the original injectors had been designed. The following chapter is organized in the following manner. Section 4.1 reviews the characteristics of DME fuel. In this section, an analysis is provided of the existing design of solenoid actuated injectors, while investigating potential difficulties in their usage for the direct injection of DME. Section 4.2 explores solutions to the challenges identified in Section 4.1 and, given these solutions, Section 4.3 presents alternative configuration concepts for the injector design. Section 4.4 will identify the configuration of choice, and discuss its advantages over the other alternatives. Section 4.5 will conclude the section on DME characteristics, injection concepts and review the specifications of the injector configuration used.

4.1 DME Characteristics And Traditional Solenoid Actuated Injectors

DME fuel (chemical symbol CH_3-O-CH_3) can be produced from natural gas and, therefore, its application can be of great importance to the Canadian economy that is so rich in natural gas resources. Its production technology has been recently upgraded for mass volume production in anticipation of its increased use as a diesel fuel.

Table 4.1.1 presents a comparison between DME, diesel fuel, and natural gas with respect to a number of key variables.

	DME	Diesel Fuel	CNG (Methane)
Chemical Structure	CH_3-O-CH_3	-	CH_4
Cetane Number	~ 60	40-55	50
Boiling Point (°C)	-20	180-370	-162
Density (g/ml)	0.66	0.84	-
Kinematic Viscosity @ 20 °C (cSt)	0.25	2.5-3.0	-
Auto Ignition Temperature (°C)	235	250	650
Stoichiometric A/F Ratio	9.0	14.6	17.2
Lower Calorific Value (MJ/Kg)	27.6	42.5	50.0
Heat of Evaporation (KJ/Kg)	410 @ 20 °C	250	-
% wt. Carbon	52.2	86.0	75.0
%wt. Hydrogen	13.0	14.0	25.0
%wt Oxygen	34.8	0	0

Table 4.1.1 - Properties of DME and Comparison Fuels [29]

The key property of DME is its high cetane number as compared to natural gas and some diesel fuels. As a result, the on set of combustion in a compression engine can be easily achieved without an ignition aid. The high cetane number indicates a shorter

ignition delay, lowering premixed burning and, thus, NOx and noise emissions. In comparison to modern diesel fuels which have a cetane number of 40-55, DME exhibits a cetane of around 60. This can also be witnessed by observing DME's lower auto-ignition temperature as compared to diesel fuels and natural gas. In fact, natural gas has an auto-ignition temperature almost 3 times higher than DME.

The chemical structure of DME is also very revealing. The fuel has a 34.8% oxygen content which, in contrast to diesel fuels and natural gas (which have 0% oxygen), DME offers the potential of a totally smoke-free combustion, if properly burned.

The main drawback of DME use lies in its low boiling point, approximately -20°C, as compared to liquid diesel fuels that can have boiling points as high as 370°C. As such, DME is gaseous at atmospheric conditions, but becomes liquid at around 5 bar pressure in a 20°C environment. As the environmental temperature rises, pressurization must increase as well, in order to keep the fuel liquid. At combustion chamber temperatures of over 500°C, the required pressure is estimated to be about 20 MPa to keep injected DME liquid.

DME has both lower density and lower calorific values, as compared to diesel fuels. Assuming the same engine efficiency, the consequence is that volumetric fuel flow rates must be around 1.7-1.8 times that of diesel fuels, in order to achieve the same level of power output. This means that 1.7-1.8 times more DME (in volume) is required than with diesel fuels.

The liquid viscosity of DME is approximately ten times lower than for diesel fuels. This can result in higher internal leakage within the supply pump, common rail and fuel injectors. Given that this leakage into the environment would cause DME to evaporate

and potentially form an explosive mixture with air, special attention has to be given to the leakage issue.

As already discussed in previous sections, DME provides substantial benefits with regards to meeting and surpassing strict emission standards. Table 4.1.2 gives a summary of DME and diesel fuel emissions in comparison to the strict Ultra-Low Emissions Vehicle guidelines required in California for medium-duty vehicles [40].

POLLUTANT	ULEV	DIESEL FUELS	DME RESULTS
Hydro Carbons	1.3	2.2	0.21
Carbon Oxide (CO)	7.2	-	3.2
NOx + NMHC	2.5	3.5 - 5.5	2.4
Particulate Matters (PM)	0.05	0.08 - 0.13	0.033
Formaldehyde (HCHO)	0.025	-	0.022

Table 4.1.2 - Emission Limits and Results (measured in g/bhp-hr)

As can be seen, DME meets and surpasses all ULEV requirements, as well as significantly outperforming diesel fuels, especially in NOx and non-methane hydrocarbon emissions (NMHC).

Before examining the problems associated with the incorporation of DME into the injection process using current designs of solenoid operated injectors, it is necessary to review the design specifications of the third generation of fuel injectors developed in 1994 at Concordia University. This injector uses an electrical solenoid to generate the pulling force necessary to open the injector needle. This force must be considerable in order to

ensure rapid opening of the needle for the proper injection timing of the fuel discharge. The injection system used a powerful high-performance Lisk L7 solenoid, which guaranteed opening at higher gas supply pressures, and included an advanced driving circuit. This circuit reduced the opening and closing delays of the injector, limited the extraneous current passing through the solenoid, and ensured that the injector would open at gas pressures up to 10 MPa. In order to absorb the heat which negatively affects the solenoid force, incoming gaseous fuel was directed around the solenoid. Two screws bolting directly into the solenoid served to hold the solenoid body firmly against a copper spacer and the cap. As long as the gap between the solenoid core and the bottom of the core cavity was larger than the needle lift itself, the lift was accurately set and was independent on the gap. This was a direct consequence of a larger diameter spring and a special retainer which were placed inside the injector body, so that a needle stopper was provided by the bottom face of the body. This spring also served to accelerate the injector's closing. Advanced as this design was in its time, it was not intended to be used with DME fuel; and, as such, has several shortcomings for this purpose.

The following challenges face the modification of the above injector design for compatibility with DME use and improved efficiency.

1. The DME fuel would be delivered by a common rail system under a high pressure of about 20 MPa, acting steadily on one side of the nozzle seat, with the presence of hot burning gases on the other side. The injector's behavior is unpredictable in such an environment. Given the low viscosity of DME, this environment presents significant threats with respect to leakage of the fuel to the combustion chamber between consecutive injections. To address this issue, and minimize the leakage, a steel to steel

sealing contact seems to be inevitable, so as to assure improved seat geometry and needle concentricity.

2. The low viscosity of DME presents a second hurdle insofar as the durability of the needle seat is concerned. The seat sealing surface would be subject to high temperature and to high frequency impacts from the needle hitting the surface. Since the DME liquid layer cannot create an appropriate cushion, there is no dampening of the needle movement and dissipating its kinetic energy, and these impacts can adversely affect the durability of the needle seat.
3. Given the lack of dense liquid fuel between the injector needle and the nozzle body, combined with a loosened fit surface in an injector with a pressure balanced needle, there is increased potential of high bouncing of the needle at both sides of its stroke; the upper stop and the bottom seat. The increased spring-back of the needle when fully open might restrict the fuel flow through the nozzle orifices, thus affecting the discharge rate characteristic, and the engine combustion process. The increased spring-back of the needle when hitting the seat would further create the unwanted post-injection of the fuel into the combustion chamber, which is detrimental to the engine combustion process. Post-injection is the delivery of fuel into the combustion system at an inappropriate time, resulting in the direct discharge of the fuel into the exhaust in the form of particulates, hydrocarbons, and other emissions. The increased spring-back of the needle also increases the impact force on the nozzle seat, which contributes to the wear of the seat, as previously described.
4. The speed and repeatability of the solenoid dynamic response, combined with the high temperatures existing in the combustion chamber, cause an increase in the

temperature of the solenoid coil itself. This heating of the solenoid coil causes a reduction in the total pulling force provided by the solenoid actuator. There can be several consequences; the extreme being a complete malfunction of the injector, where the needle does not have enough force to open. More moderate consequences include the non-uniformity in injected fuel dose and injection timing across all cylinders.

5. At any given moment, the injector nozzle stores more fuel than is needed for each individual discharge. When the needed fuel is injected, the excess remains in the nozzle, and is subject to the extremely high temperatures of the combustion chamber. Given the low boiling temperature of DME, this exposes fuel to vaporization. If this occurs, the fuel discharge rate might be adversely affected.
6. The control of the nozzle's fast opening was previously accomplished by a switching circuit which was able to withstand up to 10 MPa pressure. However, it is known that DME must be pressurized at 20 MPa in order to maintain its liquid form in the hot temperature surroundings of the combustion chamber. It is clear that the driving circuit previously used would not be applicable to an injection system operating with DME.

The preceding discussion exposed some of the fundamental problems surrounding the use of current solenoid actuated fuel injector design for use with DME as fuel. Proposed design configurations must include modifications to address the difficulties presented above, before an injection system for DME fuel can be considered viable.

4.2 Overcoming The Barriers

A commentary on each of the problems presented above is now presented with the aim of discovering solutions to them.

Comment on Problem 1

The first issue raised in the previous discussion was the leakage of fuel into the combustion chamber. Since the nozzle is protruding into the engine combustion chamber, and is surrounded by hot combustion gases, no soft material can be used for the needle seat inside the injector nozzle. The sealing technique used in conventional diesel nozzles is to create a distinct contact line at the intersection of two cones - on the needle tip and in the nozzle seat - with the cone apex angles being different by only 40 minutes. This differential angle is a compromise between the best nozzle valve sealing that is provided by a larger differential angle, and the needle seat durability provided by a smaller differential angle.

Recent manufacturing technology is able to produce the injector nozzle with very high accuracy of the hardened steel seat components. This was confirmed by tests made with conventional diesel injectors using natural gas, which would leak much more than any liquid fuel and more than DME fuel [41]. Only a very small leak rate was observed at 20 MPa gas pressure. The possibility of reducing the fuel leak by introducing a reverse cone differential angle, where the sealing contact line at the internal seat diameter would be approximately half the length, should be considered.

Comment on Problem 2

The dynamic impact of the needle when closing on the seat in the nozzle will be greater when injecting DME by the solenoid operated injectors than in the conventional

injectors. This is due to two factors - a smaller damping effect on the needle movement by the lower viscosity DME and a greater dynamic impact force on the seat from the decelerating needle with the attached heavy solenoid core. To reduce the large inertia force, a special elastic rod connected to the needle on one side, and to the solenoid core on the other, can be introduced. By damping the impact of the solenoid core, the kinetic energy conversion could be distributed in time, reducing the impact force acting on the seat.

Comment on Problem 3

The third hurdle is the high bouncing of the needle at both sides of its stroke, resulting in possible restrictions on the fuel flow through the nozzle orifices, when at the upper stop, and in undesired post-injection, when at the nozzle seat. Bouncing is caused by the spring-back of the needle while the rapidly decelerating needle is converting its kinetic energy into the elastic deformation of the contracting material. The injector needle bouncing is related to the inertia force produced by the needle, the injector rod, and the solenoid core. The same elastic rod discussed above under the Comment on Problem 2, could also serve in reducing the bouncing effect of the needle. The long elastic pulling rod could introduce the elasticity of the metal material into the design.

Comment on Problem 4

Of primary importance in the operation of solenoid actuated injectors is the ability of the solenoid to exert sufficient electromagnetic pulling force upon the injector rod. Being installed directly in the cylinder head of an engine, the solenoids are particularly vulnerable to the heat of the combustion chamber. The solenoid duty cycle and cooling have a substantial impact on the solenoid force. One solution is to place the solenoid coil

at a significant distance from the cylinder head, removing it from direct contact with the combustion chamber. The distance between the solenoid and the combustion chamber helps to reduce heat transfer to the solenoid. An improved solution is to place the solenoid inside the common rail, where fuel is consistently being re-circulated to the tank. Here, the solenoid is constantly cooled by the fuel in which it is immersed.

Comment on Problem 5

In order to reduce the possibility of boiling DME inside the nozzle, one could provide a path for re-circulation of the excess fuel coming out of the nozzle. This path could circulate the fuel out of the injector and into the common rail, the tank, the pump, or any other destination in the fuel delivery system.

Comment on Problem 6

A special solenoid driving circuit that can help overcome the 20 MPa pressure needed to keep DME in liquid state, could be designed and developed. The microprocessor would be able to control the fuel dose by varying the duration of the pulse sent to the solenoid driver circuit. The driving circuit should be able to provide the required solenoid force to overcome the increased pressure without compromising its abilities to minimize the opening and closing delays of the injector to less than 1 ms, while operating on the 12 V power supplied by standard car batteries.

Now that there are possible solutions provided for the major hurdles involved with DME use, a variety of concepts for design configurations can be explored. These configurations all present necessary modifications to the standard injectors studied thus far, possibly adapting them to be used with DME fuel.

4.3 Possible Concepts For Configurations

Several alternative design configurations were considered. They have a common DME supply system, but they differ regarding the injection process of the system, as each of their respective figures and accompanying explanations will demonstrate.

Figure 4.3.1 presents a block diagram of the DME supply system. It originates at the fuel tank, where the DME fuel is stored at 1.5 MPa pressure. The pressure has been increased

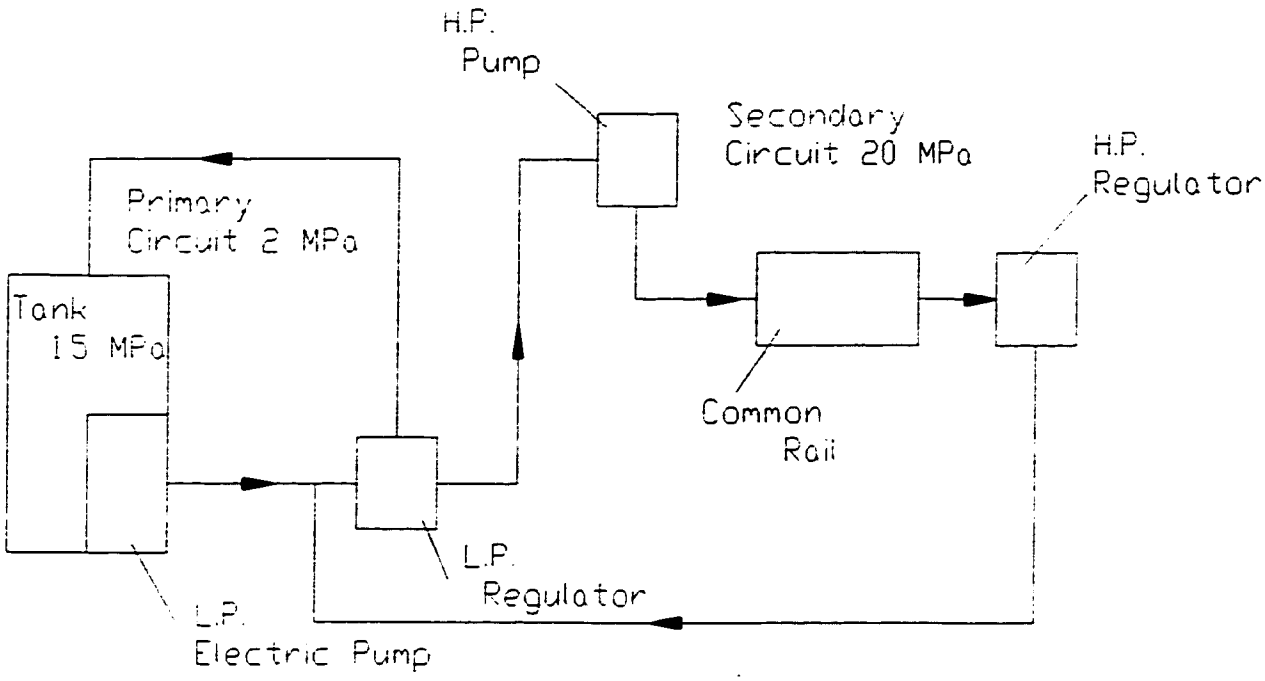

Figure 4.3.1 - Basic Schematic for DME Direct Injection Common Rail System

from the 0.5 MPa mentioned previously in order to create a safety margin for the higher atmospheric temperature. Through the use of a low pressure electric pump, the fuel pressure is increased to 2 MPa in order to circulate it through the low pressure regulator. The circulation is achieved in the primary circuit, consisting of the tank, the low pressure

electric pump, and the low pressure regulator. Once regulated to a steady pressure, the fuel is delivered to the high pressure pump in which the fuel is pressurized to 20 MPa, which is the required pressure for DME injection. The high pressure pump delivers the fuel to the common rail and, subsequently, to the individual injectors. The amount of fuel required for combustion is injected into the chamber, and the remaining fuel flows through the high pressure regulator and is returned to the primary circuit. By simply varying the low pressure regulator's characteristics, the pressure level obtained by the high pressure pump can be adjusted.

The remainder of this chapter analyzes 6 separate, though related, configurations for the injection process within the common rail and individual injectors, and finish by identifying the configuration design of choice, evaluating in contrast to the other options presented.

Configuration 1

The first configuration is, in principle, the 3rd generation solenoid actuated injector previously analyzed. The only modification made was the connecting of the injectors to a common rail delivery system. In this configuration, as with the previous design, the main disadvantage lies in the fact that the efficiency of the solenoid is adversely affected, due mainly to the high temperature of the near-by combustion chamber. In this modified configuration, presented in Figure 4.3.2, the fuel is delivered to the common rail from the high pressure pump pressurizing the fuel to 20 MPa. From the common rail, fuel is guided to the solenoid operated injectors. Once the solenoid is energized, the injector is opened and fuel is delivered to the combustion chamber. The excess of fuel is released to the primary circuit through the pressure regulator.

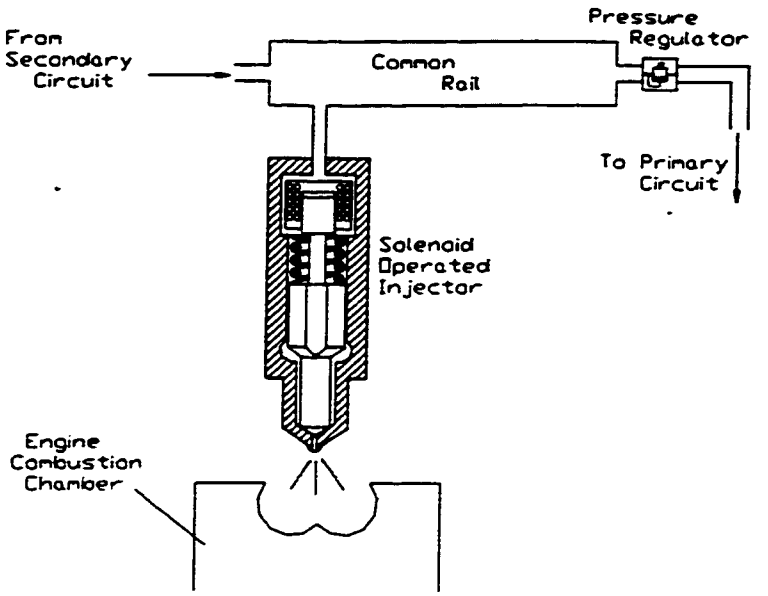

Figure 4.3.2 - Configuration 1

Configuration 2

As a result of the main disadvantage of the first configuration, regarding the proximity to the combustion chamber and the high temperature effect on the solenoid, a second configuration is proposed. In this configuration, the solenoid is located in the common rail and is cooled by the fuel flowing inside. The solenoid core is connected to the needle using a long hollow rod (Figure 4.3.3). The use of a long connecting rod made from a thin wall pipe should help to reduce the bouncing of the needle by dampening the kinetic energy impact. The two main drawbacks of this configuration are that the excess DME inside the nozzle tip is still susceptible to boiling and vaporization. Furthermore, fuel leakage remains a concern in this design as well.

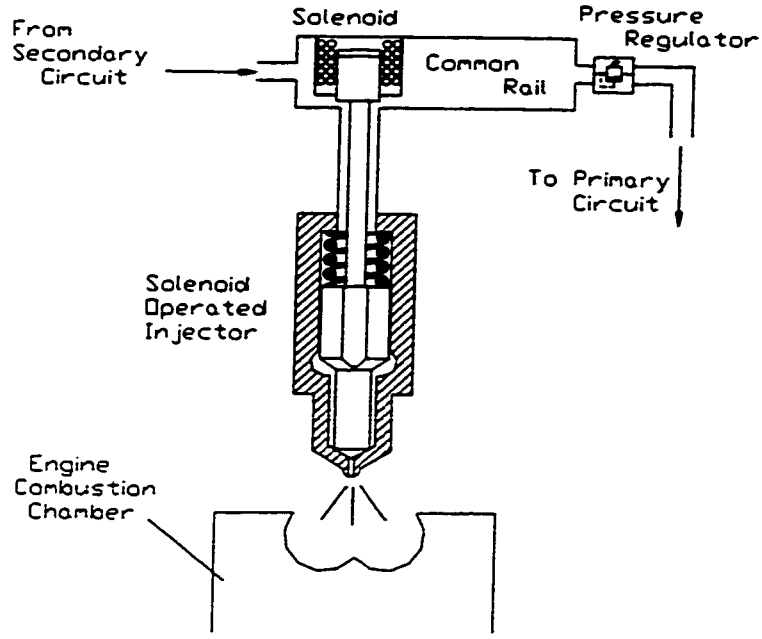

Figure 4.3.3 - Configuration 2

Configuration 3

The third configuration is conceived in order to address the possibility of DME boiling in the nozzle tip, by providing a circulation path for the excess fuel left in the injector. It is similar to the second configuration, insofar that the solenoid is placed inside the common rail in this design as well. A variable metering orifice is added in order to control the fuel's ability to escape into the primary circuit. This is important, since only fuel susceptible to undesired boiling should be allowed out of the injector nozzle. With this configuration, the potential for the DME to vaporize in the nozzle is reduced, without impairing the necessary operations of the injector system. The configuration is presented in Figure 4.3.4.

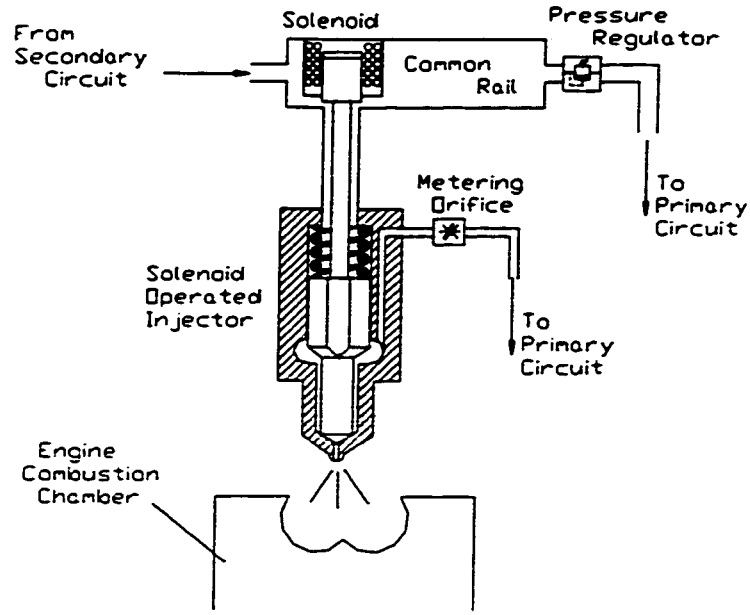

Figure 4.3.4 - Configuration 3

Configuration 4

In this design, similar to configurations 2 and 3, the solenoid is placed inside the common rail (Figure 4.3.5). However, instead of using a solenoid operated injector, a solenoid operated valve is used and the fuel is injected through a pressure operated injector. By opening the valve and generating a pressure wave, the solenoid controls the opening of the pressure operated injector. Due to the lower pressure in the nozzle between injections, fuel leakage is reduced. However, as a result of the low pressure, the possibility of DME boiling is greatly increased.

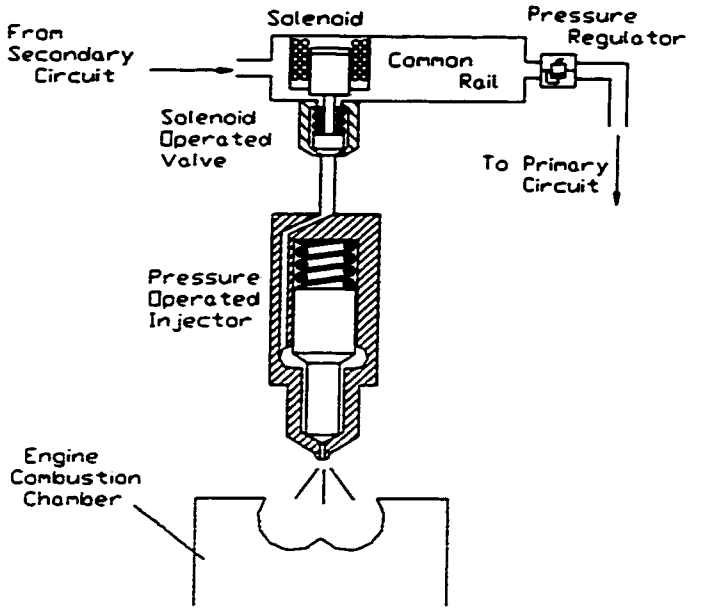

Figure 4.3.5 - Configuration 4

Configuration 5

In this configuration, as in the previous one, a solenoid operated valve is used to

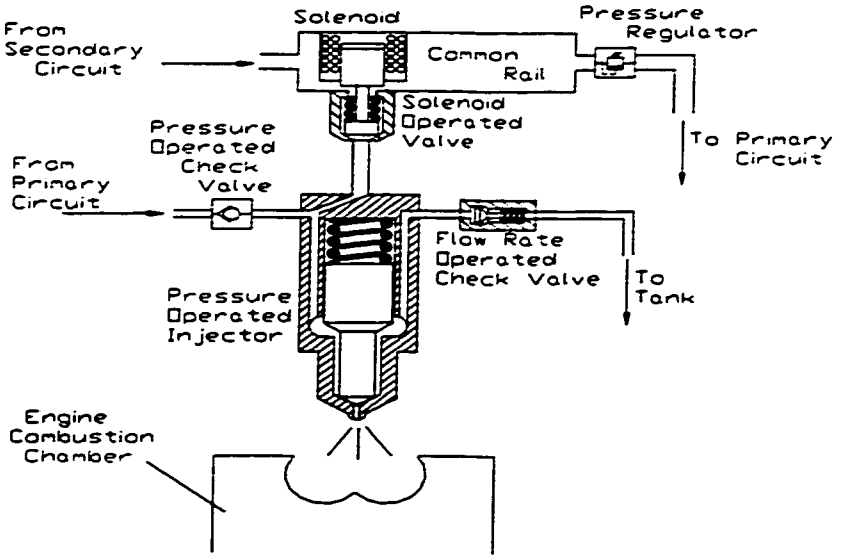

Figure 4.3.6 - Configuration 5

supply a pressure operated injector (Figure 4.3.6). However, in this system, the fuel is circulated through the injectors between the injections, in order to reduce the potential of DME boiling. During the injection period, by opening the solenoid operated valve, the pressure wave generated in the injector causes the pressure operated check valve, and the flow rate operated check valve, to close. When these two check valves are closed, the fuel circulation is interrupted and the pressure inside the injector lifts the needle, allowing fuel injection to occur.

Between injection periods, while the solenoid operated valve is closed, the fuel from the primary circuit flows inside the injector. Due to the low pressure in the primary circuit, the flow rate operated check valve remains open allowing the fuel to circulate. However, it is unclear if the response of the solenoid that triggers the opening and closing of the check valves, is rapid enough to produce a fast fuel injection process.

Configuration 6

In this last configuration, a solenoid is used to control the opening and closing of a valve at the exit path from the injector. During the injection period, the solenoid operated valve remains closed, and the high pressure to open the injector is controlled through a variable metering orifice. In order to close the injector, the solenoid operated valve is opened, creating a pressure drop inside the injector.

In this system, the fuel is circulated through the injector between the injections, and helps the DME to remain in liquid state. As in the first configuration, the high temperature caused by the proximity of the combustion chamber presents an increased possibility of reduced efficiency of the solenoid. By placing the solenoid inside the

common rail, this problem would be addressed, since the solenoid could be cooled by the surrounding fuel. Figure 4.3.7 illustrates this system.

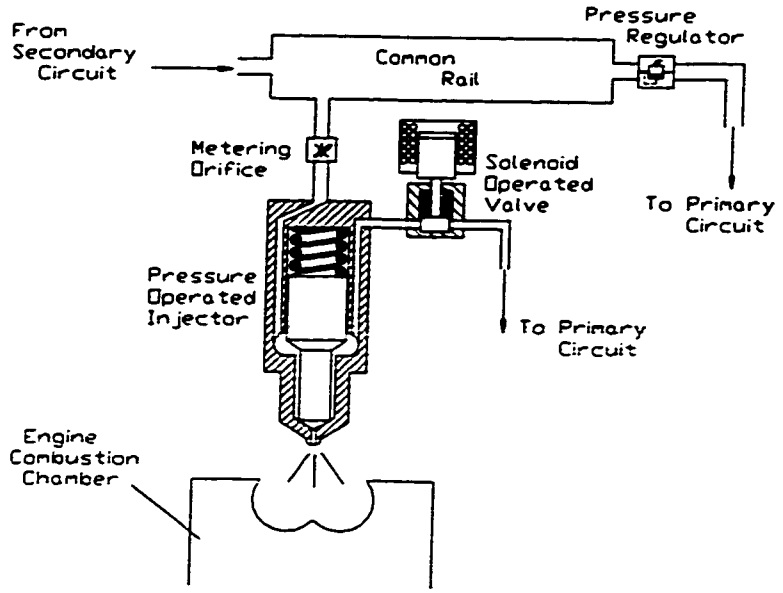

Figure 4.3.7 - Configuration 6

4.4 Configuration Of Choice

Of the six designs, Configuration 3 is the most complete. While maintaining a great degree of simplicity, the design addresses most of the problems identified with the adaptation of injectors for use with DME, and does so more effectively than any of its counterparts.

The first characteristic of note in the configuration of choice is that a circulation path through a metering orifice is provided for the excess fuel left in the nozzle between discharges, in order to avoid fuel vaporization in the nozzle (solution to problem 5). This circulation path is not found in Configurations 1, 2 or 4.

Next, it is important to highlight that the length of the injector rod has been increased, removing the solenoid from direct exposure to the heat of the combustion chamber. Furthermore, the solenoid is placed inside the common rail, where circulating fuel provides a cooling mechanism. As such, the risk of the solenoid's efficiency being adversely affected due to overheating is greatly reduced (solution to problem 4). In Configuration 1, the rod length is not increased, nor is the solenoid placed in the common rail. As such, the configuration jeopardizes the ability of the solenoid to function unimpaired by excess thermal challenges.

Furthermore, the long elastic rod in Configuration 3 dampens the spring-induced bouncing, dissipating its kinetic energy, and thus reducing the resultant post-injection and decreased durability of the needle seat (solution to problems 2 and 3). Configurations 1, 4, 5, and 6 do not have the lengthened rod and, as such, are vulnerable to increased seat wear, and post-injection caused increases in toxic emissions.

Finally, the design also includes a new driving circuit which can withstand 20 MPa pressure (solution to problem 6). Insofar as the risk of leakage is concerned, modifications to the injector needle (discussed in subsequent sections), as opposed to the configuration, are required to address the issue.

Furthermore, there exist other important advantages to the selected configuration which, though not addressing any specific problem raised earlier, help position the design as the most effective one proposed.

Configuration 3 maintains the solenoid actuation, and all the resulting benefits. This is in contrast to Configurations 4, 5, and 6, which are all non-pressure balanced designs. Injector characteristics such as flow rate, timing, etc. are no longer independent

of pressure without the solenoid actuation. Furthermore, in these configurations, the injector operates through a pressure buildup in the nozzle causing the needle to open and discharge the fuel. As previously mentioned, the rate of pressure buildup is an unknown variable, leaving doubt as to whether fast and controllable injection can be achieved. These problems further complicate the design of the driving circuit, which must now account for a greater number of variables (i.e. pressure).

Configuration 3 also maintains a significant level of simplicity in its design. Configuration 5, for example, has 2 additional valves resulting in an increased risk of leakage due valves themselves and to the additional piping, connections, etc. It is clear that the simpler design would also be the most inexpensive and adaptable design, indicating that Configuration 3 also passes the tests of cost-effectiveness and flexibility.

4.5 Summary

The preceding section was focused on the adaptation of the configuration design of the third generation of fuel injectors for use with DME fuel. In order to accomplish this, the characteristics of the fuel itself were reviewed and analyzed. The most significant factors surrounding DME are its high cetane number allowing for more reliable auto-ignition and, therefore, a shorter ignition delay; its high oxygen composition allowing for substantial reductions in NOx, PM, HC and other emissions; its low boiling point, forcing the maintenance of a high pressure environment throughout the injection process; and a substantially lower viscosity than alternate fuels, increasing the probability of leakage in the fuel delivery system.

After reviewing the characteristics displayed by DME, the adaptation of existing fuel injector configuration designs to accommodate the intended fuel source was

investigated. The analysis revealed that there were a number of fundamental problems in the design of current injectors that needed to be addressed for effective functionality with DME fuel. Among these were modifications to reduce increased needle seat wear, post injection, solenoid coil overheating, fuel vaporization in the injector nozzle, and to increase the pressure tolerance of the driving circuit. Six alternative configurations were presented and analyzed on the basis of their effectiveness in addressing the identified problems, as well as overall efficiency, simplicity, and cost effectiveness. Configuration 3 was identified as the best overall design, and it is with this configuration that the rest of the research proceeds.

CHAPTER 5
INJECTOR AND DRIVING CIRCUIT DESIGN

In the previous chapter, several different possible configurations for the injection of DME in a diesel engine were presented. It is important to reiterate that the chosen schematic was that of Configuration 3, presented in Figure 4.3.4. This chapter builds upon the configuration, transforming it into an injector design. As such, Section 5.1 will begin with an examination of the previous generation of injector, drawing attention to their design objectives and attributes. Section 5.2 will then present a technical analysis of the selected injection system design, presenting the characteristics and benefits of the solenoid integration in the common rail, and the injector's ability to reduce needle seat force. As mentioned in previous chapters, a new driving circuit was developed for this particular injection system, and Section 5.3 will finish with an analysis of the driving circuit's design and application.

5.1 Past Injector's Design

The previous generation of injectors developed at Concordia University was, as already discussed in previous chapters, the starting point for the design presented in this thesis. The design of these injectors is presented in Figure 5.1.1, which is a detailed representation of Configuration 1. These injectors, introduced in 1993, listed 5 basic objectives for their design. These included minimizing the opening and closing delays to under 1 ms, reducing the heat build-up affecting the solenoid, as well as the injector needle's bouncing, minimizing injector seat wear, and the ability of the injector to operate at a fuel pressure up to 12 MPa.

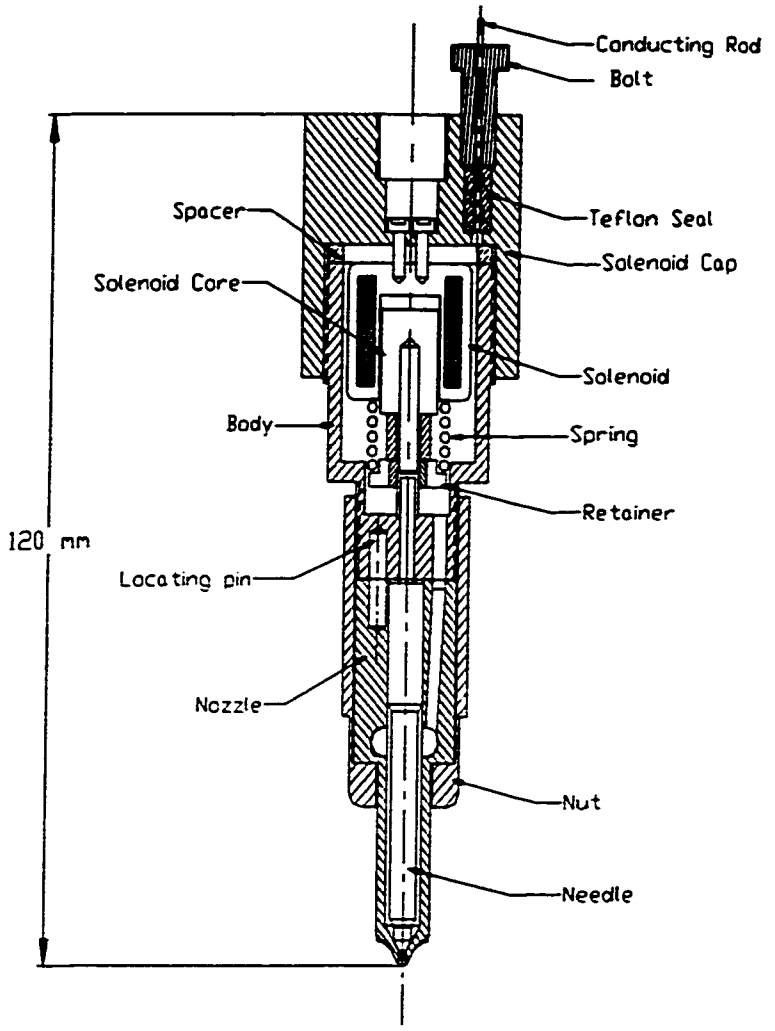

Figure 5.1.1 - Past Injector Design

The solenoid shown in Figure 5.1.1 was a high performance Lisk L7 solenoid, which was attached to the upper cap, against a copper spacer, by two small screws bolting directly into the solenoid. The solenoid's electric wires were soldered to the conducting rod and fastened with teflon seals in order to prevent fuel leakage. Under the solenoid, a large diameter spring and a special retainer were placed, so that the bottom of the solenoid

could act as a stopper for the spring. The retainer, which is connected to the needle through the sleeve, moves in tandem with the needle lift, compressing the spring. The needle had longitudinal grooves cut along its axis so that the pressure on either side of the needle are equal. The injector nozzle was remade from a Lucas CAV type BDLL150S6571 originally used for diesel engines. Fuel was supplied from the top of the injector, flowed around the solenoid on its way down to the nozzle. Upon the solenoid becoming energized, and the injector opening, fuel was discharged into the combustion chamber. The length of the entire injector was approximately 120 mm.

5.2 Current Design

The unit injector design of this thesis is illustrated in Figure 5.2.1. The detail diagrams of individual injector parts can be found in Appendix A. The total length of the new injector is 210 mm. The main cause of the large increase in length from the previous design is the presence of a lengthened elastic rod which measures 87 mm. The lengthened rod is introduced to remove the solenoid from direct contact with the combustion chamber, and reducing seat force with greater rod elasticity. Furthermore, the length of the injector prototype is larger than that of working models, in order to install various measuring devices such as pressure transducers and the LVTD for experimental purposes. Optimization of the entire system, combined with the elimination of the exaggerated dimensions of the prototype, would yield an injector size much more comparable to the previous design, and to other designs currently on the market.

The operation of each of the major components of the injector will now be examined.

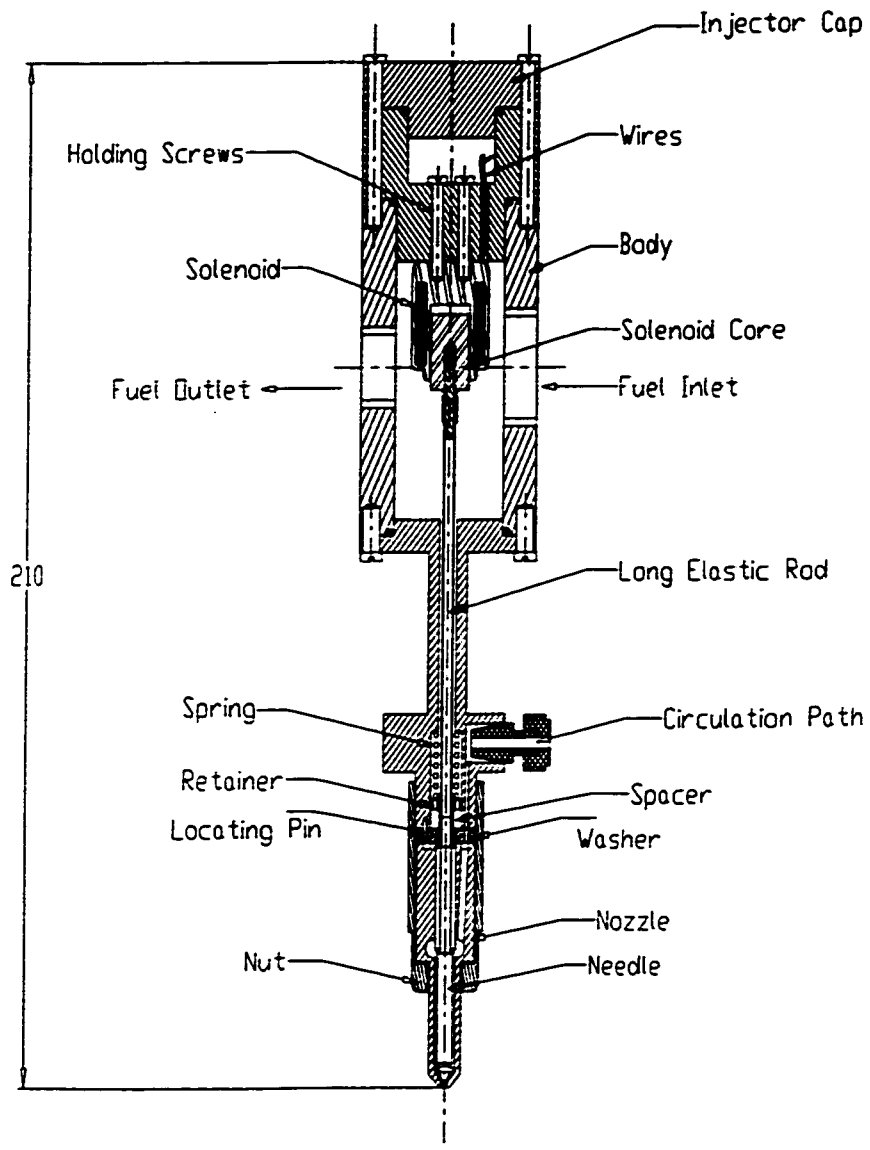

Figure 5.2.1 - Injector Design

5.2.1 Nozzle and Needle

The nozzle used is for the injector of size "S", according to the classifications given by Bosch, which has a body diameter of 9 mm and a head diameter of 17 mm. These injectors are readily available for commercial diesel engines. The nozzle needle incorporates the modification of cut grooves along the needle axis for differential pressure balance to reduce the force necessary to lift the needle for injector opening. Part of the longitudinal area are left to provide needle piloting as it moves relative to the nozzle body. The unbalanced pressure force opposing the needle to open can be further reduced by reversing the differential angle between the conical end of the needle and the nozzle seat. The effect of changing the needle cone angle from 60° 20" to 59° 40" reduces considerably the area under the nozzle that is exposed to fuel pressure. This decreased exposure results in a reduced fuel pressure force that opposes the opening of the needle. However, this same fuel pressure force aids in the lifting of the needle after the nozzle opening and can be thus harnessed to reduce the opening delay. The design presented in this thesis does not reverse the aforementioned differential angle. In order to counteract the pressure force's opposition to the needle opening, a more powerful driving circuit was devleloped, as described below. The nozzle tip is presented with in Figure 5.2.2.

Along the side of the conventional diesel nozzle, there exists a channel which is used to direct the fuel below the needle to create a pressure force that would open the injector needle. Such designs are called pressure operated injectors. However, since electronic actuation is being used, the needle's opening is being controlled with the use of a solenoid.

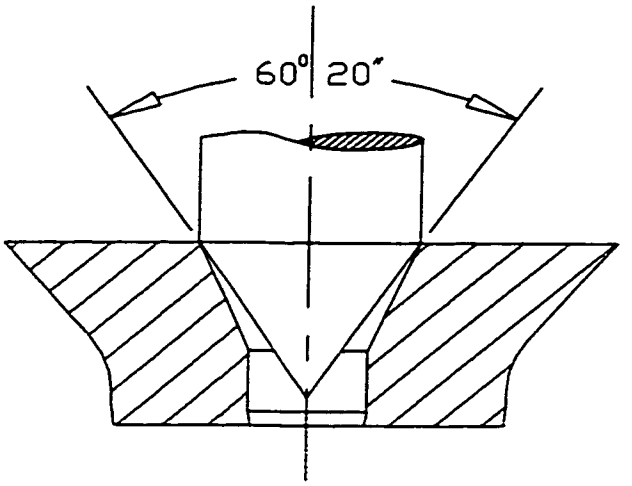

ORIGINAL NOZZLE WITH CUT TIP

Figure 5.2.2 - Needle Tip Modifications

This channel, therefore, was left unused as in previous solenoid actuated injector designs. It has already been mentioned in previous chapters, that the DME fuel in the nozzle tip maybe susceptible to boiling, due to the heat emanating from the combustion chamber. The design in this thesis makes use of this channel in order to circulate the DME in the nozzle tip through the metering valve back to the primary circuit, reducing the possibility of the fuel's boiling.

Between the top of the needle and the bottom of the nozzle holder body, there exists a 0.6 mm air gap when the injector is closed, which determines the stroke that the needle can travel. A 3 mm stiff steel washer is placed on the nozzle body, providing a stop for the needle during lifting. A locating pin has been placed in the washer, preventing its

rotation, and subsequent interference with the fuel path. The washer, which is adjacent to the nozzle on one side and the body on the other side, helps create a metal to metal sealing which prevents fuel leakage through the nut.

5.2.2 Spring, Retainer and Spacer

The spring retainer, as mentioned in the discussion regarding the previous injector's design, moves in tandem with the needle. In order to keep the nozzle closed and to overcome the gas pressure force from the combustion chamber, inherent force sealing the injector is achieved by a pre-compression of the spring during assembly. The force that the spring exerts upon the needle is called the pre-load. Between the nozzle and the retainer, a hollow tube called the spacer is placed, as shown in Figure 5.2.3. The length of the spacer determines the spring pre-load. The amount of pre-load should be greater than the force from the combustion chamber, which has been calculated as 20 N, to provide a force on the needle to seal the injector.

However, since the fuel pressure inside the injector has 20 MPa pressure, as compared with a maximum 4 MPa pressure in the combustion chamber, the pre-load could be considered as unnecessary in order to keep the injector closed. It becomes useful, however, since its force is an aiding factor in the injector needle's closing process; the combination of the spring pre-load and spring force increase caused by the needle-lift generated compression, help to achieve a fast closing of the injector.

Given a spacer length of 8 mm which compresses the spring by 1 mm, a spring stiffness constant of 20 N/mm, and the pre-load force of the injector as 20 N, result in a total downward spring force of 32 N.

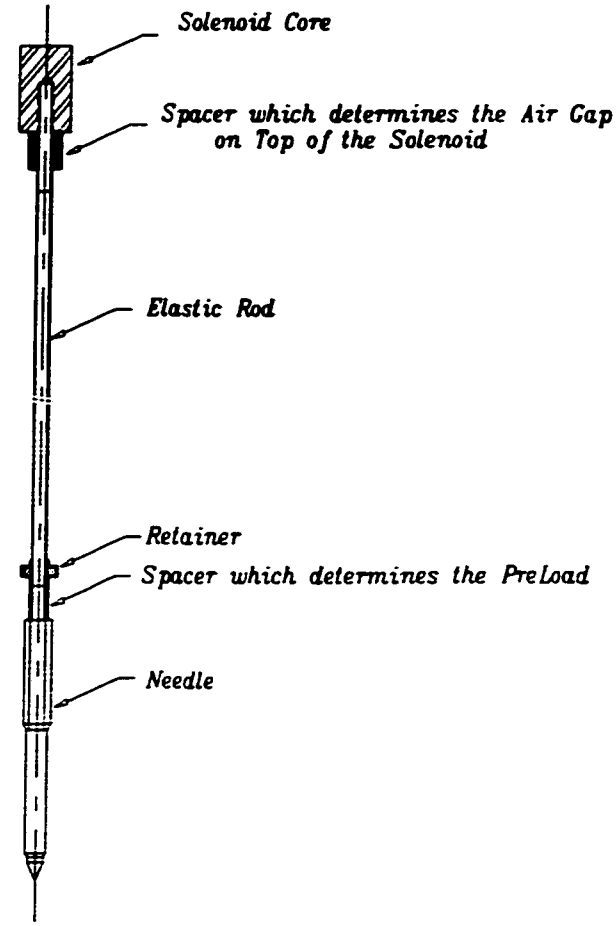

Figure 5.2.3 - Needle Assembly

5.2.3 Elastic Rod

One of the most important aspects of the injector design is the use of a long elastic rod. This hollow tube rod, 87 mm in length, attaches the solenoid core to the injector needle and, through it, the solenoid is allowed to exert its pulling force to lift open the needle. The rod has an outside diameter of 3.25 mm and an inside diameter of 2.75 mm, which indicates a total wall thickness of 0.25 mm. The stainless steel rod has a stiffness of 5308.21 N/mm, the calculation for which is presented in the following section. The first

consequence of using such a long rod is that the solenoid is at a considerable distance from the combustion chamber. As mentioned in previous chapters, the solenoid's proximity to the heat emanating from the combustion chamber can hamper its ability to provide force. Furthermore, the elastic rod reduces the spring-induced bouncing of the needle thus reducing fuel post-injection and needle seat wear. These issues were addressed in the previous chapter.

5.2.4 Solenoid

Attached to the elastic rod is the solenoid core. A Lisk L7 short body solenoid has been used, with 150 W power. Figure 5.2.4 gives a cross-section illustration of the solenoid.

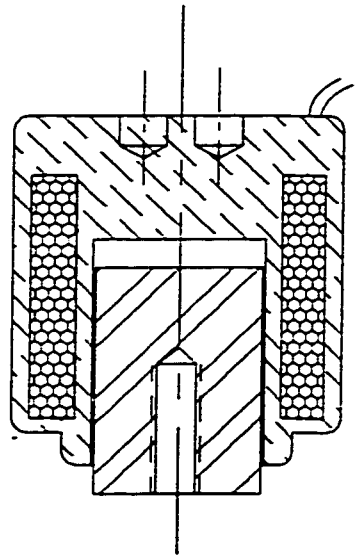

Figure 5.2.4 - Solenoid Cross Section

When energized, the electromagnetic force created by the solenoid pulls the elastic rod, attached to the injector needle, opening the nozzle. The total movement expected from the solenoid is 0.6 mm. This is the stroke of the solenoid which has an inverse relationship to its force; that is to say, the shorter the stroke, the higher the force. The force of the Lisk L7, given a 0.6 mm stroke and a 10% duty cycle is approximately 120 N [42]. In order to open the injector, a high force is required to overcome initial resistant forces and to quickly accelerate the needle assembly. Once open, a lower force is needed to maintain the nozzle opening, implying that the duty cycle, on average, will be approximately 4%. The consequence is that more current can be applied to the solenoid, without causing coil overheating. Given these design attributes, the total force of the solenoid can be much higher than the conventional 120 N, by applying a higher voltage. As such, the extra force that is provided by the extra current made possible by the shorter duty cycle, guarantees a shorter opening delay. This issue will be further explored at the end of this section, in the discussion of the driving circuit.

The solenoid body, as in the previous design, is mounted unto the solenoid housing with the use of two small screws, and is immersed in fuel. This constant flow of fuel around the solenoid serves as a coolant, further enhancing its performance. To prevent fuel leakage through the screws and the hole provided for the wires, a cap has been mounted with an O-ring above the solenoid housing. The wires are no longer soldered to a conducting rod, but rather, are passed through the plastic teflon sealing directly. Figure5.2.5 illustrates the electronic wire path of the solenoid.

On the extension connecting the solenoid core to the elastic rod, a spacer has been placed. Varying the spacer's length allows for an adjustment of the air gap existing with respect to the core's initial position relative to the solenoid pole end. The greater the air gap, the lower the force generated by the solenoid. When the solenoid is not energized, a minimum air gap of 0.6mm is required in order to allow for the ensuing needle lift. This injector has an air gap of 0.7 mm. The extra 0.1 mm is provided so that the core will not touch the solenoid pole so as to disallow the effect of residual magnetism which tends to

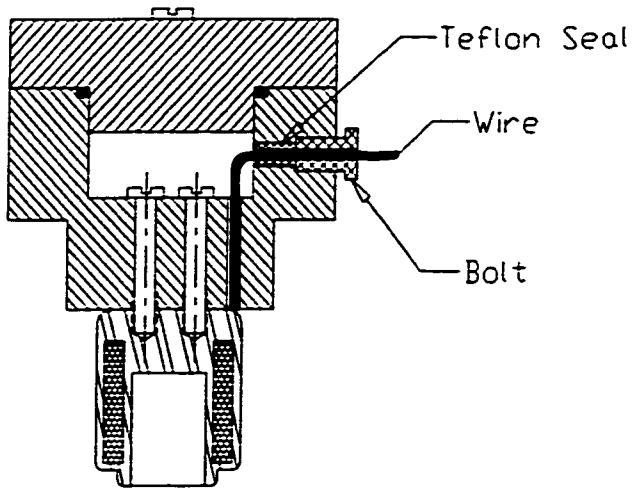

Figure 5.2.5 - Solenoid Assembly With Wires' Path To Driving Circuit

increase the injector needle closing time.

5.2.5 Common Rail

Two fundamentally different designs for the common rail system were investigated. The first, shown in Figure 5.2.6, has a square, steel tube as a common rail linking the two

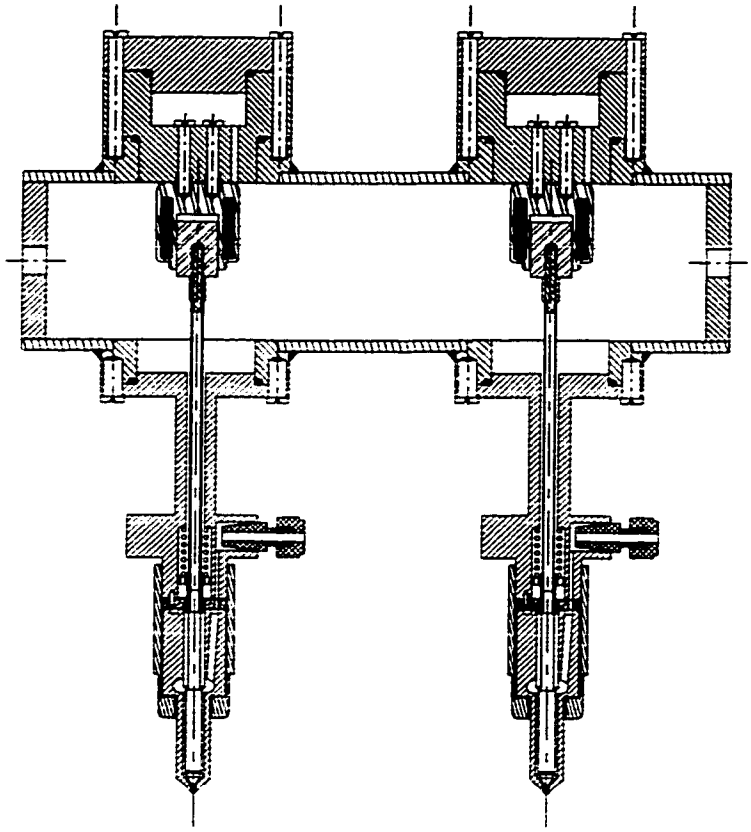

Figure 5.2.6 - Original Common Rail System Design

injectors of the engine. The square shape of the tube facilitates the installation and insulation of the solenoids inside the common rail. The fuel delivered from the secondary circuit through an intake valve fills the common rail, acting as a coolant for the solenoids, and is recycled to the primary circuit through an exit valve. In order to withstand the stress caused by the fuel's 20 MPa pressure, a steel tube has to have a thickness of at least 3 mm (see Appendix B for calculations). In fact, during original testing, the common rail

with this thickness (which incorporates a safety factor of 3) was warped under the stress caused by the fuel pressure. The tube's inability to cope with the stress is caused by the necessary modifications (hole drilling, welding, etc.) that were undertaken in order to adapt it for the installation of the solenoid units. The substantial thickness required for the tube, combined with the necessary length for a four cylinder engine results in a considerable addition to the weight of the vehicle. Alternative metals to steel would obviously require much larger thicknesses or would be accompanied by sizable cost burdens. Furthermore, even with today's advanced technology, an engine is still subjected to a fair amount of vibration during its operation. The inflexibility of this common rail system, brought about mainly by its steel construction, complicates its alignment and installation. Since each injector is imbedded in the common rail, should one injector fail during the course of its life, repairs would require the removal of the entire system as opposed to just the problematic injector. For the above reasons, the common rail design presented in Figure 5.2.6 was not used in this fuel injection system. The alternative design, shown in Figure 5.2.7, addresses these concerns. The injection system links unit injectors through the use of a high-pressure, hydraulic tube. This tube's ability to withstand the stress of high pressures allows the injection system to be constructed within reasonable weight limits. The common rail's flexibility allows it to adapt to the engine vibrations, facilitating both the installation and insulation of the injection system. The flexibility of the tube also makes the entire system suitable for the multiple engine size variations that currently exist, making its standardization a relatively simpler task. Among problems facing the first design was the issue of repair difficulties should the need arise. Since, in the second design, unit injectors are not imbedded into the common rail,

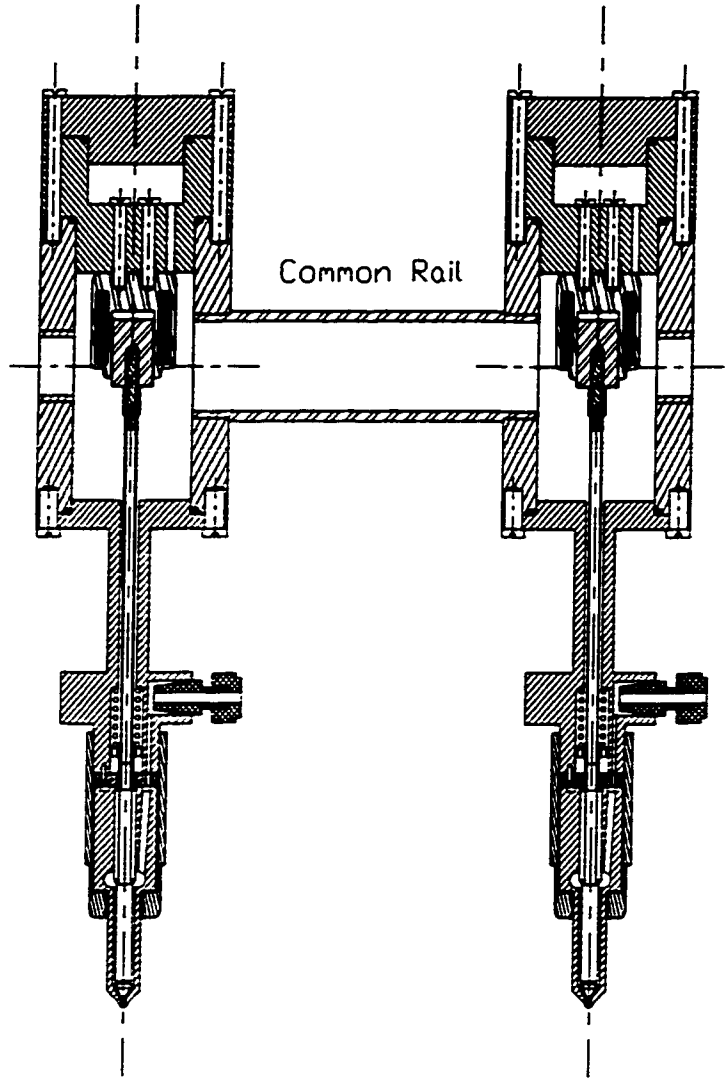

Figure 5.2.7 - Revised Common Rail System Design

facilitated repairs can be affected by simply disconnecting problematic units from the overall system.

Finally, as can be seen in Figure 5.2.7, the solenoids are still placed within a constant flow of fuel providing the necessary cooling. It is this common rail which was incorporated into the overall injection design.

5.3 Driving Circuit: Design and Application

The injection electronic control system presented in the block diagram in Figure 5.3.1, is made of four different sections: micro-controller, charge pump, 80V feedback signal conditioning and injector power switch. The micro-controller is commanding the injectors opening and closing time via the CHA2. It also controls the charge pump output voltage, which is desired to be 80 VDC. The signal feedback conditioning section makes

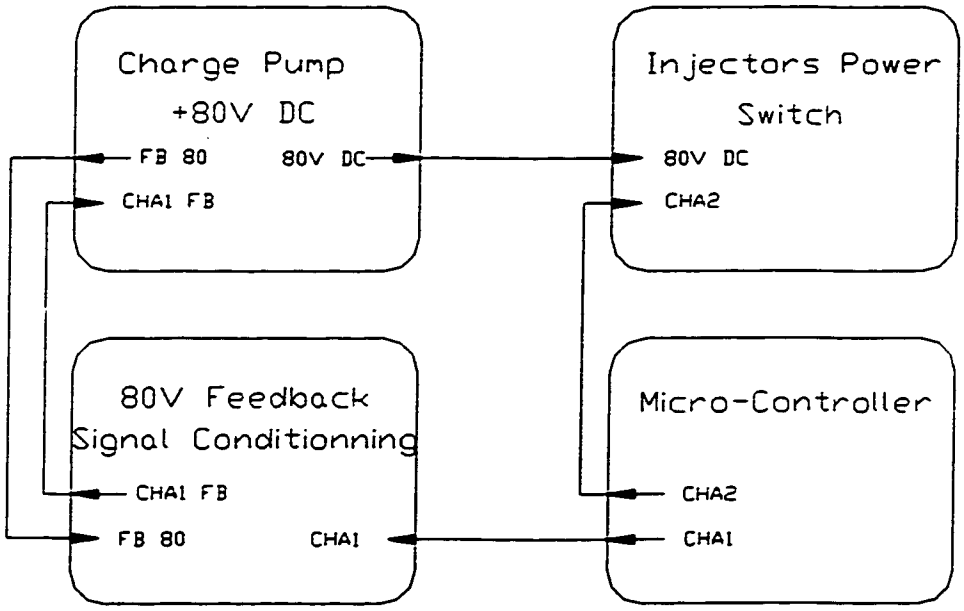

Figure 5.3.1

Block Diagram of the Solenoid Driving Circuit

sure that the charge pump maintains a constant output voltage level to provide enough electrical energy to the power switch. The injector power switch (MOSFET) varies the duty-cycle through the solenoid core which moves the injector needle and allows the DME to be injected inside the combustion chamber of the internal combustion engine.

5.3.1. Charge Pump

The charge pump circuit (Figure 5.3.2) is built according to the fly-back converter principle [43] to be able to supply the sufficient voltage to the power switch. By switching a MOSFET (Q1) the energy in the transformer is transferred to capacitor C1. The frequency and duty cycle for switching Q1 to obtain the 80 VDC has been determined

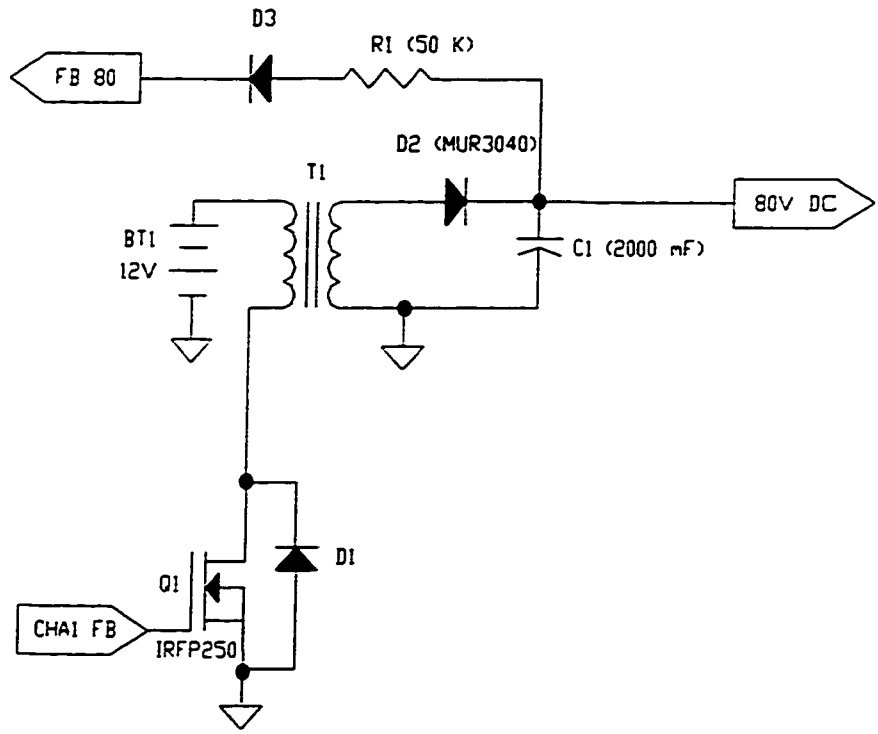

Figure 5.3.2 - Charge Pump Schematic

experimentally. The 80 VDC is needed to obtain sufficient power in order to open the injector. The capacitor C1 acts as a temporary storage element so the injector power

switch is always fed with the proper voltage when a large amount of current is required to open the injector. The diode D2 rectifies the spike of current, coming from the transformer, feeding C1 with high positive voltage (spike of 150V).

5.3.2 Feedback Signal Conditioning

The purpose of the feedback signal conditioning circuit (Figure 5.3.3) is to limit the output voltage of the charge pump at 80 VDC. Higher voltage may damage the injector solenoid or the MOSFET power switch. The output voltage of the charge pump is monitored and compared with a reference voltage that can be varied by resistor R5. A comparator circuit is added to control the charge pump (on/off). If the voltage is lower

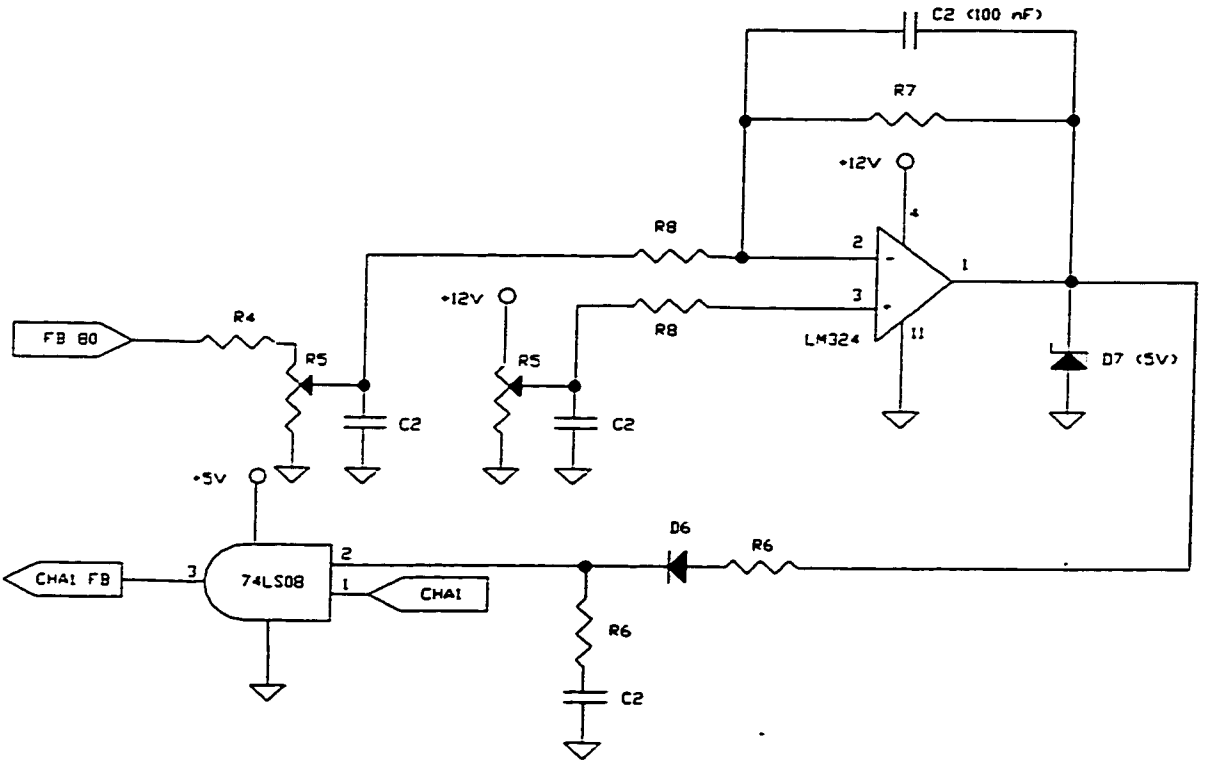

Figure 5.3.3 - 80 VDC Feedback Signal Conditioning

than the required value, the charge pump turns on and if the voltage is higher than the required value, it turns off. In the case that the feedback indicates a low voltage, the output of the comparator becomes positive. A zener diode (D7) drops the voltage to approximately 5 V to supply a desirable voltage level to the AND-gate (74LS08). When the charge pump control signal CHA1 from the micro-controller is activated, in other words, when the micro-controller sends a signal (frequency and duty cycle), the AND-gate output follows the micro-controller signal if the feedback conditioning circuit has detected that the voltage is lower than 80 VDC. And if the voltage is higher than 80 VDC, the And-gate stops the charge pump. A small capacitor C2 is added to avoid high oscillation of the comparator.

5.3.3 The injector power switch

The injector power switch circuit (Figure 5.3.4) is interfacing the control elements (micro-controller) which are operated at low voltage (+12VDC) and the high voltage components (MOSFET) that are used to drive the injector solenoid. A constant voltage of 80 VDC is applied to one end of the solenoid. The MOSFET (IRFP250) is used as a power switch to bring the other end of the solenoid to ground. This closes the circuit loop and activates the magnetic field in the solenoid core. Diodes D4 and D5 are freewheel diodes, which are connected across the injector solenoid and the power MOSFET to protect the MOSFET from the surge of current when the injector switches close. In addition, the freewheel diode D4 helps the injector to close faster. As safety, an opto-coupler (not shown) is used to isolate the micro-controller signal (CHA2) from the high voltage supplied to the injector solenoid. Many protection circuits can be added to prevent any damages to the

MOSFET or the injector solenoid. Over power dissipation, over current and short circuit protections are some examples.

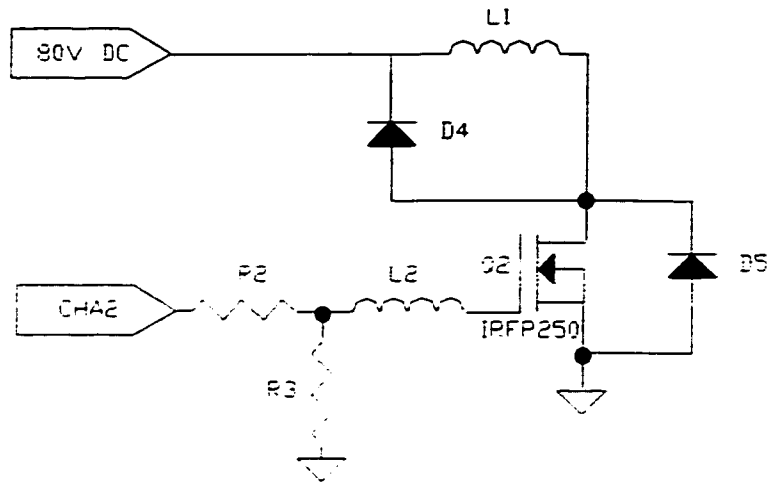

Figure 5.3.4 - Power Switch

5.3.4 Micro-Controller (PIC 16C74)

A micro-controller from Microchip (PIC 16C74) using an internal clock of 20 MHz is managing the electronic injection system. A pulse width modulator (PWM) configuration is used to reduce power consumption and temperature of the injector solenoid. A complete injection cycle for one injector consists of three different parts. First, the output of the PWM is controlling the opening spike to initiate the solenoid core to move. Second, a PWM square wave form with a duty cycle of 20% is then sent to maintain (steady state) the solenoid active for a determined amount of time. Third, at the end of the opening cycle, a signal is sent to the injectors power switches to turn off the

magnetic field of the solenoid core. The micro-controller falls on standby mode until a new cycle is demanded. The timing process determines the exact time when to begin the injection cycle. The timing signal comes from an external source such as a computer, programmable logic controller (PLC) or camshaft sensors. The injection cycle of the injector is determined by the physical variables that follow the behavior of the internal combustion engine (temperature, revolution per minute (RPM), airflow mass sensor and acceleration pedal level).

CHAPTER 6

MODELING AND SIMULATION

A mathematical model describing the injector's performance and characteristics, is needed to be built for computer simulation. This model includes both the mechanical and electrical components of the injection system. The model of the injector needle and the solenoid core, dynamic by design, is considered to be a mass-spring-damper model of the injector needle assembly. It was simulated in a C language program using the fourth order Runge-Kutta integration method for solving differential equations. The model and simulation results are presented in this section, while the injector's laboratory tests and corresponding results are presented in the next Chapter. Chapter 7 will also compare the simulation and test results, validating the model developed in this section, and giving further simulation results conducted after model validation.

6.1 Mathematical Model of the Injector and Driving Circuit

Figure 6.1.1 illustrates the lumped mass-spring-damper model of the injector

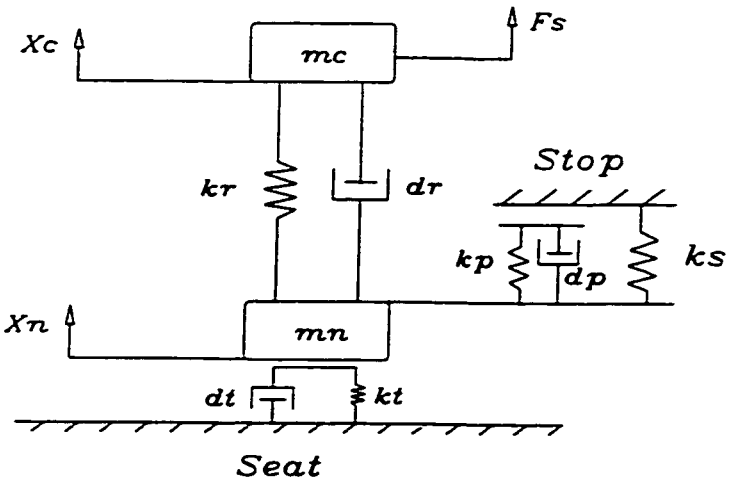

Figure 6.1.1 - Mathematical Model of the Elastic Rod

needle assembly. The mass m_n of the injector needle is connected to the solenoid core of mass m_c via a long hollow elastic rod which is modelled with a spring stiffness k_r and material damping d_r. The rod spring rate can be determined from geometry and material properties, which is given by:

$$k_r = \frac{\pi E (d_o^2 - d_i^2)}{4 l} \tag{6.1}$$

where d_o and d_i are respectively the outside and inside diameters of the hollow metal rod, l is the rod length, and E is the modulus of elasticity of the rod material. For a solid rod, the inner diameter d_i is omitted from Equation (6.1).

When the needle closes the injector upon its seat, the needle-to-seat interface is modelled with a spring stiffness k_t and material damping d_t. Similarly, when the injector needle is fully opened which is limited by the physical stop, the needle-to-stop interface is represented by a spring k_p and damper d_p. k_s represents the stiffness of the injector return spring, and K_{PR} is the spring preload. F_S is the electromagnetic pulling force created by the energized solenoid. x_n and x_c represent respectively the needle and core displacements, which are taken as positive in the upward direction.

The dynamics of the solenoid core and injector needle are mathematically modelled, respectively, by the following equations:

$$m_c \ddot{x}_c + d_r \mid \dot{x}_c - \dot{x}_n \mid sgn (\dot{x}_c) + k_r (x_c - x_n) + f d_c = F_S + m_c g \tag{6.2}$$

$$m_n \ddot{x}_n + d_r \mid \dot{x}_n - \dot{x}_c \mid sgn (\dot{x}_n) + k_r (x_n - x_c) + k_s x_n + K_{PR} + F_P + f d_n = F_R + m_n g \tag{6.3}$$

and, the needle reaction force F_R with the seat or stopper depends on the following conditions:

$$\begin{aligned} F_R &= 0 && \text{for } 0 < x_n < H_{MAX} \\ F_R &= -k_t x_n - d_t \dot{x}_n && \text{for } x_n \le 0 \\ F_R &= -k_p (x_n - H_{MAX}) - d_p \dot{x}_n && \text{for } x_n \ge H_{MAX} \end{aligned} \tag{6.4}$$

With reference to Equations (6.2) and (6.3), the second term on the left hand side of both equations represents the material damping force of the long connecting rod between the solenoid core and needle masses. This damping term is considered to be always dissipative in the direction of mass motion, as indicated by the sign (*sgn*) of the velocity components.

With reference to the needle reaction force conditions, when the needle displacement is $x_n \le 0$, which represents the needle hitting the seat, the seat has a reaction spring force that pushes the needle upwards. When the needle hits its upper stop, for $x_n \ge H_{MAX}$, where H_{MAX} represents the maximum needle lift, the stop reacts with a spring force by pushing the needle downwards. The material damping forces due to the seat or stop are always dissipative.

F_P is the fuel pressure force acting on the injector needle and resulting from the pressure drop across the injector nozzle orifice, and it is approximated by [18]:

$$F_P = A_m(P - P_e) \tag{6.5}$$

where the differential pressure $P - P_e$ acts on the effective needle area which is a function of the needle lift x_n, given by:

$$A_m = \pi \bullet \left(\frac{d}{2} - x_n \bullet \sin\theta \bullet \cos\theta\right)^2 \tag{6.6}$$

P is the pressure inside the injector above the effective area, and P_e is the pressure below this area. d is the seat diameter of the nozzle orifice and θ is the angle of the needle conical tip.

fd_n and fd_c are respectively, the viscous damping forces due to the needle and core motion relative to the fluid viscosity inside the injector. These forces are assumed negligible for gaseous fuels and low viscosity DME. This assumption is further justified by the fact of the large clearance between the core and solenoid housing, and by the longitudinal grooves cut along the axis of the needle which provides a large clearance with the walls of the needle holder.

The electromagnetic force of the core attraction created by the solenoid is determined from the stored magnetic energy [44] $W(\varphi,h)_{mag}$:

$$F_s = - \frac{\partial W(\phi, h)_{mag}}{\partial h} = - \frac{\phi^2}{2 A_l \mu_0} \tag{6.7}$$

where $h = G_{MAX} - x_c$ represents the air-gap between the solenoid magnetic pole and moving core, and G_{MAX} is the maximum air-gap. The negative sign in Equation (6.7) indicates that the force is directed towards the magnetic pole, and it tends to reduce the air-gap reluctance. Thus, the solenoid force increases as the magnetic flux φ increases due to smaller air-gaps and increase of coil current. A_l is the pole end effective area, and μ_o is the permeability of free space.

6.2 Simulation and Results

In order to study the motion and seat force dynamics of the injector system, the mathematical model of the needle assembly was computer simulated. The model was incorporated into an existing program that simulated the dynamic model of the solenoid to generate the electromagnetic force to pull open the injector needle [45]. Certain assumptions regarding initial test conditions and parameters needed for the simulation are as follows.

Parameter Estimations and Assumptions

1) The ambient temperature in the laboratory setting was assumed to be 300 K. Since the model validation would be performed vis-a-vis the results in an experimental setting, the 300 K assumed temperature was deemed to be appropriate for the purposes of validation, even though actual engine temperatures can reach approximately 800 K. The injectors were tested for only one opening cycle and then were rested to ensure that it remained at room temperature for the next test.
2) The pressure inside the common rail and unit injectors was assumed constant at 20 MPa. This is justified by the fact that in the actual engine implementation of the fuel delivery system, the common rail will be supported with an accumulator to eliminate pressure fluctuation. The ambient pressure was assumed to be 0.101 MPa. This assumption was deemed appropriate for the purposes of validation with respect to test results obtained in the laboratory environment.
3) For the results regarding seat force as a function of needle movement, the simulation was run without considering the fuel flow and its related effects. This was done since seat force measurement (discussed in the next chapter) was not possible in a fuel

present environment. For validation purposes, the simulation setting was set to mirror the laboratory environment.

4) The engine speed was assumed to be 2000 rpm, the nominal speed of a four stroke engine. Injection timing is, in part, dependent on the engine speed. The time corresponding to one engine cycle is calculated as:

$$(60\ s) \times (2\ rev.) / (2000\ rpm) = 0.060\ s\ or\ 60\ ms$$

The above 60 ms is the duration between each injection. Individual injections is assumed to occur within 60° around top dead center of crankshaft revolution. Therefore, the corresponding injection time is calculated as:

$$injection\ time = 60° / 720° \times 60\ ms = 5\ ms$$

5) Equation (6.2) and Equation (6.3) have mass variables for the solenoid core and the injector needle. However, there are other positive mass injector components other than the core and needle, such as the rod, spring, retainer, etc. Their combined mass was divided on a 50-50 basis between the core mass and the needle mass for the purposes of the lumped mass model.

6) The material damping for the three different rods were assumed to be the same. This was for the purpose of simplifying comparison of the results.

7) Approximate values for the spring and material damping coefficients of the seat, k_t and d_t, and stop, k_p and d_p, in equation (6.4) can be estimated by observing and matching the oscilloscope traces of the needle displacement (see Appendix C for values).

The simulation was performed with the above assumptions and given the voltage source of 80 V, a pre-load of 20 N and, a spring constant of 20 kN/m. The predicted

results with respect to the model variables presented in Equation (6.2) and Equation (6.3) are presented in the following.

Figure 6.2.1 shows the injector needle motion and solenoid force variations, as well as the current profile across time for a needle-core assembly using a hollow steel connecting rod. At time zero, the solenoid force starts increasing as a result of the boosted current passing through the solenoid from the driving circuit. The injector does not begin to open until the solenoid force reaches above 80 N, which occurs at approximately 0.2 ms. Before this time, the solenoid force is insufficient to counteract the pre-load, gravity and fuel pressure forces acting downward on the needle. There is a delay of approximately 0.5 ms between the peaks in the force and current, with the former lagging behind the latter. Although the boost current reaches a maximum of about 85 A and then removed, the solenoid force continues to increase because force increases for smaller air-gaps. This is because once the needle-rod-core assembly starts to accelerate upwards, the assembly will continue to accelerate because of its inertia, and thus the air-gap still reduces with less needed current. The solenoid force is seen to increase to a maximum of 155 N, at full injector needle opening, and takes about 1.5 ms to fully open. A decrease in the spring stiffness would reduce this delay, although it would increase the closing delay. By increasing the spring stiffness and reducing the pre-compression, an optimal pre-load and spring stiffness can be achieved, optimizing both opening and closing delays.

It can further be observed in Figure 6.2.1 that there is a substantial change in the slope of the solenoid force after 80 N when the needle velocity starts to increase rapidly. This is because of the magnetizing current that is creating the solenoid force decreases due

to the back emf which is a function of needle velocity [45][46]. As can be seen, once the needle hits the upper stop, it bounces off the stop, and when it hits the needle seat, it bounces off the seat as well. The result of this bouncing at the upper stop changes the air-gap and causes the force to fluctuate. The final point of interest regarding Figure 6.2.1 is that the total time of injection, from the beginning of the needle lift until it closes, is approximately the previously calculated 6 ms.

The current profile is also presented in Figure 6.2.1. This graph depicts the simulated results on the driving circuit design. Approximately 85 A of current is transmitted to the solenoid in the first millisecond of operation. It is this boosted current that provides the necessary solenoid force to start the injector needle to accelerate towards its fully open position. Once the needle is fully lifted, less current is required to keep the injector needle open. This is achieved by controlling the average current through the coil, resulting from the voltage pulse width modulation (PWM), as can be seen by the short pulses of current applied. There are additional force oscillations which are due to the profile of the current pulses. The initial bouncing of the needle off the stop, occurring simultaneously with a decrease in current transmission, causes a abrupt decrease in solenoid force. Here, the air-gap increases sharply as the needle is bouncing off the stop, once again causing an increase in the gap reluctance.

The comparison between needle and solenoid core movement versus time is presented in Figure 6.2.2. The difference that can be witnessed between needle and core displacement results from the extension and compression of the elastic rod. The rod absorbs a portion of the energy to be transferred from the core to the needle, and vice-

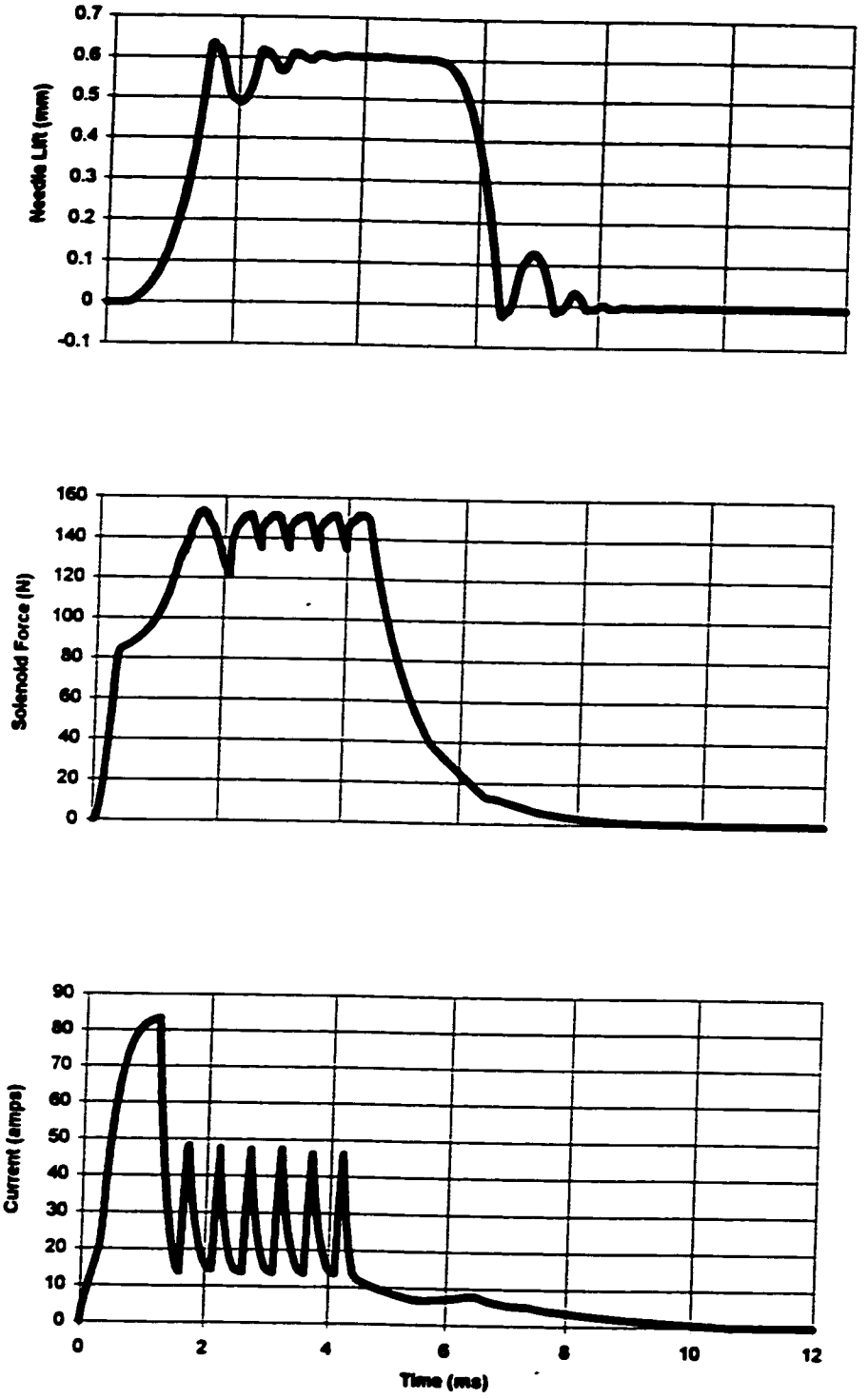

Figure 6.2.1
Needle Movement,Solenoid Force and Current profile over time [Hollow Steel Rod]

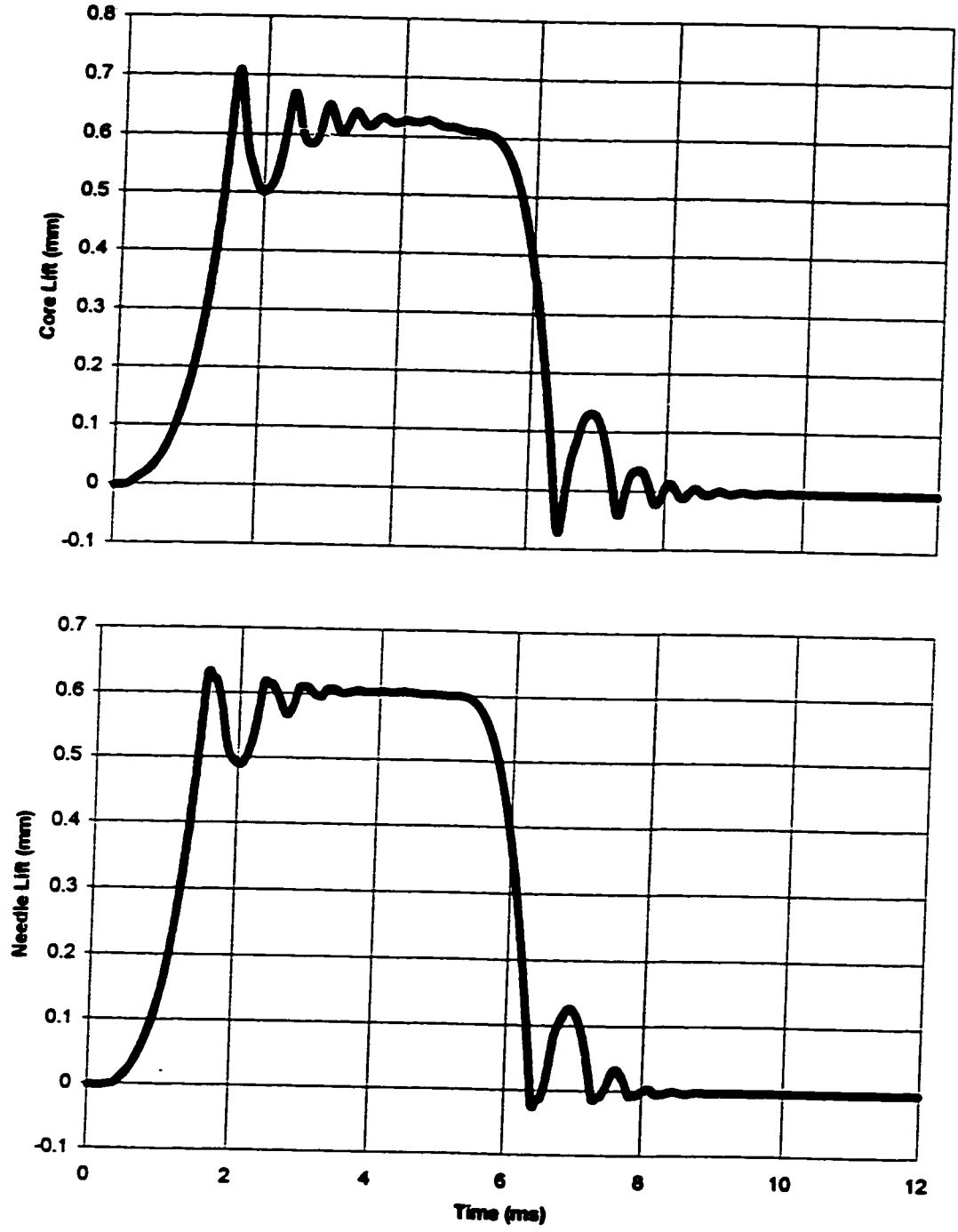

Figure 6.2.2
Needle Lift and Core Movement [Hollow Steel Rod]

versa, so that the needle's bouncing is reduced. A perfectly stiff rod would result in a perfect correlation between the displacement of both the needle and core and would result in more bouncing with higher amplitude. As can be seen, the core lift reaches over 0.7 mm, a full 0.1 mm more than the required lift height. The air gap between the core and the solenoid pole end, which persists even after the injector is fully open, allows the core to displace by more than the 0.6 mm maximum needle lift. The mass concentration in the solenoid core allows for a greater force pull on the injector needle, increasing its extension.

Figures 6.2.3 - 6.2.5 show the core bouncing and seat force as a function of core movement over time for three different injector rods. Figure 6.2.3 is derived using a hollow stainless steel tube with stiffness of 5.3 kN/mm, Figure 6.2.4 shows the effects using a solid stainless steel rod with stiffness 17.5 kN/mm, and Figure 6.2.5 gives the results with a hollow aluminum rod with stiffness 1.8 kN/mm. Keeping the material constant, one can observe the effects of a hollow rod by comparing the results of the first two graphs.

When the needle is pulled up by the solenoid, it accelerates and hits the upper stop, transferring all its inertia force to the stop, which causes the needle to bounce back down, where the solenoid force pulls it back up. This process repeats itself, causing a bouncing effect on the upper stop. Once the solenoid is de-energized, the spring pushes the rod down; the latter accelerates and finally hits the needle seat. Due to the impact, the seat shows first an elastic deformation which then causes the needle to bounce upwards, compressing the spring again, perpetuating the process, and beginning a high frequency

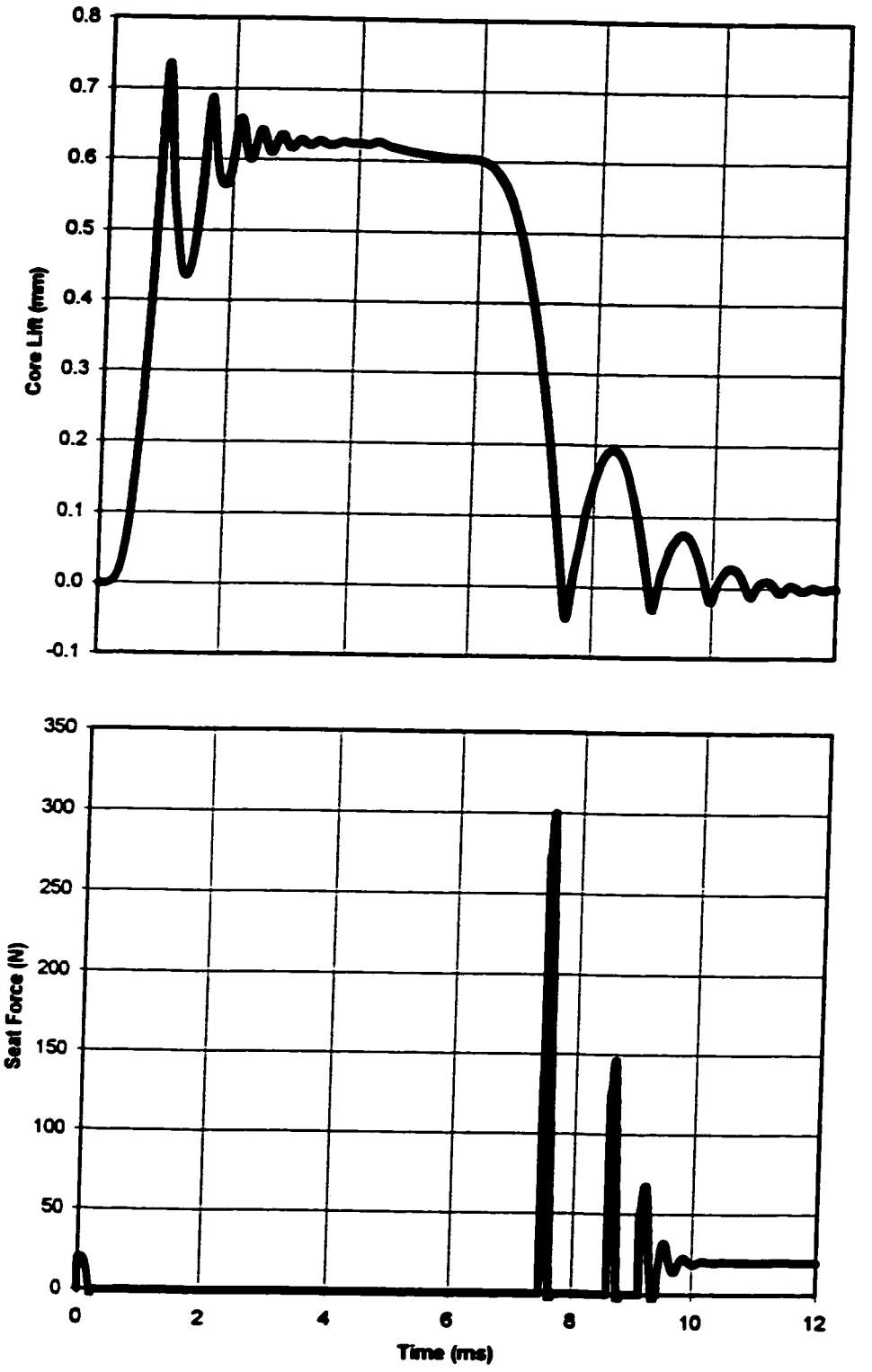

Figure 6.2.3
Core Movement and Seat Force of a Hollow Steel Rod

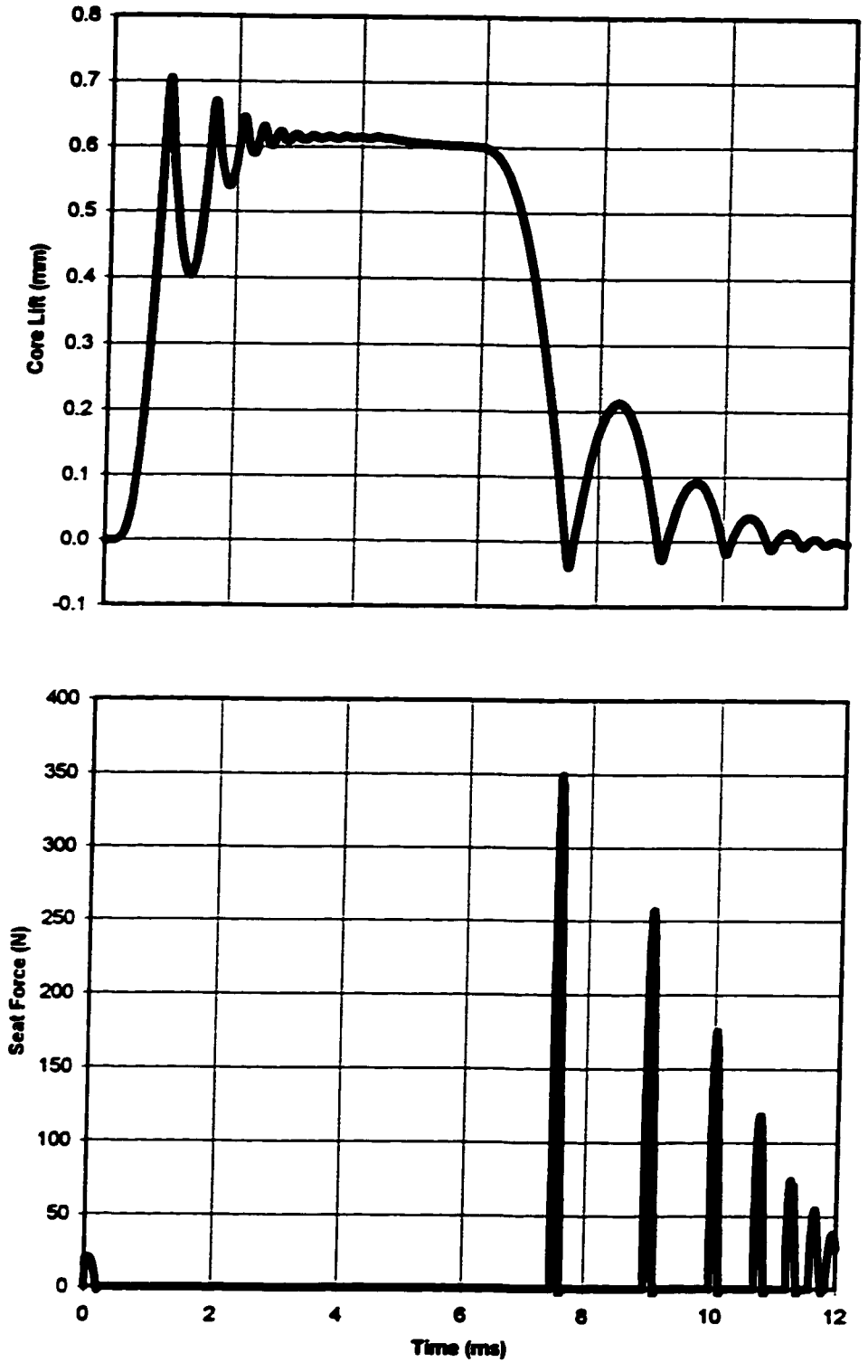

Figure 6.2.4
Core Movement and Seat Force of a Solid Steel Rod

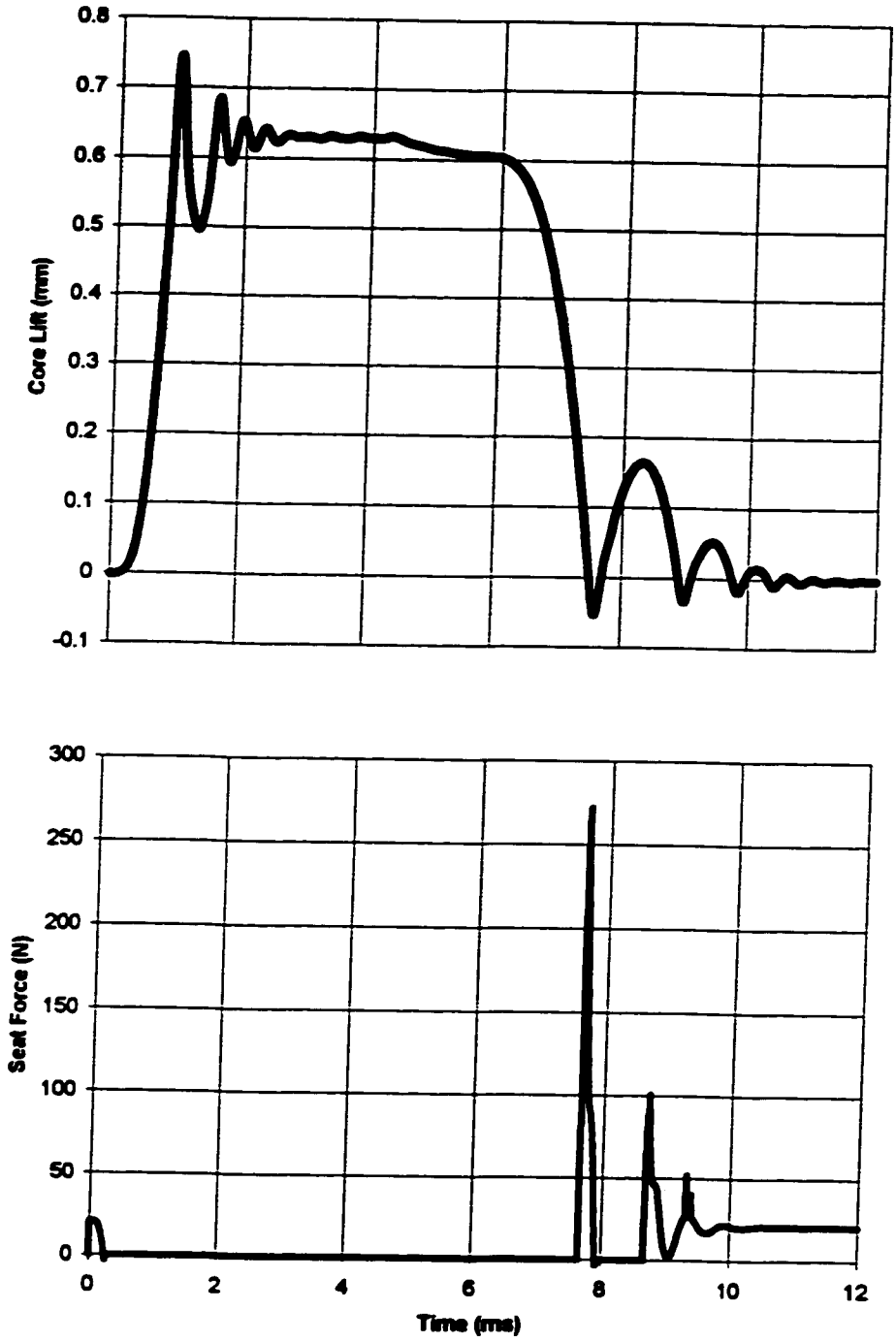

Figure 6.2.5
Core Movement and Seat Force of a Hollow Aluminum Rod

hollow tube also has less bouncing on the needle seat, where the transfer of inertia energy from the core to the needle is dampened. Here the effect can be measured in terms of the needle seat force, which is 350 N using the steel rod, as compared to 300 N with the hollow tube for the original impact alone. Given that this occurs every 60 ms the engine is running, the use of a hollow tube can significantly reduce the wear on the needle seat. Furthermore, the bouncing effect on the seat results in post-injection with the resultant excess pollution. For the solid steel rod the amplitude of seat bouncing is higher and would result in more fuel post-injection.

Keeping the hollow characteristic constant, while changing the material, one can compare Figure 6.2.3 and Figure 6.2.5 to observe the respective influence of steel and aluminum tubes. The aluminum tube has less bouncing on both the stop and seat. The original impact force on the latter is reduced to 270 N from the 300 N caused by the hollow steel tube. Again, the driving factor is the comparative elasticities, where steel, as a material, is significantly stiffer than aluminum. Combining these results with the previous discussion, one can conclude that the use of a hollow aluminum rod is most effective in reducing needle seat wear and post-injection. However, given that steel is a substantially more durable material than aluminum, the benefits with regards to reducing the needle bouncing must be weighed against other considerations, before actually incorporating an aluminum rod in an injector design.

It is important to note that the rod length in the above simulations was held constant. The main conclusion that can be drawn from the above analysis is that the important factor in determining the dampening effect is the stiffness of the rod. A less stiff rod allows more relative motion between the core and needle masses, which then can be

absorbed by the material damping. Thus, the transfer of inertia forces between the two masses are reduced which results in less bouncing and impact forces at the needle-seat interface and at the core-stop interface. Since rod stiffness is inversely proportional to its length, longer rods, other things equal, have a greater dampening effect with a correspondingly lower amount of seat wear and post-injection. As mentioned in the previous section, the design of the injector in this thesis includes a lengthened rod, for the very reason of its increased elasticity.

The purpose of the simulation is to allow a validation of the mathematical model based upon the test results. The simulation variables were set to mimic laboratory conditions, in order to facilitate and justify comparison between the two sets of results. The next section will present the actual experimental work performed on the injector, along with the corresponding results, while comparing those results to the ones presented in this section, aiming to provide a validation of the model.

CHAPTER 7

TESTING AND VALIDATION

In the previous chapter, a mathematical model of the injector design was presented and simulations were performed. In order to validate the model, the injector was tested in a laboratory setting, where the results can be cross-referenced to those obtained in the simulation. If the two sets of results are consistent with each other, the model can be considered validated, allowing for the viability of changes to the proposed design to be gauged in the computer simulation. The laboratory test results also provide an understanding of the injector design's performance within a real automobile engine. Section 7.1 will present a detailed account of the testing performed on the injector, including the experimental setup. Section 7.2 presents the obtained results, comparing them to those obtained in the simulation, and provide commentary of the validity of the mathematical model found therein. Section 7.3 will conclude by revisiting the simulation, and analyze its predictions with regards to varied experimental conditions, given the validation found in Section 7.2.

7.1 Setup and Testing

The main equipment used in the testing process were a Linear Variable Differential Transformer (LVDT), and piezo electric force cell. The former is used to measure core movement, through the use of an iron core attached to a nonmagnetic rod affixed to the solenoid core. When the core is displaced, the nonmagnetic rod moves into the magnetic field above the solenoid core. As the rod enters, the iron core distorts the magnetic field, creating a signal that is captured by the amplifier. The amplifier transfers the signal to an oscilloscope which graphs the core movement. In order to attach the rod to the solenoid

core, a 1 mm hole was drilled through the injector cap and the solenoid core was tapped. The rod was passed through the hole and was threaded to the core. Figure 7.1.1 illustrates the LVDT setup.

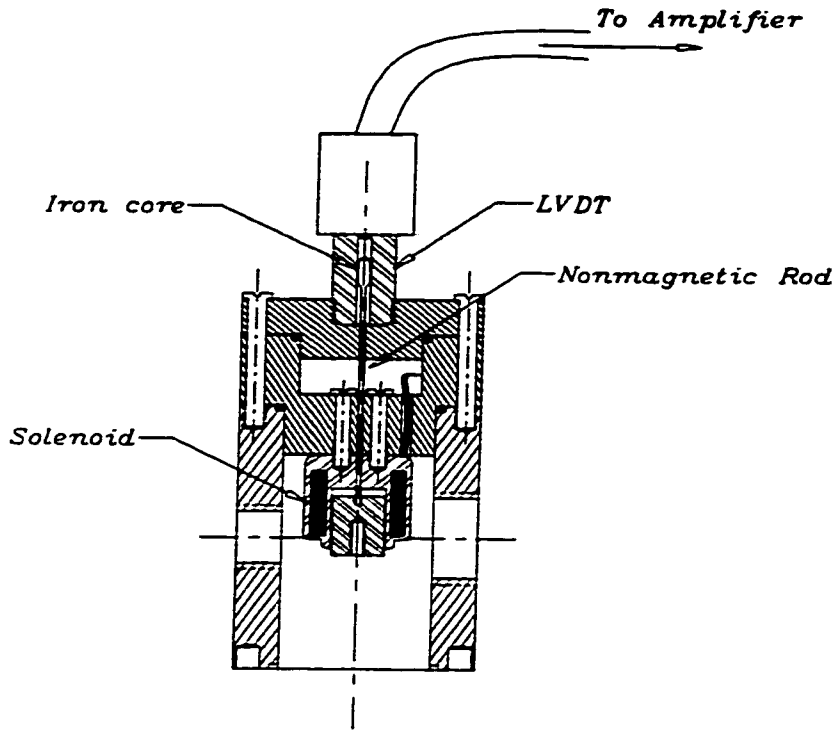

Figure 7.1.1 - LVDT Setup

The second main equipment used was a piezo electric force cell. This force transducer was used to measure the force acting upon the needle seat. The force cell is placed underneath the injector nozzle so that it can record the force when the nozzle hits its seat and transmits the signal to a charge amplifier. The record of the force is conveyed from the amplifier to an oscilloscope which traces the patterns of the seat force. A diagram of the piezo cell setup is shown if Figure 7.1.2. As can be seen, the nozzle has been cut approximately 8 mm above its tip. This allows for the seat force to be transferred

to the piezo cell, where it can be measured. A sleeve was provided so that the nozzle's alignment would not be compromised, and in order to keep both sections connected after the cut has been performed, a sliding fit was added to the sides of the nozzle tip end. In order for the nozzle to fit unto the load cell, a washer had to be placed above the cell,

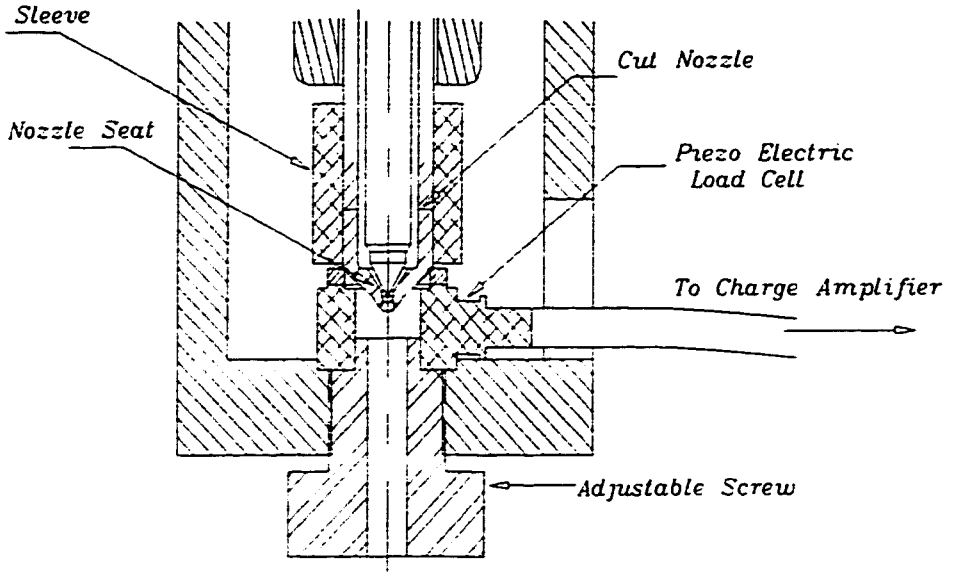

Figure 7.1.2 - Piezo Load Cell

creating a flat surface on which the modified nozzle can rest. The adjustable screw located at the end of the injector serves to provide the piezo cell with the a pre-load necessary for the cell's proper performance. The calibration data and characteristics for both the LVDT and the piezo cell can be found in Appendix D. Figure 7.1.3 shows the overall experimental setup and assembly. As can be seen, the nozzle section has been placed inside a steel casing, tightened with a screw at the top.

assembly. As can be seen, the nozzle section has been placed inside a steel casing, tightened with a screw at the top.

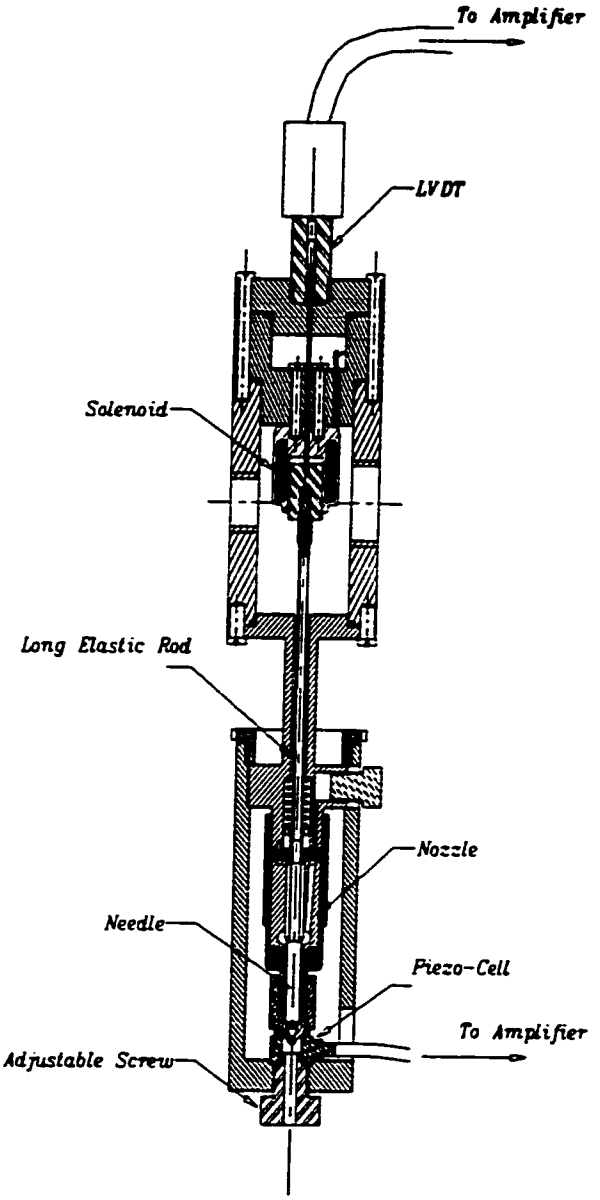

Figure 7.1.3 Experimental Setup Equipped With Piezo Cell And LVDT

The testing was conducted in two major sets. The first set, aimed at testing injector performance, with particular respect to opening and closing delays, core movement, circuit performance, etc., was run using nitrogen fuel at a pressure of 20 MPa.

The setup had an initial air-gap of 0.3 mm, a total lift of 0.6 mm, with a hollow, stainless steel tube injection rod. Since fuel would leak through the cut nozzle and because the cut nozzle would also change important configuration variables, this set of tests were run without the piezo cell installation and related design modifications. Although the design of the injector was intended for use with DME fuel, the tests could not be conducted with DME due to safety and regulatory factors.

The second part of the testing was performed without fuel, and with the main intention of measuring the seat force. As such, an injector such as the one in Figure 7.1.3 with the appropriate modifications for the piezo cell was used, and testing was performed using three different rods. The simulation results for each of these rods - a solid steel rod, a hollow steel tube, and a hollow aluminum tube - were presented in the previous section. Since the simulation results regarding seat force were also derived from a no fuel setup, validation of these results would still be possible. For this part of the testing, one important assumption had to be made. As an approximation, since the dynamics of the masses between the seat and piezo cell are difficult to measure, the effect of moving masses on the cell were not considered. Given the stiffness of the piezo cell, and the fact that the masses cannot be accelerating greatly, this assumption can be a valid one. However, even if it is not, the impact would only lie in an overstatement of the absolute value of the seat force. Since it is the relative, and not absolute, value of the seat force that is of importance, even an error in this assumption would not undermine the basic conclusions of the experiment. It is important to note, that, given this consideration, the prediction would be that there would be a slight variance in the seat force results obtained in the computer simulation and in the laboratory testing.

7.2 Test Results

7.2.1 Test Results for Hollow Steel Rod for Different Current Profiles

As core lift originates with the current provided by the driving circuit, the variation of core movement with respect to different current profiles is presented. To begin with, a voltage source of 80 V and a pulse width modulation with 20% duty cycle was applied to the solenoid core with a 20 MPa fuel pressure and injection period of 60 ms. Figure 7.2.1 shows the effect of the current on the core movement. As can be seen, the current has two peaks, with only one occurring once the injector is fully open at approximately 1.5 ms. This single peak, with an amplitude of close to 50 amps, was not powerful enough to keep the injector open beyond 3.5 ms. In the previous section, it was shown that the required injection time is approximately 5 ms. Simulating this identical current profile, similar results were obtained for core movement as in the laboratory testing. Figure 7.2.2 presents the simulation results for this current profile. The single peak existing after the injector is fully open has an amplitude of 48 amps and occurs at approximately 1.5 ms in the simulation as well.

To increase the power, either the amplitude of the peak, or the number of peaks must be increased. It is important to note that the original burst of current, reaching 83 A for 1.0 ms was not varied, since it was the minimum requirement to open the injector. As such, this original burst was kept constant in the experiments, and only subsequent peaks were varied. The first step was to increase the amplitude of the single peak existing after the injector is open to 72 amps. This was accomplished by increasing the duty cycle to 30% and keeping voltage constant. Figure 7.2.3 shows that the injector's opening time increases to a little over 4 ms. The increase in current amplitude keeps the injector open.

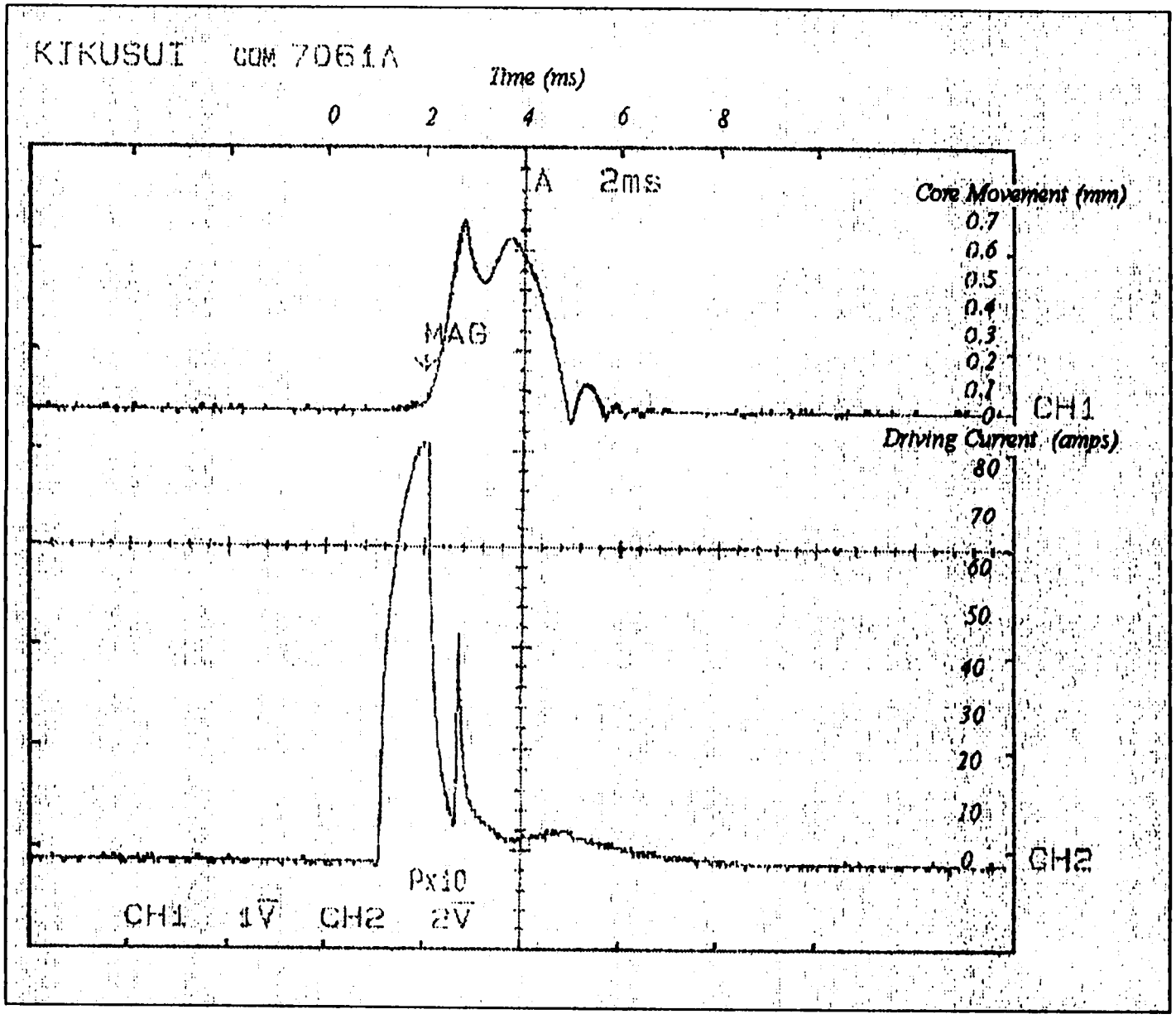

Figure 7.2.1
Core Movement for a low peak Current (experimental)

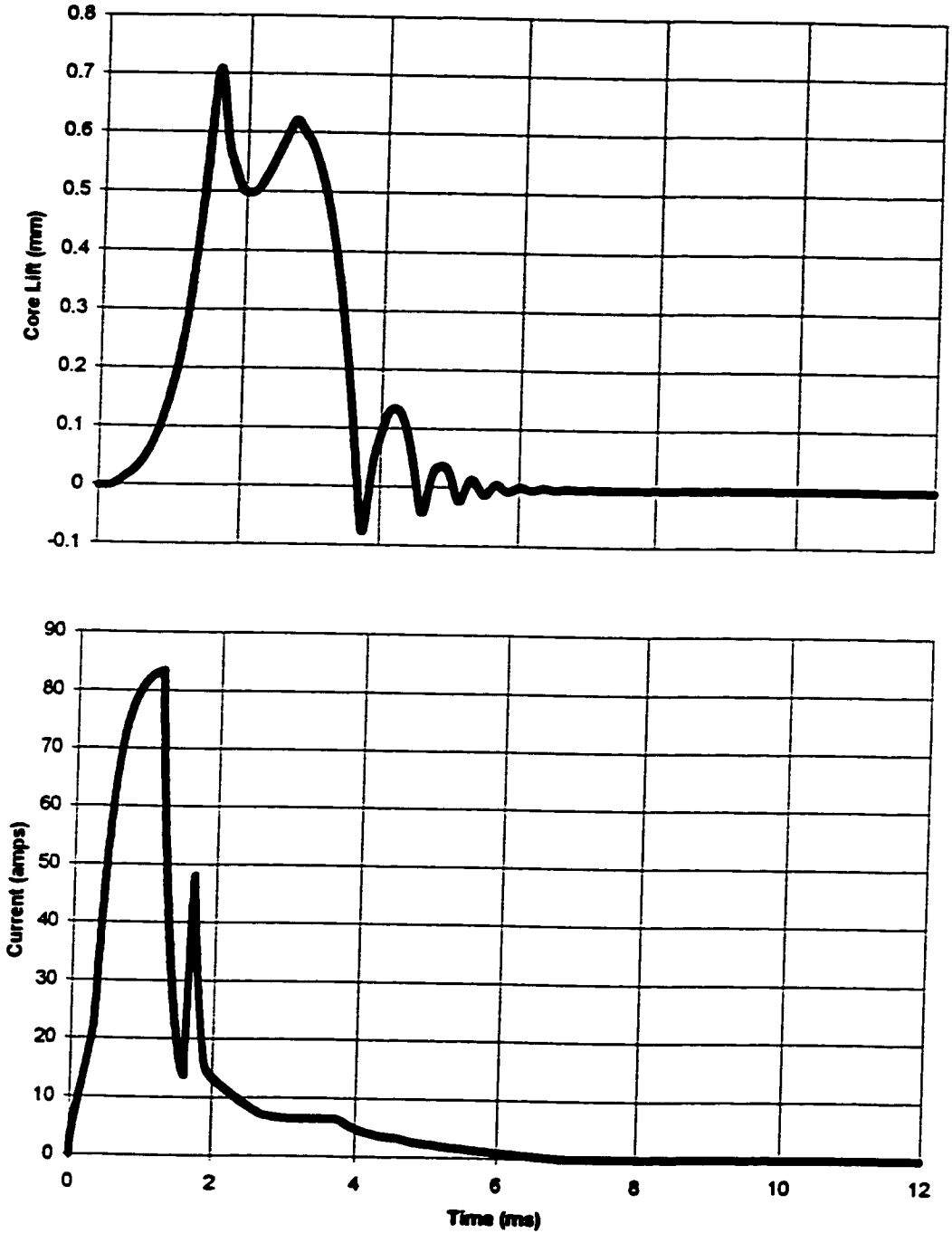

Figure 7.2.2
Core Movement for a low peak of Current

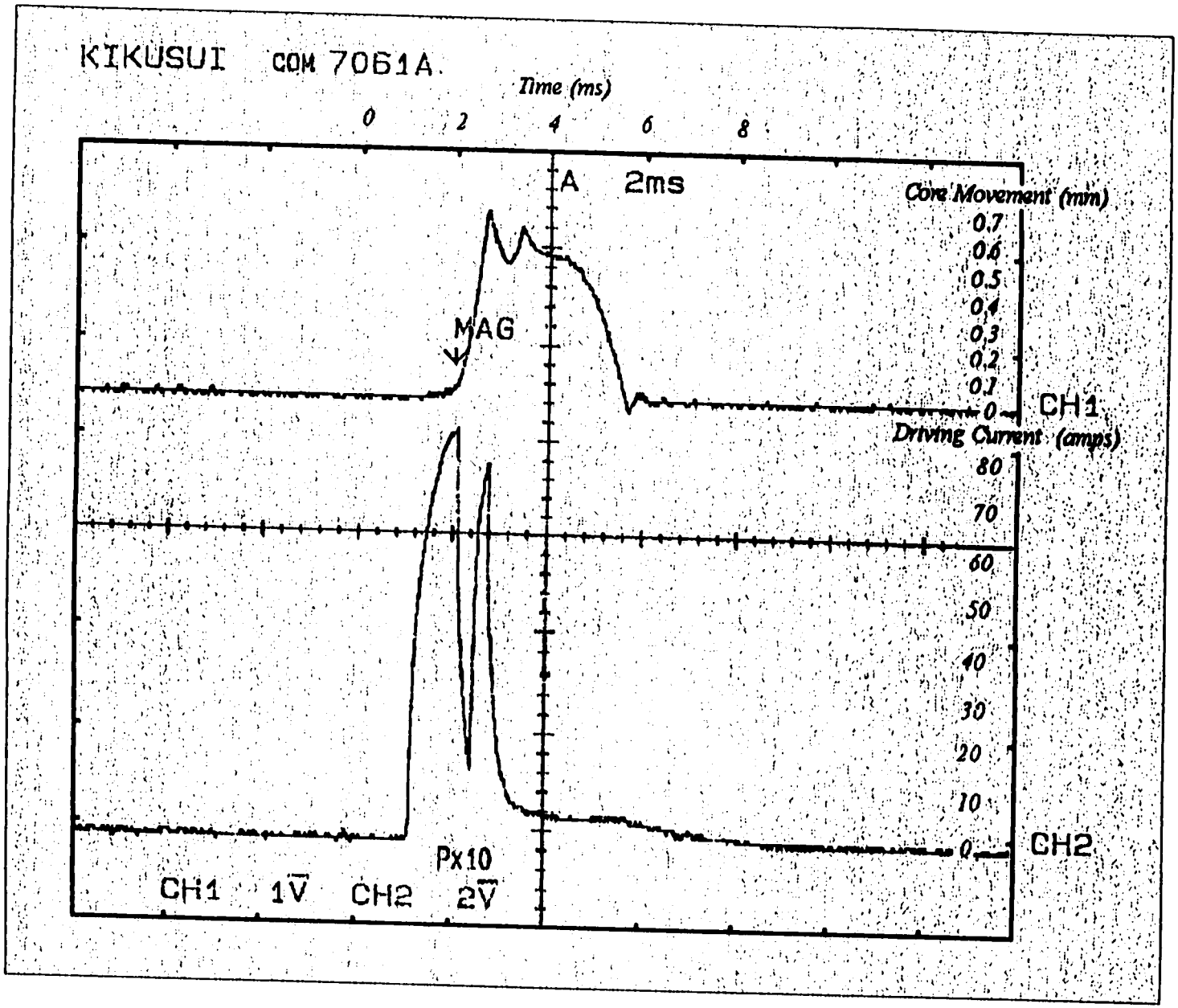

Figure 7.2.3
Core Movement for a high peak or Current (experimental)

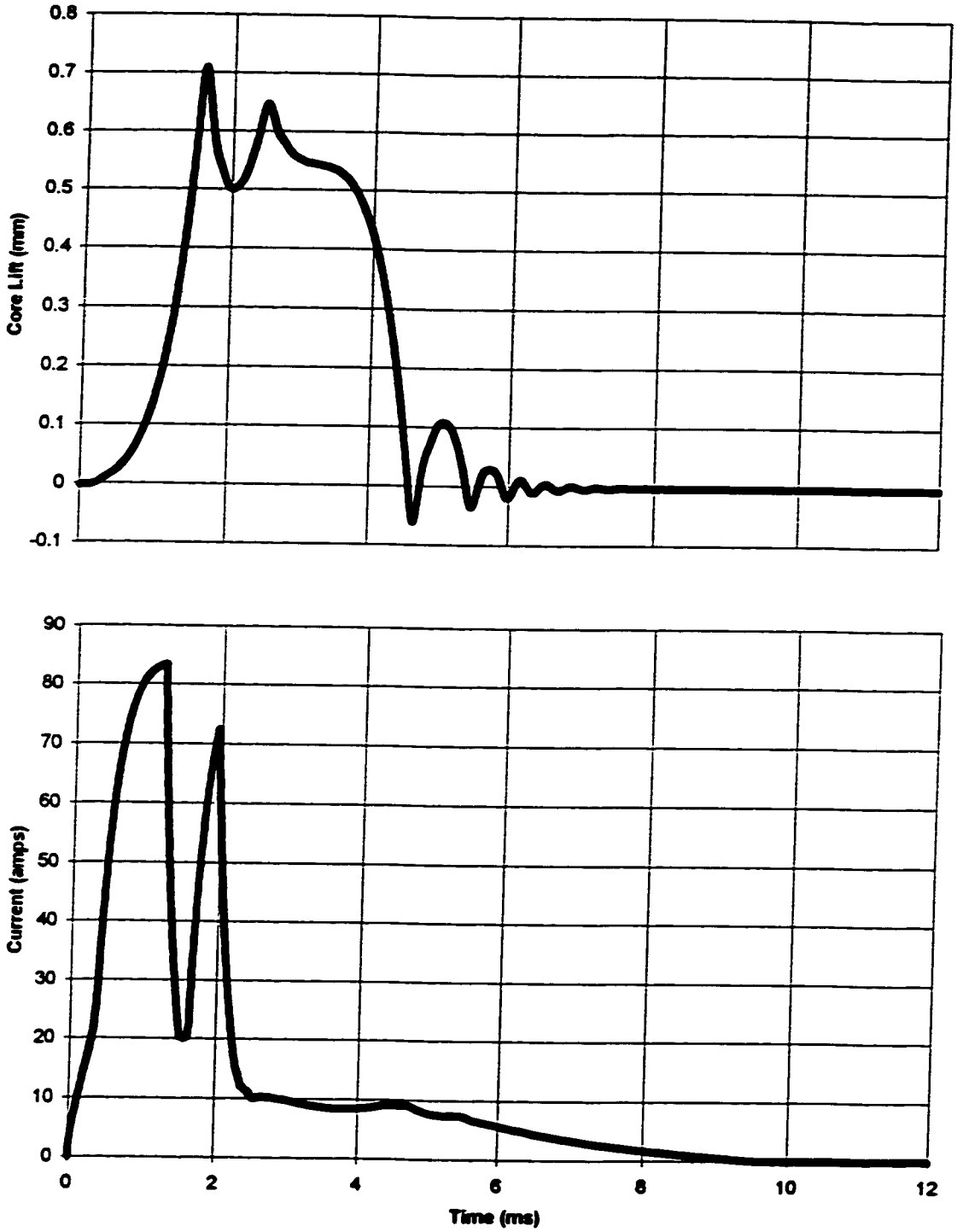

Figure7.2.4
Core Movement for a high peak of Current

for a longer period of time, before it begins to close. The corresponding simulation is presented graphically in Figure 7.2.4, and, as can be seen, similar results were again obtained. In practice, the drawback of increasing the current amplitude to keep the injector open for a controllable amount of time is not a feasible control scheme since the magnitude and duration are unknown. Since the Lisk L7 solenoid used in the injector is designed to withstand 6 V, which translates to 25 A for a given power of 150 W, a scheme that leads to good controllability is by applying voltage pulse width modulation (PWM). Thus, the average of the number of resulting current peaks can be controlled to equal the nominal 25 A as recommended by the manufacturer.

Figure 7.2.5 shows the effect of maintaining a 20% duty cycle at a 80 voltage and increasing the number of pulses to 8. Total injection time was increased to 8 ms, as the current peaks were kept at 48 A. Once the needle's original bouncing off the stop, the injector needle's opening stays constant at 0.6mm. This can be compared to the similar results which were derived from the simulation, and can be found in Figure 7.2.6.

Since 8 ms exceeds the desired total injection time, resulting in fuel waste, the number of peaks was reduced to 6. Here, injection time was brought down to just under 6 ms, as can be seen in Figure 7.2.7, by decreasing the number of pulses at the same duty cycle of, 20% and also keeping other variables constant. For the same current profile, the results of the simulation are presented in Figure 7.2.8.

Up to now, different current profiles were presented for a fuel pressure of 20 MPa. Visible in these graphs is the needle's bouncing at both the stop and seat, which is shown affecting the core movement. Removing the pressure originating from fuel existence,

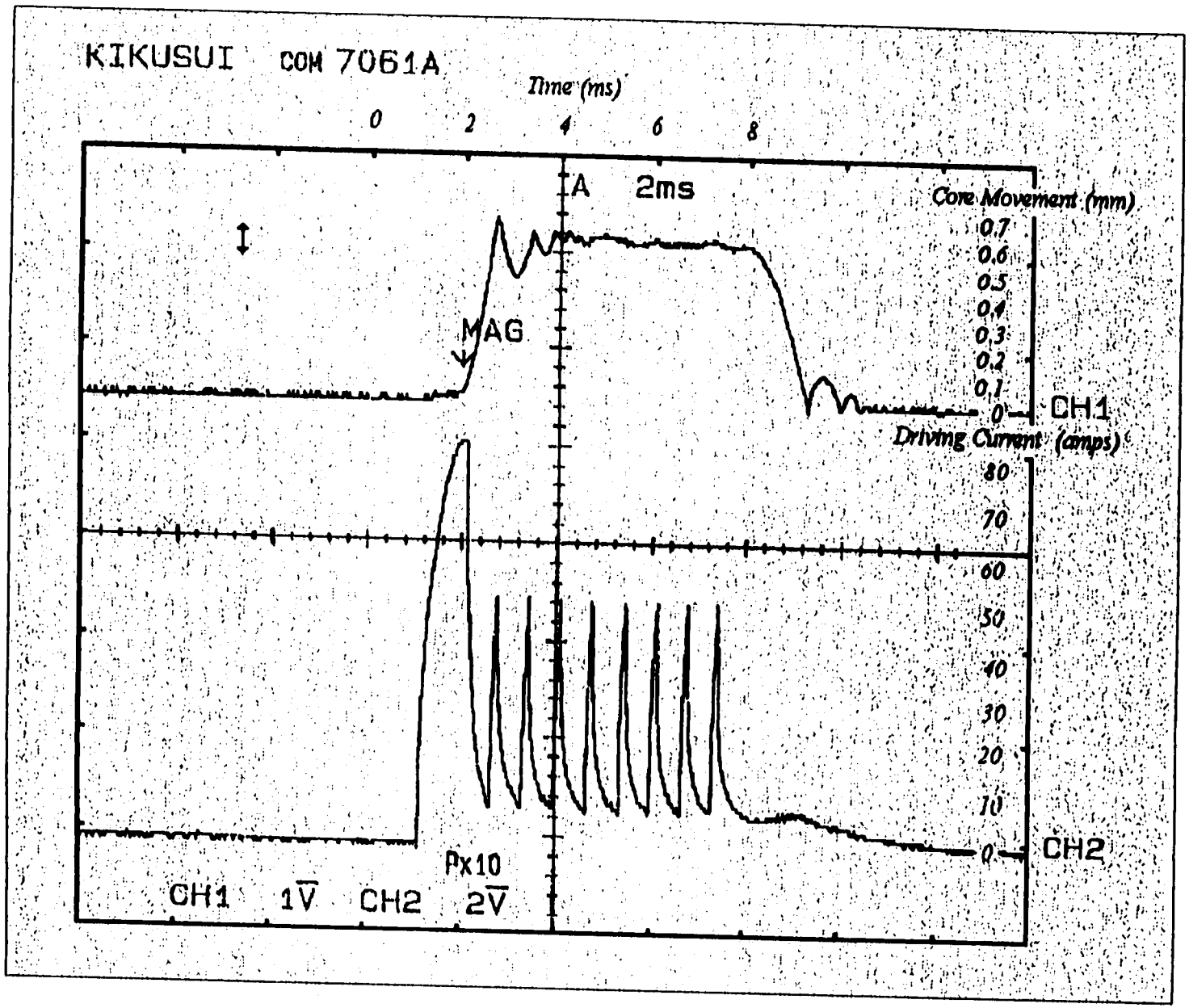

Figure 7.2.5
Core Movement for 8 low peaks of Current (experimental)

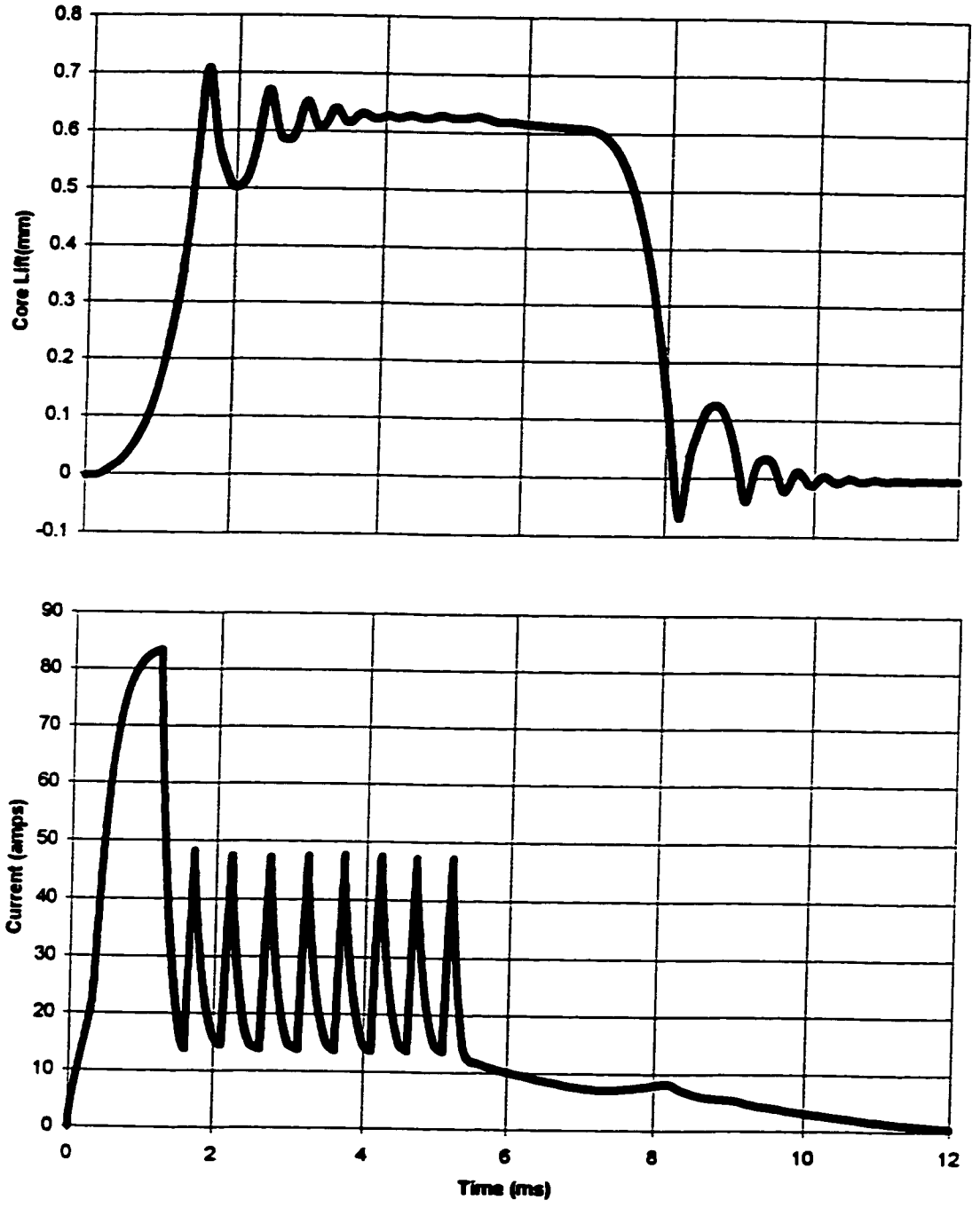

Figure7.2.6
Core Movement for 8 low peaks of Current

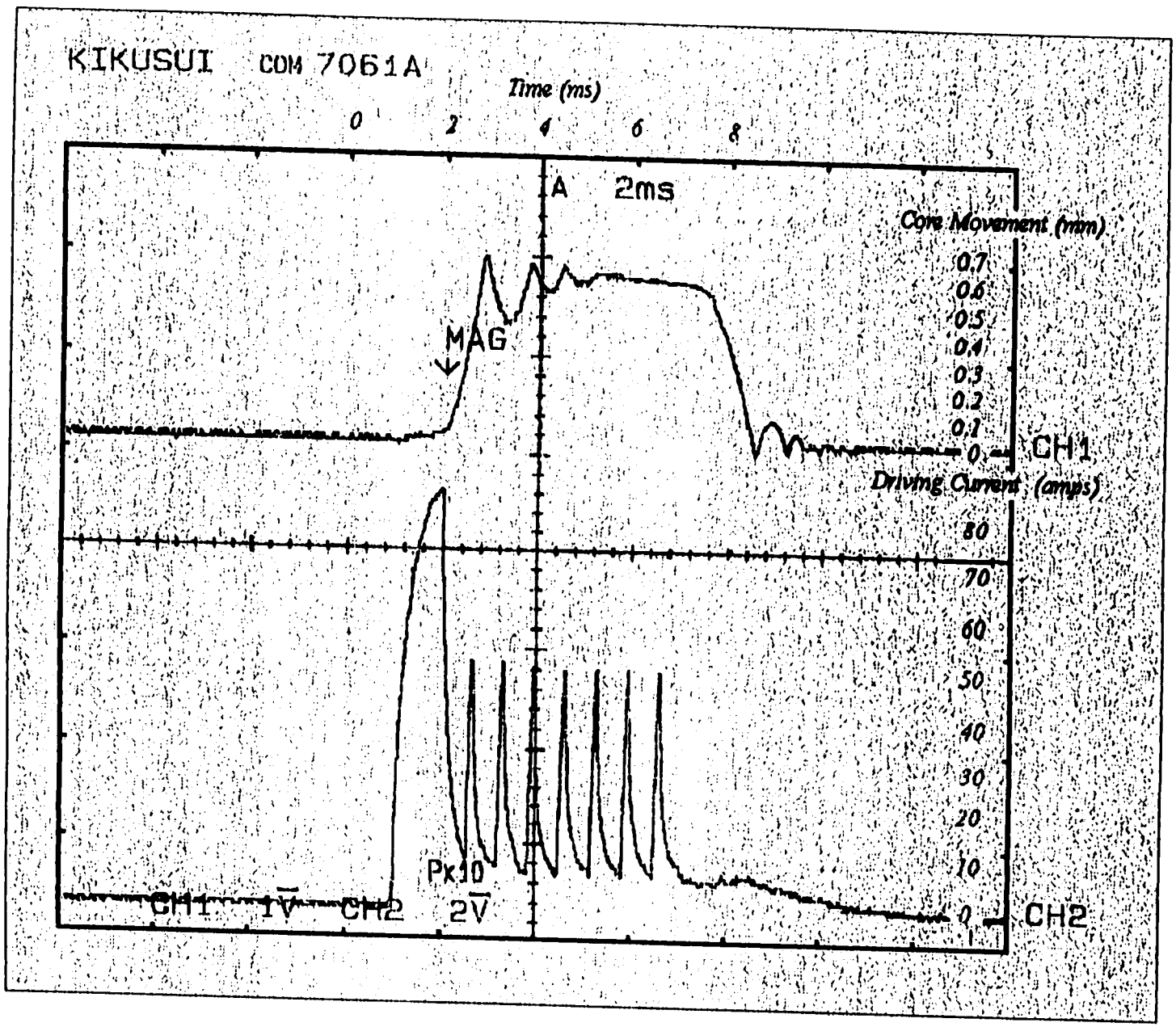

Figure 7.2.7
Core Movement for an optimal Current profile (experimental)

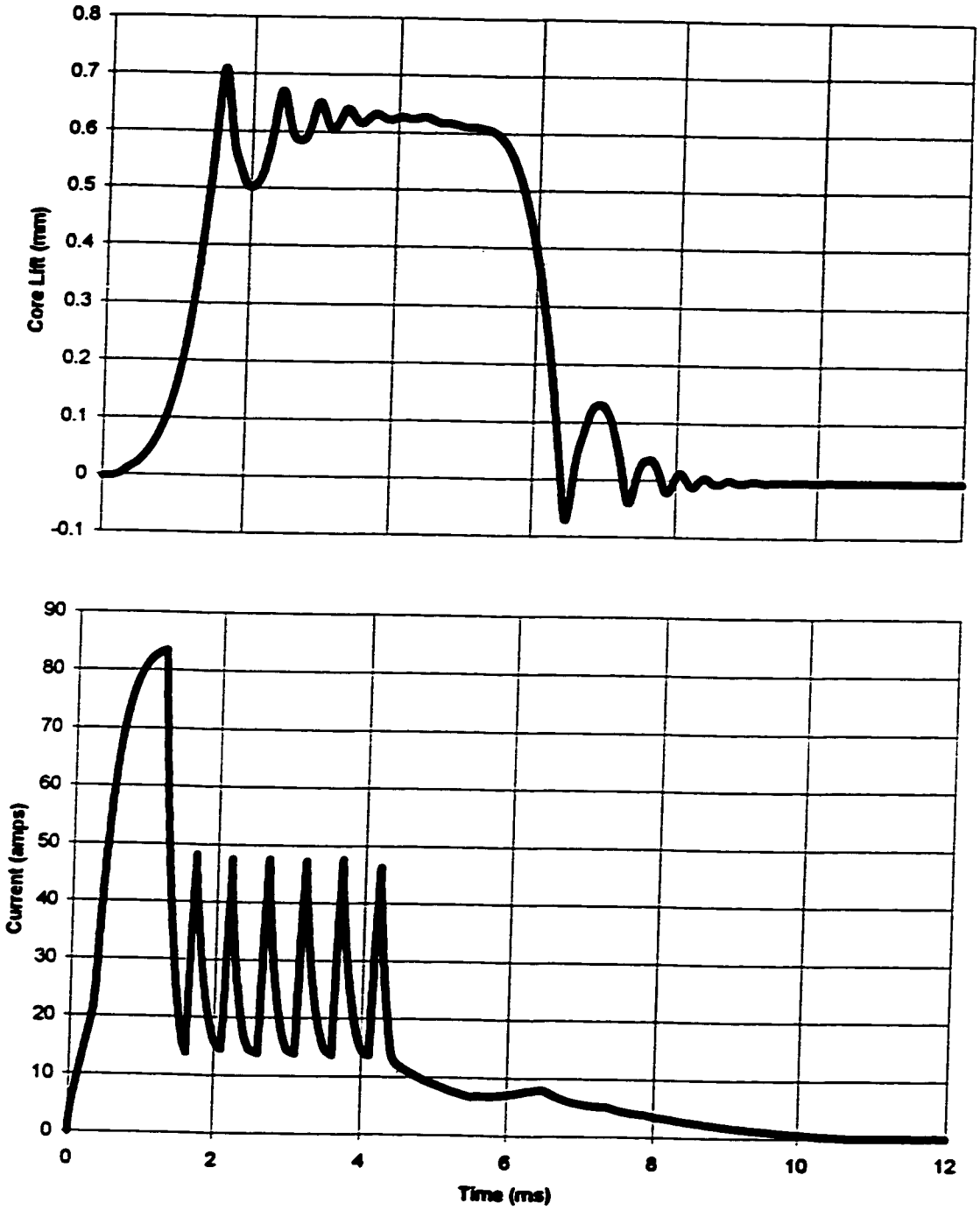

Figure7.2.8
Core Movement for an optimal Current profile with 6 peaks of low Current

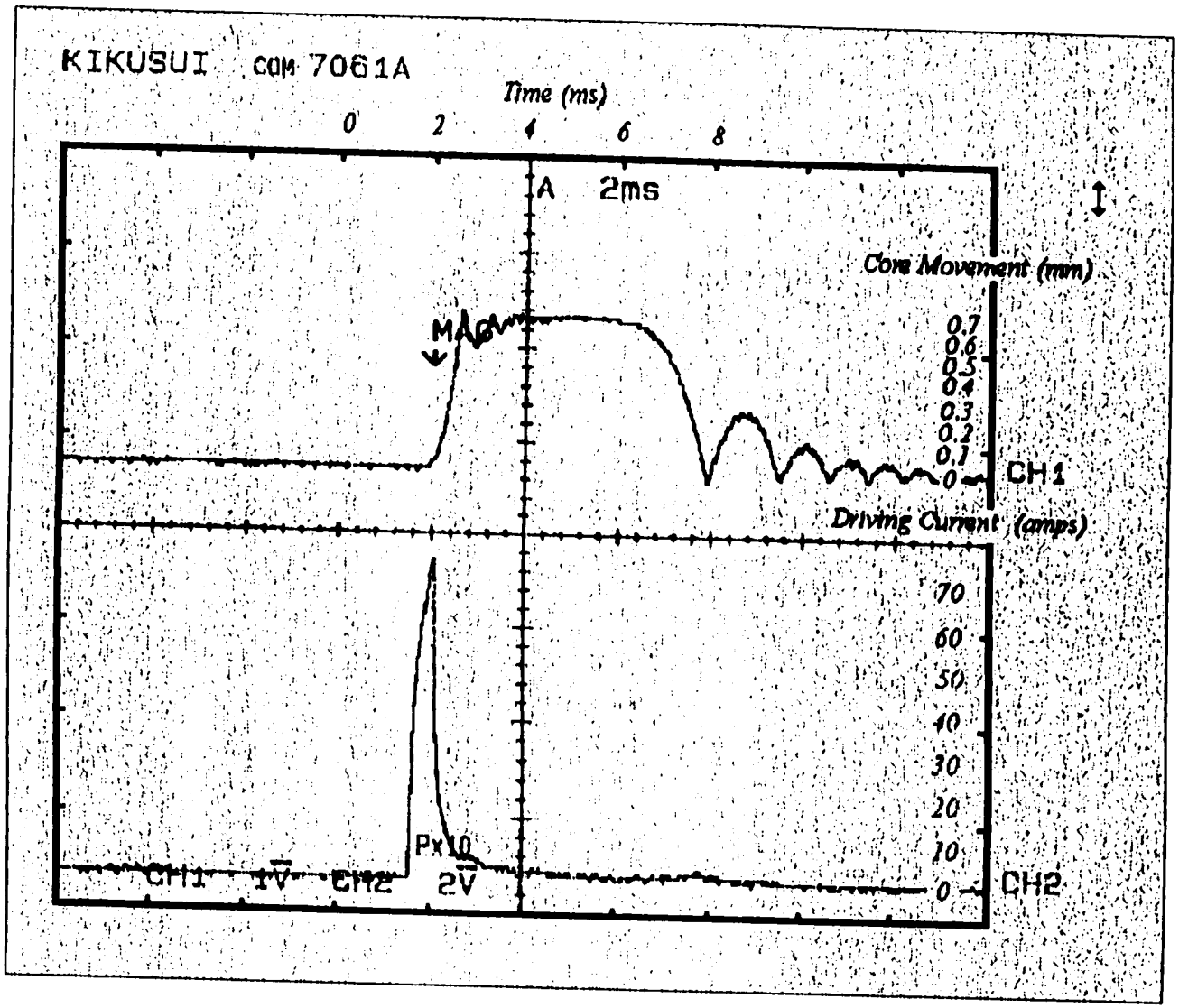

Figure 7.2.9
Core Movement and Current profile for zero pressure (experimental)

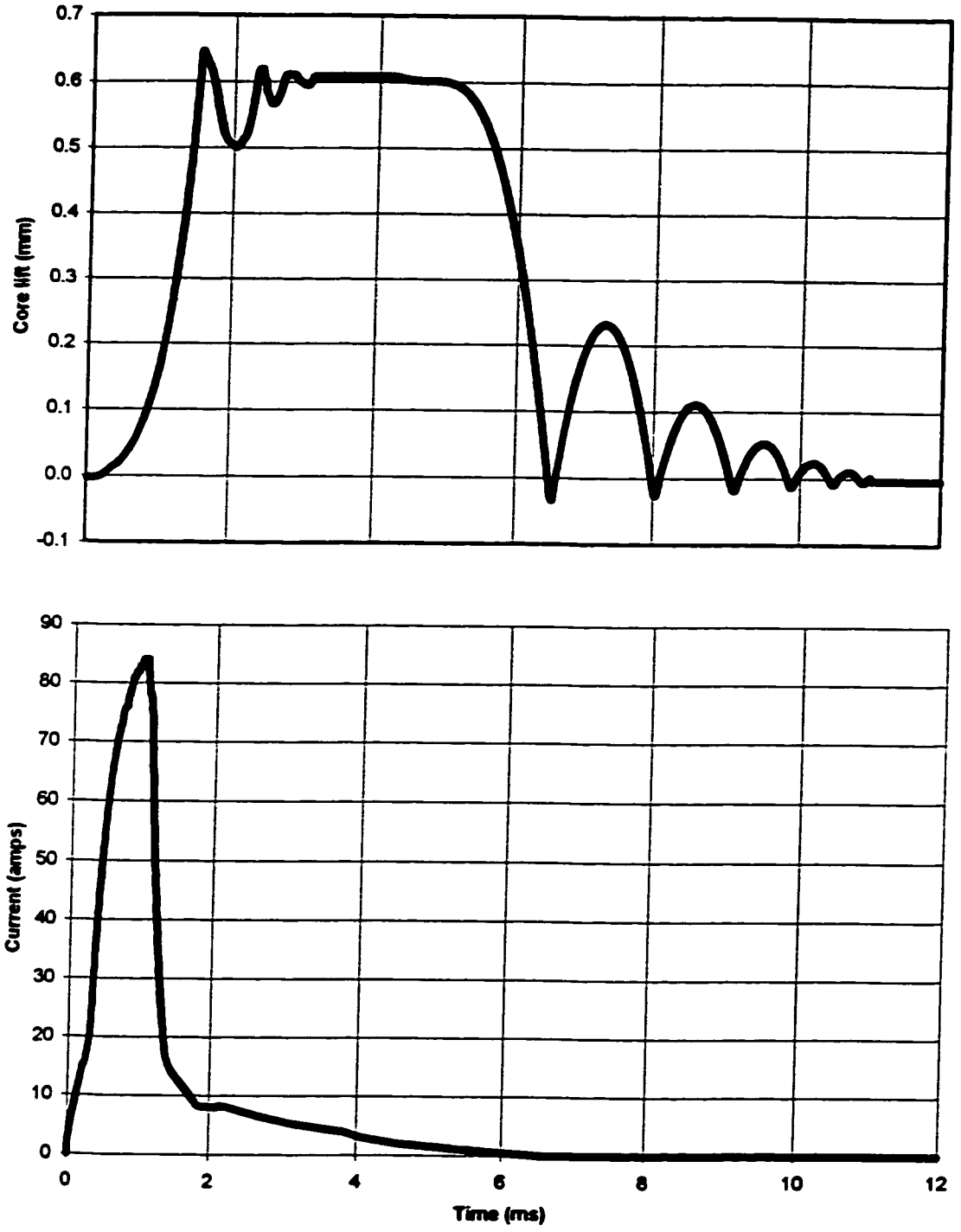

Figure 7.2.10
Core Movement and Current profile for zero pressure inside the injector

Figure 7.2.9 reveals a different bouncing pattern. The lack of downwards fuel pressure results in a minimization of the bouncing at the stop, while increasing the bouncing at the seat, as compared to Figure 7.2.7. With no pressure acting downwards inside the injector, the original current peak is sufficient to keep the injector needle open for almost 6 ms, and as such, no need for additional pulses in the current profile. The results obtained from the simulation are presented in 7.2.10 and show similar effects both in terms of the bouncing and current effects.

Comparing each of the above laboratory tests on varying current profiles with their simulation counterparts, and noting that these are only a sample of different current profiles tested, one can observe consistent similarities in the patterns displayed, validating the model presented in the previous section.

7.2.2 Force Measurement Results for 3 Different Rods

The preceding discussion was based on the first set of tests performed using the LVDT. As previously mentioned, the experimental setup was modified in order to allow the piezo cell installation, and for the measurement of seat force with three different sample rods, and the experiment was run with no fuel pressure. Figure 7.2.11 - 7.2.13 represent the results regarding seat force and core movement over time for a hollow steel tube, a stiff steel rod, and a hollow aluminum tube respectively. The simulation results for these tests were discussed in Chapter 6 with the appropriate graphs being 6.2.3 - 6.2.5. In the previous chapter, the forces acting upon the needle causing the bouncing effect that is witnessed was explained. It is important to add that the bouncing is a result of only the reversible absorption of kinetic energy provided by the injector's movement. Part of the kinetic energy is absorbed irreversibly in the internal molecular structure as internal

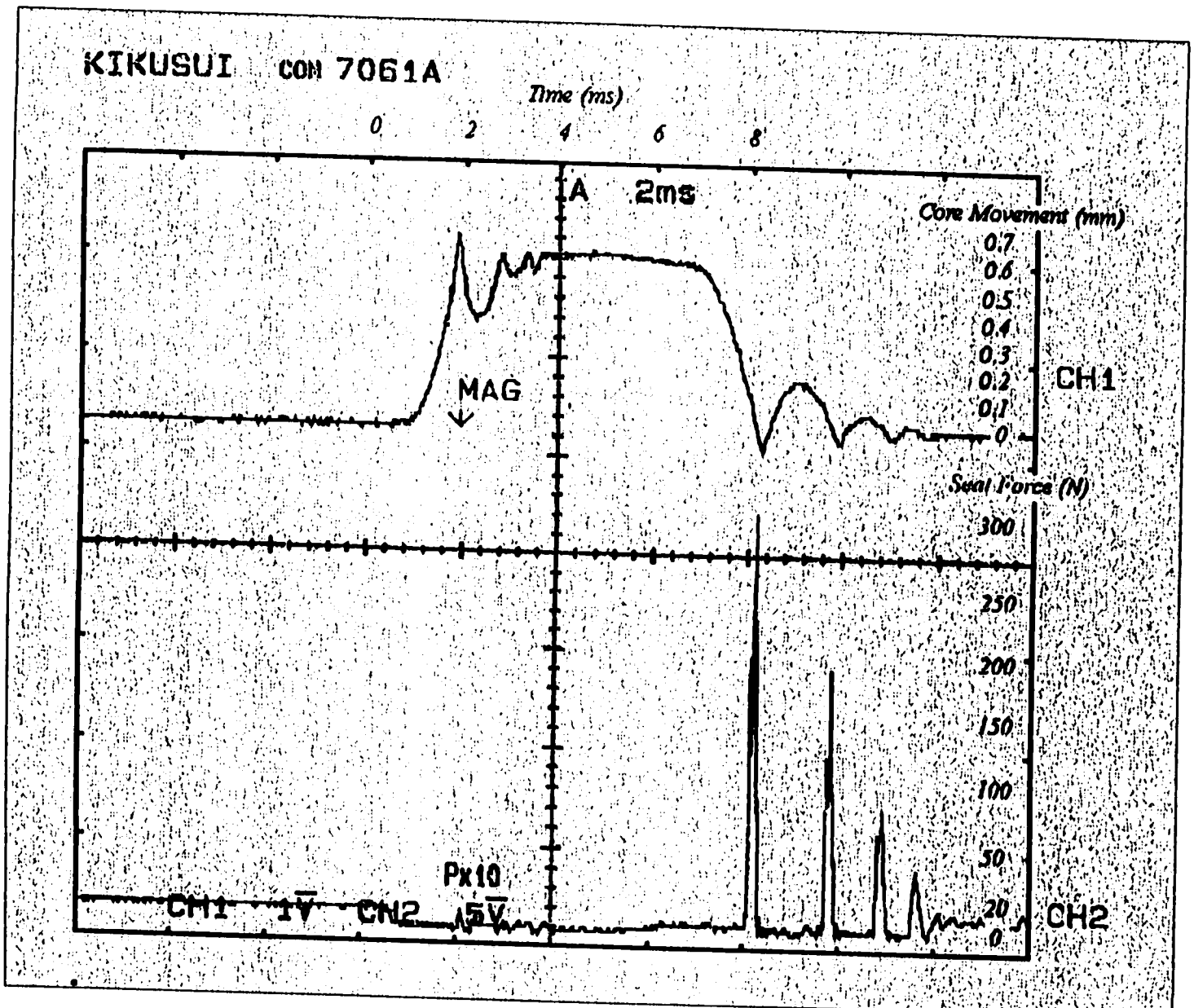

Figure 7.2.11
Core Movement and Seat Force of a Hollow Steel Rod

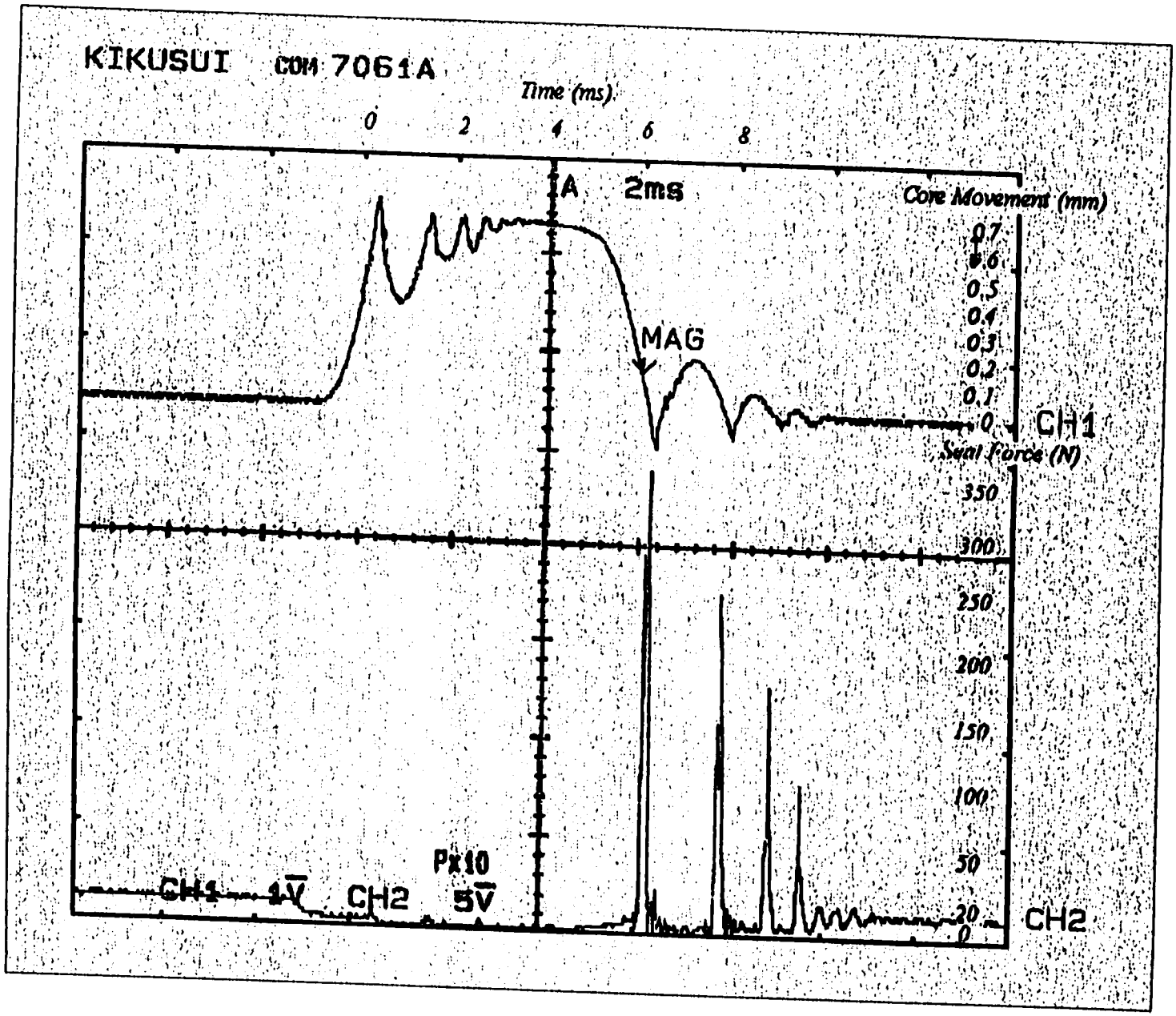

Figure 7.2.12
Core Movement and Seat Force of a Solid Steel Rod

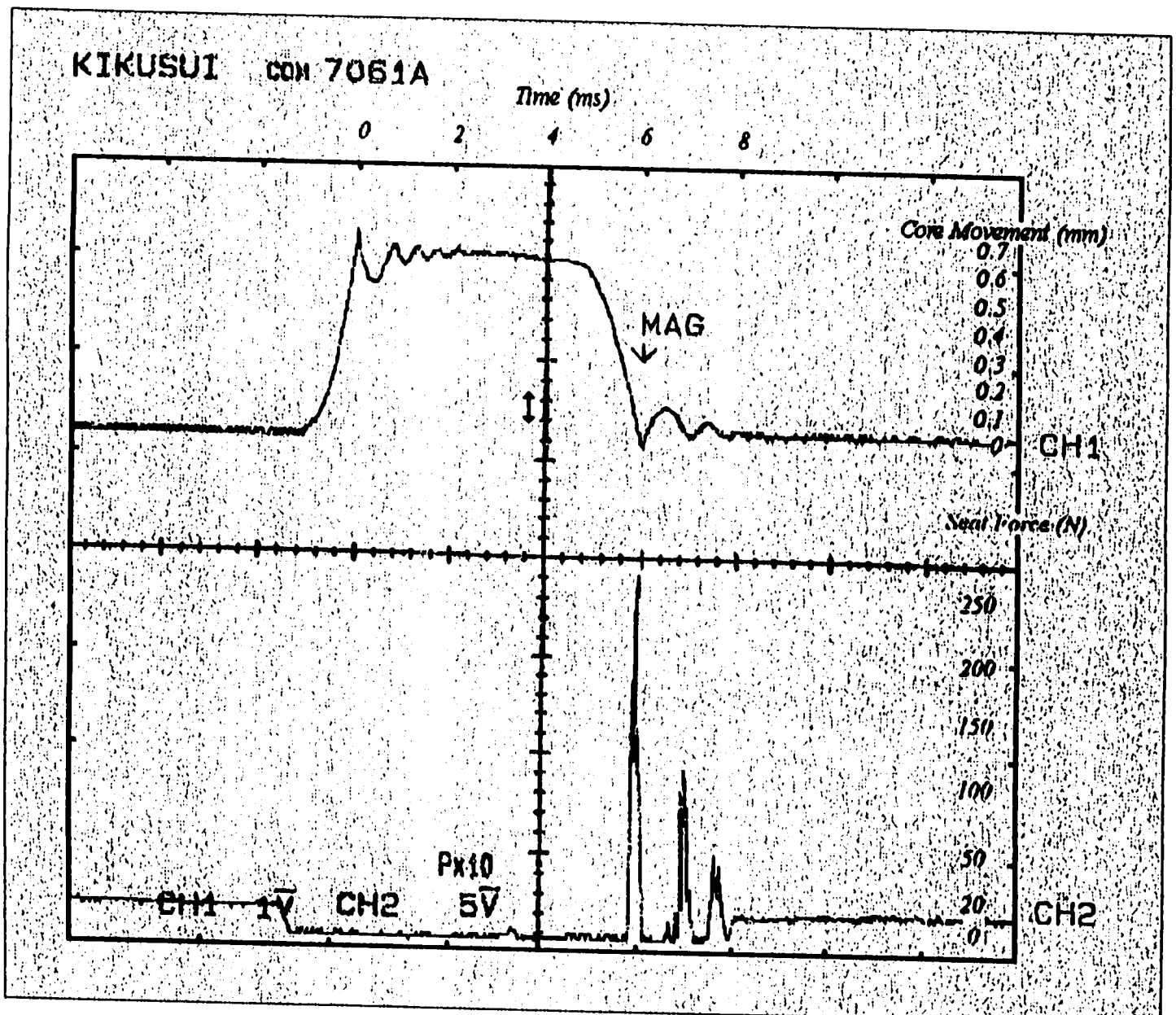

Figure 7.2.13
Core Movement and Seat Force of a Hollow Alumimum Rod

friction of the rod. More deformation in rods with higher elasticities causes a greater portion of irreversible energy absorption, reducing the bouncing effect. For the hollow steel tube, the initial seat force was measured at about 310 N, as compared to 300 N in the simulation. The testing provided a 360- 370 N seat force for the steel rod, which corresponds to 350 N in the simulation. Finally, the aluminum rod measured in at approximately 250 N, the same as in simulation. Common to all the rods is the presence of a small dip in seat force, immediately upon the injector's opening. This is a result of the alleviation of the pre-load force acting downwards upon the seat. This force reduction is equal for all three rods, and is also present in the simulation, since pre-load is kept constant in the experiment. Once again, the consistent parallels between the test results and simulation data lead to a validation of the model of Chapter 6.

Figure 7.2.14 is an extended time base plot analyzing a single impact of the needle on its seat for the hollow tube rod. The figure depicts the kinetic energy release distribution versus time as a two peak force phenomenon per needle impact. This is the result of the inertia of the two lump-masses, concentrated at the needle and at the solenoid. The first peak occurs as the needle hits the seat. With a small time lag of about 0.02 ms, the inertia of the solenoid core transfers all of its kinetic energy to the needle, causing a second, slightly smaller peak in seat force. This phenomenon is common to all individual impacts of the needle.

7.3 Further Simulation

Since the model in Chapter 6 can now be considered valid, one can observe the effects of changing a myriad of variables without actually running the experiments. The variables can be amended in the computer program, running the simulation, and recording

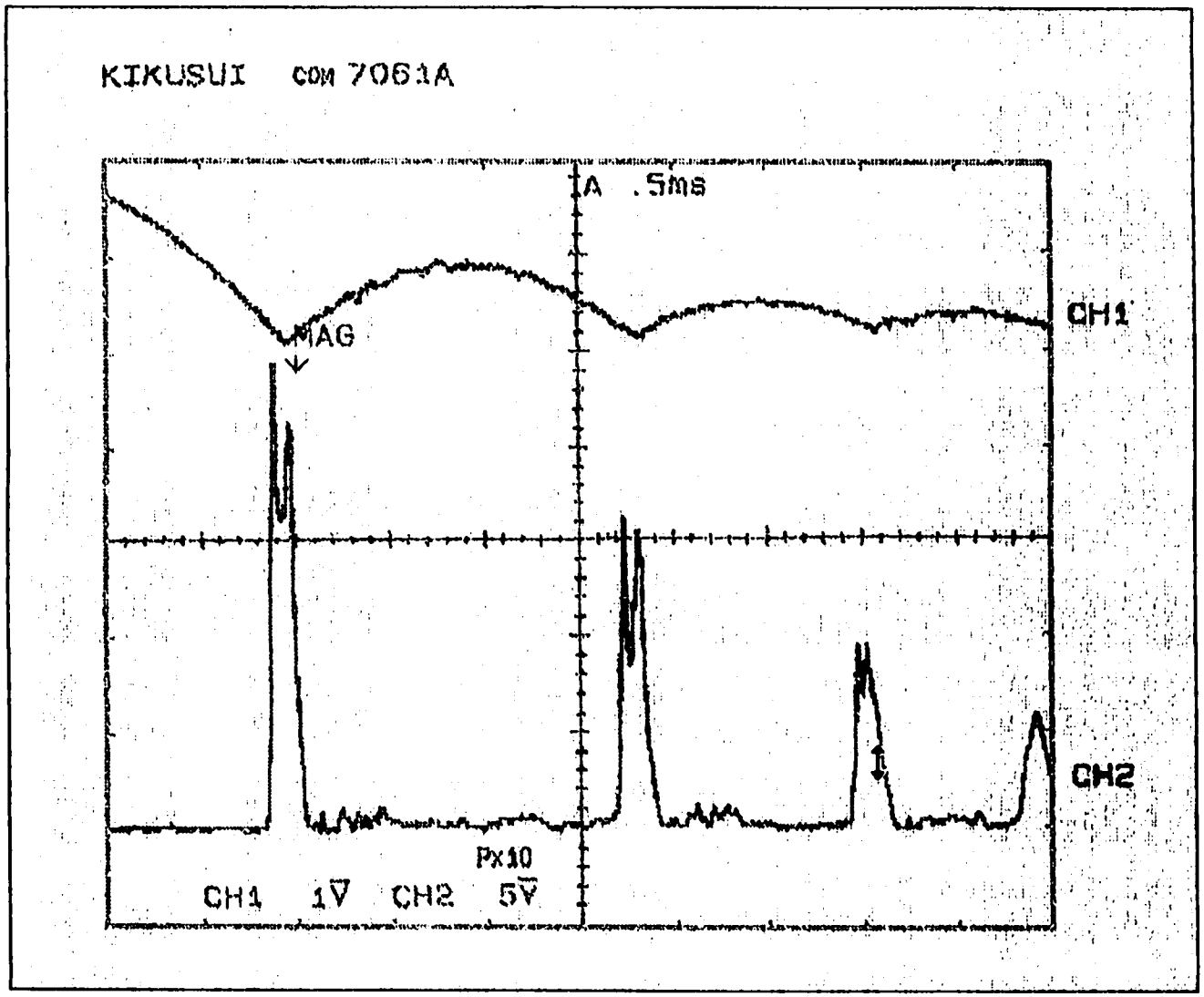

Figure 7.2.14
Extended time-base plot for the impact force in the nozzle seat

the results. Since the testing that has been discussed was performed with nitrogen fuel, and whereas a primary interest of this thesis is the adaptation of injectors for use with DME, a variable which is an obvious candidate for amendment is the fuel source. As such, the computer simulation is revisited with the necessary revisions for DME use.

The main difference between DME and nitrogen with respect to the fuels' impact on core movement is their damping effect. It has already been discussed that DME has a very low viscosity, and thus low damping factor. As such, changing the fuel to DME should not be expected to produce significant variations in the needle's operation as a result of the current provided. Figure 7.3.1 shows the core movement and current provided by the driving circuit across time, and corresponds to Figure 7.2.8 with nitrogen fuel. As can be seen, the two graphs are almost identical with respect to the injection opening, closing, bouncing, and total injection time.

The presence of fuel pressure acting downward on the needle would be expected to increase the measured seat force. Adding DME fuel, with the corresponding 20 MPa pressure, to the simulation using an elastic rod, the results provided in Figure 7.3.2 are obtained. As can be seen, the original impact force does rise from the 300 N with no fuel pressure, to 490 with DME. The fuel pressure helps the damping effects to increase, but increases the impact force on the seat. This result is not a comparison between DME and alternative fuels, but, rather, between DME and no fuel. Since other fuels operate at positive pressure, the under performance of DME in this regard is therefore overstated. However, since 20 MPa is the fuel pressure maintained to prevent the DME from boiling, it would be expected that seat force would be somewhat more pronounced using DME than other fuels able to operate at lower pressure environments.

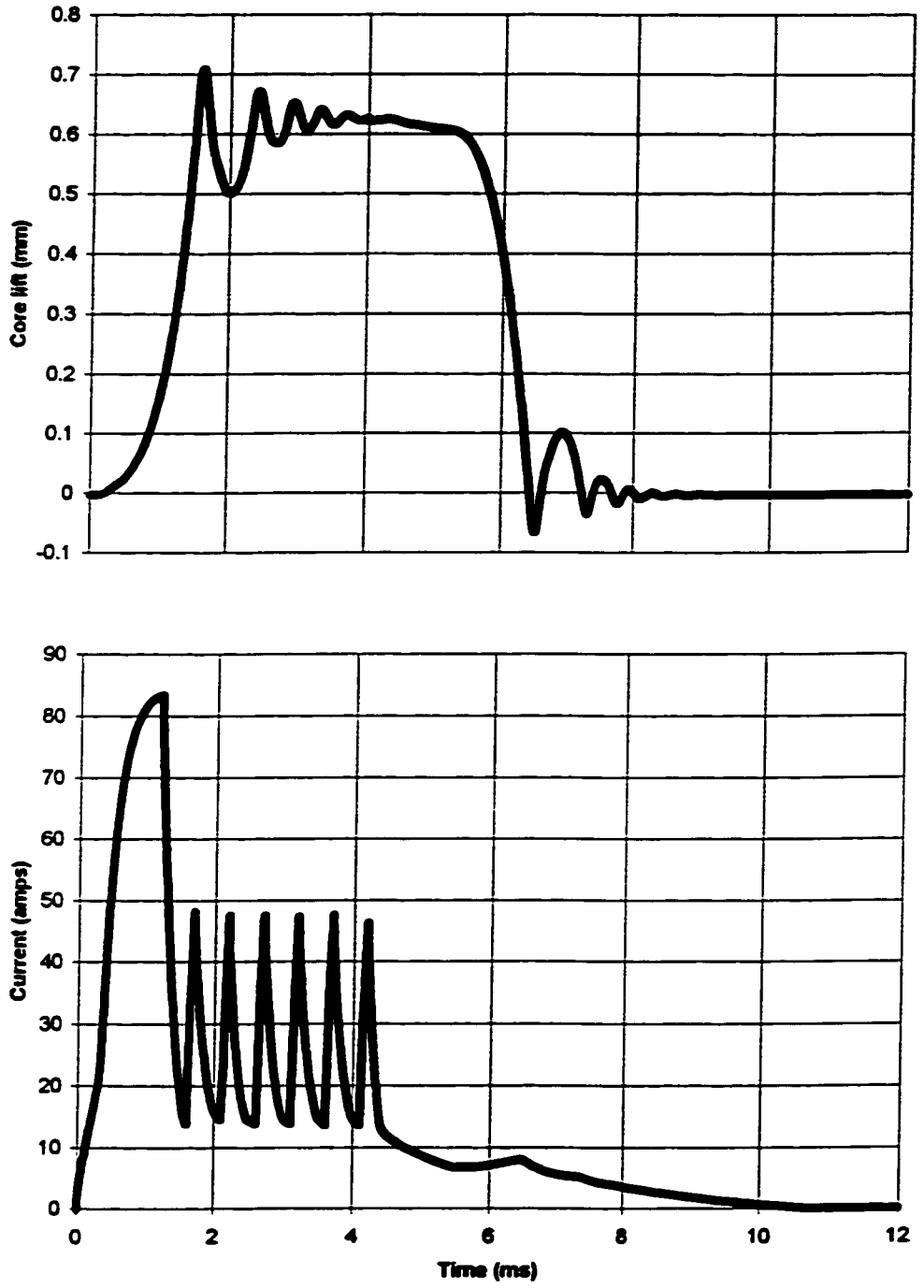

Figure 7.3.1
Core Movement and Current profile using DME as fuel

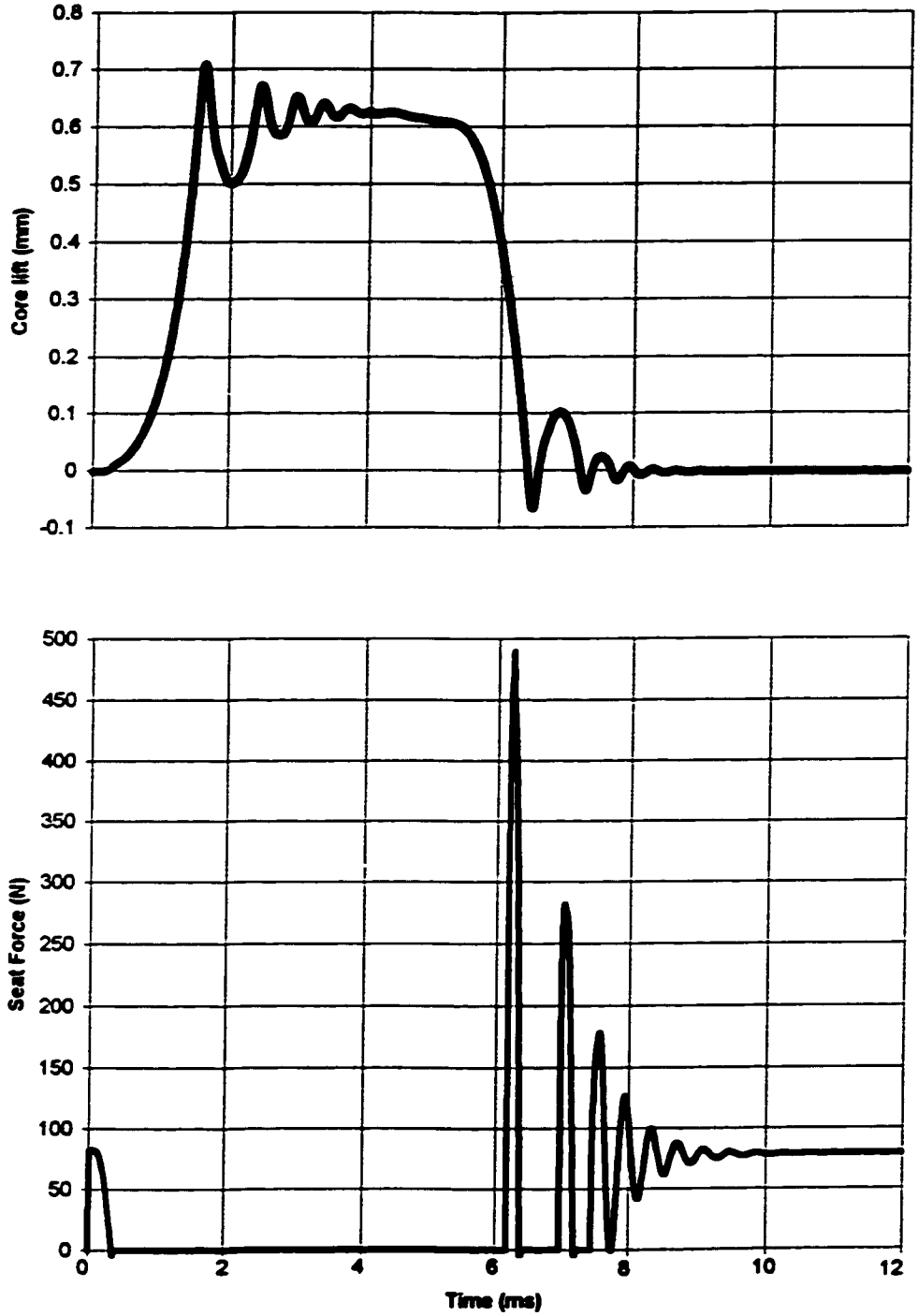

Figure 7.3.2

Core Movement and Seat Force of a Hollow Steel Rod using DME as fuel

Finally, as one of the highlights of this injector design is the lengthened elastic rod intended to reduce seat force, it would be of interest to review the effect of rod length on this force. Figure 7.3.2 already presented the seat force using DME with a long elastic rod. Shortening the rod length from 87 mm to 20 mm, the appropriate simulated results are found in Figure 7.3.3. As can be witnessed, the longer rod providing greater elasticity reduces seat force to 650 N from 490 N using a short rod, as expected.

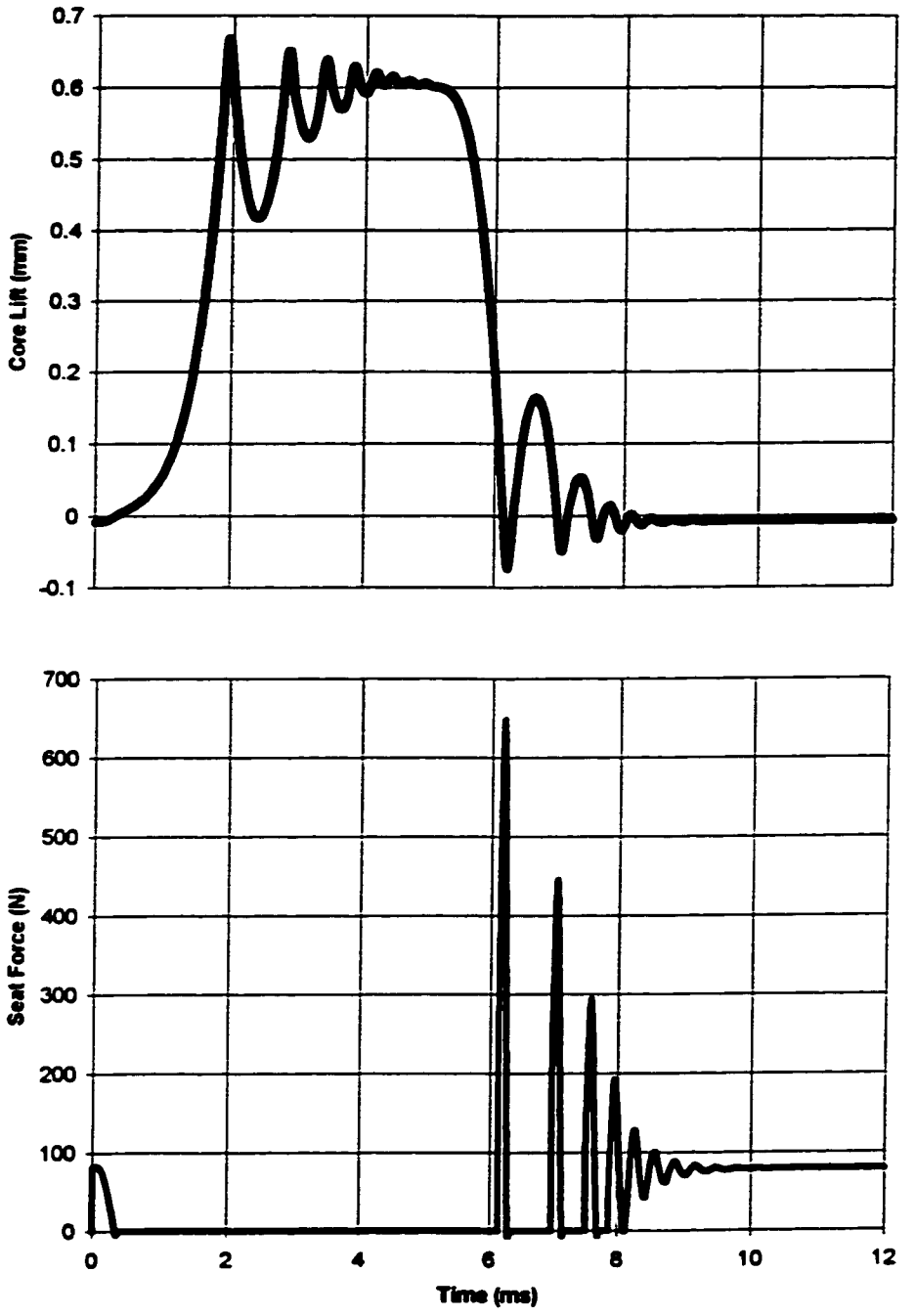

Figure 7.3.3
Core Movement and Seat Force of a Short Solid Steel Rod using DME as fuel

CHAPTER 8
CONCLUSION

Over the last ten years, a considerable amount of research energy in the field of fuel injection has been directed towards electronic actuation and alternative fuel development. The research has consistently shown that improved injector performance and pollution reduction were attainable with the incorporation of solenoids in the injector design, as well as with the use of DME fuel. This thesis has had as its aim the development of an electronically controlled injector design that could be used with DME. It has had, as a second objective, the intent of modifying traditional designs to also reduce needle seat wear, and the post-injection of fuel in the injection process. As a corollary to this latter goal, the thesis set out to develop a method whereby the needle seat force could be measured in a laboratory setting, in order to observe first-hand the effects on this force of adjusting several variables in the injector design.

8.1 Research Summary

DME fuel presents several challenges to the development of a fuel injector design that would be compatible with its use. Though its high cetane number reveals that it is easily ignitable, with corresponding advantages with respect to NOx emissions, DME has a very low boiling point as compared to other fuels. As such, it has been found that, to keep it from boiling, the fuel needs to be kept pressurized at approximately 20 MPa in the fuel injection process. DME's low boiling point also presents challenges insofar as excess fuel left in the injector nozzle after injection is concerned. Given the proximity of fuel left in the nozzle to the high temperature of the combustion chamber, it is possible for this

excess DME to evaporate, affecting the total fuel discharge rate. Furthermore, the liquid viscosity of DME is almost 10% that of diesel fuels. This reduces its cushioning ability and also provides a greater risk of internal leakage of fuel. However, DME has repeatedly shown that it has significant benefits with respect to its emission of a host of pollutants, including PM, NOx, HCHO, CO, and HC. It is for its potential in this area that DME is quickly gaining popularity as the next fuel of choice in diesel engines.

In order to counteract the potential for leakage to the fuel's low liquid viscosity, a steel to steel sealing was incorporated into the design, improving seat geometry and needle concentricity. In order to overcome the reduced damping factor involved with DME fuel, the injector design incorporated a long elastic rod, the elasticity of which would reduce the impact on the nozzle seat. This lengthened elastic rod also had the virtue of reducing the bouncing effect of the needle on its seat, thereby reducing the resultant post-injection. The 20 MPa pressure required to keep DME in liquid form was too great for the driving circuit used in past injector designs. As such, a new driving circuit, able to overcome the 20 MPa pressure environment, was developed to be used with the Lisk L7 solenoid. Finally, so as to reduce the potential for DME left inside the nozzle to evaporate, a circulation path for the excess fuel coming out of the nozzle was provided, re-directing the fuel out of the injector and back to the primary circuit. These general concepts were incorporated in the injector design, thereby allowing the injector to be used with any gaseous fuel, as well as with DME.

The issue of seat force reduction was a major concern in this thesis. Seat force is a result of the dynamic impact of the needle when closing on the seat in the nozzle, and is aggravated by the lower viscosity of DME, as well as the heavy solenoid core attached to

the decelerating needle. This seat force can cause significant strain on the needle seat, wearing it out over time, thus possibly causing injector malfunction. The elasticity of the injector rod was identified as an important variable in reducing seat force. To reduce the large inertia force, a hollow stainless steel elastic rod connected to the needle on one side, and to the solenoid core on the other, was introduced. The rod's length was also increased to 87 mm from that of the previous design of 20 mm, as elasticity is positively correlated to rod length. By damping the transfer of the solenoid core inertia force, the impact force acting on the nozzle seat was reduced. The initial impact on the nozzle seat was reduced by almost 25% with the introduction of the new rod. Since post-injection is the result of the needle bouncing off the nozzle seat, the reduced bouncing effect that was observed in the testing would also cause a reduction in post-injection.

Heretofore in the literature, there was no technique available to measure seat force. By placing a piezo cell underneath the injector nozzle, the force generated when the nozzle hit its seat was recorded and transmitted to a charge amplifier. The nozzle was cut approximately 8 mm above its tip, allowing for the seat force to be transferred to the piezo cell, where it could be measured. So that the nozzle's alignment would not be compromised, and in order to keep both sections connected after the cut had been made, a sliding fit was added to the sides of a sleeve containing the nozzle, and a washer was placed above the cell creating a flat surface on which the nozzle could rest. These and other design modifications were done for experimental conditions and measurement only, and does not appear in the actual injector design.

The design of the injector also encountered challenges with respect to its electronic actuation. Crucial to the injector's effective operation is the solenoid force that lifts the

injector needle. If the solenoid core were exposed to excessive heat, its performance could be compromised, with a reduction and variability in its ability to generate enough force to properly operate the injector. The subject of solenoid overheating was therefore of primary concern in the injector design. The main risk of heat affecting the solenoid originates from the high temperature environment of the combustion chamber. The first step taken was to distance the solenoid from the chamber, a process achieved through the use of the lengthened injector rod. The second was to use the fuel as a coolant for the solenoid. Unit injectors were inter-connected to form a common rail configuration, in which the solenoid core was placed, and where continuously flowing fuel can cool the solenoid.

The design of the common rail itself had several advantages. Unit injectors were linked through the use of a high-pressure, hydraulic tube. This tube's ability to withstand the stress of high pressures allows the injection system to be relatively light-weight. Its flexibility facilitates its installation and insulation of the system, while making its standardization and repair work more convenient.

A mathematical model was developed and was validated through a comparison of simulation results and laboratory testing. The model of the injector needle and the solenoid core, a mass-spring-damper model, was of a dynamic nature. It was simulated in a C language program using the fourth-order Runge-Kutta method for differential equation solving. Laboratory test results mirrored their simulation counterparts with respect to the effects on core lift of a variety of current profiles for different injection pressures, and the effects on seat force using a melange of injector rods. The model presented was thus validated, allowing it to be used in future research and experiments.

8.2 Further Research and Recommendations

There are seven separate areas in which further research to build on the work presented in this thesis can be conducted to add significant value to the literature.

1. System optimization. Based on past experience and research, the variable values in the injector design, such as rod length, conical angle of the nozzle tip, rod material, spring stiffness, etc. were chosen. To improve the injector performance, an optimization procedure that would establish an optimal set of design variables, could be conducted. An optimized injector could minimize seat force, opening and closing delays, improve the profile of the needle motion, while further enhancing other injector performance characteristics.
2. Real environment testing. Both optimized and non-optimized injectors could be tested in a non-laboratory setting, identifying the injectors' performance levels in an uncontrolled environment. The injector's ability to withstand the variations of the fuel temperature, combustion chamber temperature and pressure without suffering solenoid overheating and the boiling of excess fuel left in the nozzle tip.
3. DME testing. As already mentioned, for safety and regulatory concerns, the injector presented in this thesis, though designed for DME use, was not actually tested with this fuel. Although, after model validation, its performance can be estimated in the computer simulation, future work can incorporate the use of DME in laboratory and real environment testing.
4. Other variable measurements. The main concentration of this thesis was on injector needle movement and characteristic, and seat force measurement. Other variables,

such as gas discharge rates, heat transfer, spray, leakage, dynamic response, etc. could be measured and optimized in future research.

5. Endurance tests. Both the complete injector, and its electronic system, comprised of the solenoid and driving circuit, should be tested for endurance, or total life. Facilities constraints did not allow for these tests to be conducted for this thesis.
6. Micro-controller integration. The pulse width modulation of the driving circuit is controlled through a computer program which runs the driving circuit, in order to control the injector's performance. In a real automobile, the computer program would have to originate from a micro-controller system. Past designs have used, for example, the 80C196KC as part of the Intel EV80C196KC evaluation board [20].
7. Two coil solenoid integration. The solenoid used in this thesis was a pulling solenoid. Upon being energized, it would lift the core, opening the injector needle, and allowing fuel to be injected. When de-energized, the spring force would push the rod back down to close the injector. A two coil solenoid basically has two separate solenoids in one body with a single output connection. When one coil is energized, the solenoid pulls the injector needle, which stays open until the other coil is energized pulling the needle back down. With a specially designed driving circuit, this type of solenoid could, theoretically, both open and close the needle. The advantages of electronic actuation on a myriad of variables were document in the literature review chapter. Further gains could be achieved, improving injector performance with the integration of two-way electronic actuation. Furthermore, this type of solenoid could lead to a simplification of the overall injector design, making such components as the spring, retainer, spacer, etc. extraneous.

Each of these areas is a separate area for research, and their combination could greatly improve the performance of solenoid injectors with DME fuel.

REFERENCES

1. Belaire, R.C., Boggs, D.L. and Foulkes, D.M., "The Development of Small Direct-Injection Diesel Engines for Europe and US", AVL Conference Engine and Environment, 1997, pp. 156-166.

2. "Office of Advanced Automotive Technologies R&D plan", US Department of Energy, Office of Advanced Automotive Technologies, March 1998.

3. Mikulic, L., "Diesel 2000 - Future Trends and Technologies for Passenger Car Diesel Engines", AVL Conference Engine and Environment 97, pp. 48-66.

4. J.F. Wakenell, G.G. O'Neal, Q.A. Baker, C.M, Urban, "An Investigation of High Pressure/ Late Cycle Injection of CNG as a Fuel for Rail Applications", Report, Southwest Research Institute, 1988.

5. Karpuk, M.E. and Cowley, S.W., "On Board Dimethyl Ether Generation to Assist Methanol Engine Cold Starting", SAE Paper No. 881678, 1988.

6. Miele, D., Krepec, T. and Giannacopoulos, T., "Electronic Injection System for Natural Gas in a Diesel Engine - Development and Testing", SAE Paper No. 890852, 1989.

7. Green, C.J. and Wallace, J.S., "Electrically Actuated Injectors for Gaseous Fuels", SAE Paper No. 892143, 1989.

8. Beck, N.J., Johnson, W.P., George, A.F., Petersen, P.W., van der Lee, B. and Klopp, G., "Electronic Fuel Injection for Dual Fuel Diesel Methane", SAE Paper No. 891652, 1989.

9. Lom, E.J. and Ly, K.H., "High Pressure Injection of Natural Gas in a Two Stroke Diesel Engine", SAE Paper No. 902230, 1990.

10. Johnson, W.P., Beck, N.J., Lovkov, O., van der Lee, A., Koshkin, V.K. and Piatov, I.S., "All Electronic Dual Fuel Injection System for the Belarus D-144 Diesel Engine", SAE Paper No. 901502, 1990.

11. Green, C.J., Cockshutt, N.A. and King, L. "Dimethyl Ether as a Methanol Ignition Improver: Substitution Requirements and Exhaust Emissions Impact", SAE Paper No. 902155, 1990.

12. Lauvin, P., Loeffler, A., Schmitt, A., Zimmermann, W. and Fuchs, W., "Electronically Controlled High Pressure Unit Injector System for Diesel Engines", SAE Paper No. 911819, 1991.

13. Karpuk, M.E., Wright, J.D., Dippo, J.L. and Jantzen, D.E., "Dimethyl Ether as an Ignition Enhancer for Methanol-Fueled Diesel Engines", SAE Paper No. 912420, 1991.

14. Miyaki, M., Fujisawa, H., Masuda, A. and Yamamoto, Y., "Development of New Electronically Controlled Fuel Injection System ECD-U2 for Diesel Engines", SAE Paper No. 910252, 1991.

15. McCarthy, C.I., Slodowske, W.J., Sienicki, E.J. and Jass, R.E., "Diesel Fuel Property Effects on Exhaust Emissions from a Heavy Duty Diesel Engine that Meets 1994 Emissions Requirements", SAE Paper No. 922267, 1992.

16. Yang, M. and Sorenson, S.C., " Direct Digital Control of the Diesel Fuel Injection Process", SAE Paper No. 920626, 1992.

17. Hower, M.J., Mueller, R.A., Oehlerking, D.A. and Zielke, M.R., "The New Navistar T 444E Direct-Injection Turbocharged Diesel Engine", SAE Paper No. 930269, 1993.

18. Hong, H., Krepec, T. and Cheng, R.M.H., "Optimization of Electronically Controlled Injectors for Direct Injection of Natural Gas in Diesel Engines", SAE Paper No. 930928, 1993.

19. Cuenca, R.M., "Evolution of Diesel Fuel Injection Equipment - The Last 20 Years", SAE Paper No. 933015, 1993.

20. Kekedjian, H. and Krepec, T., "Further Development of Solenoid Operated Gas Injectors with Fast Opening and Closing", SAE Paper No. 940450, 1994.

21. Guo, J., Chikahisa, T., Murayama, T. and Miyano, M., " Improvement of Performance and Emissions of a Compression Ignition Methanol Engine with Dimethyl Ether", SAE Paper No. 941908, 1994.

22. Yamaki, Y., Mori, K., Kamikubo, H., Kohketsu, S., Mori, K. and Kato, T., "Application of Common Rail Fuel Injection System to a Heavy Duty Diesel Engine", SAE Paper No. 942294, 1994.

23. Dolenc, A. and Waras, H., " High Pressure Fuel System for High Speed DI Diesel Engines with Suitable Electronic Control", SAE Paper No. 942293, 1994.

24. Sturman, O.E., Pena, J.A. and Petersen, P.W., "A CNG Specific Fuel Injector Using Latching Solenoid Technology", SAE Paper No. 951914, 1995.

25. Barkhimer, R.L. and Wong, H., " Application of Digital, Pulse - Width - Modulated, Sonic Flow Injectors for Gaseous Fuels", SAE Paper No. 951912, 1995.

26. Yudanov, S.V., "Development of the Hydraulically Actuated Electronically Controlled Unit Injector for Diesel Engines", SAE Paper No. 952057, 1995.

27. Yao-qing, D., "The Investigation on the Development of New-fashioned Low-Inertia Injector for Small-Medium IDI Diesel Engines", SAE Paper No. 951803, 1995.

28. Fleisch, T., McCarthy, C., Basu, A., Udovich, C., Charbonneau, P., Slodowske, W., Mikkelsen, S. and McCandless, J., " A New Clean Diesel Technology: Demonstration of ULEV Emissions on a Navistar Diesel Engine Fueled with Dimethyl Ether", SAE Paper No. 950061, 1995.

29. Kapus, P. and Ofner, H., " Development of Fuel Injection Equipment and Combustion System for DI Diesels Operated on Dimethyl Ether", SAE Paper No. 950062, 1995.

30. S. C. Sorenson, " Performance and emissions of a 0.273 liter direct injection diesel engine fuelled with neat dimethyl ether", Technical University of Denmark; and Svend-Erik Mikkelsen, Haldor Topsoe. SAE Paper No. 950064, 1995.

31. Hansen, J.B., Voss, B., Joensen, F. and Sigurdardottir, I.D., "Large Scale Manufacture of Dimethyl Ether - a New Alternative Diesel Fuel from Natural Gas", SAE Paper No. 950063, 1995.

32. Stumpp, G. and Ricco, M., "Common Rail - An Attractive Fuel Injection System for Passenger Car DI Diesel Engines", SAE Paper No. 960870, 1996.

33. Hong, H., Krepec, T. and Kekedjian, H., "Shaping of Fuel Delivery Characteristics for Solenoid Operated Diesel Engine Gaseous Injectors", SAE Paper No. 960869, 1996.

34. McCandless, J.C. and Li, S., "Development of a Novel Fuel Injection System (NFIS) for Dimethyl Ether - and Other Clean Alternative Fuels", SAE Paper No. 970220, 1997.

35. Endo, S., Adachi, Y., Ihara, Y., Terasawa, M. and Suenaga, K., "Development of J-Series Engine and Adoption of Common-Rail Fuel Injection System", SAE Paper No. 970818, 1997.

36. Yoda, T. and Tsuda, T., "Influence of Injection Nozzle Improvement on DI Diesel Engine", SAE Paper No. 970356, 1997.

37. Arcoumanis, C., Gavaises, M., Yamanishi, M. and Oiwa, J., "Application of a FIE Computer Model to an In-Line Pump-Based Injection System for Diesel Engines", SAE Paper No. 970348, 1997.

38. Guerrassi, N. and Dupraz, P., "A Common Rail Injection System For High Speed Direct Injection Diesel Engines", SAE Paper No. 980803, 1998.

39. Kato, T., Koyama, T., Sasaki, K., Mori, K. and Mori K., "Common Rail Fuel Injection System for Improvement of Engine Performance on Heavy Duty Diesel Engine", SAE Paper No. 980806.

40. Poulton, M.L., " Alternative Fuels for Road Vehicles", Computational Mechanics Inc., 1994.

41. Bosch R. GMBH, "Bosch Worldwide: Your Partner in Diesel Technology" - A catalog of Bosch Diesel Systems,1998.

42. Lisk Company, Inc. Tubular Solenoids. Catalog 9A.

43. Irving M. Gottlieb, "Power Supplies", fourth edition, pp.418-424.

44. Msjmufst, H., "Electromechanical Energy Converters", Allyn and Bacon, Inc., Boston,1965, pp.64-65.

45. Hong, H. "Optimum Performance of Solenoid Injectors for Direct Injection of Gaseous Fuels in IC Engines", A Thesis in The Department of Mechanical Engineering, Concordia University, Montreal, Quebec, 1995.

46. Hong, H., Krepec, T. and Cheng, R.P.M., " Transient Response of Fast Acting Solenoids in Automotive Applications", Journal of Circuits, Systems, and Computers, World Scientific Publishing Co., Vol.4, No.4, 1994.

APPENDIX A

Injector Detailed Drawings

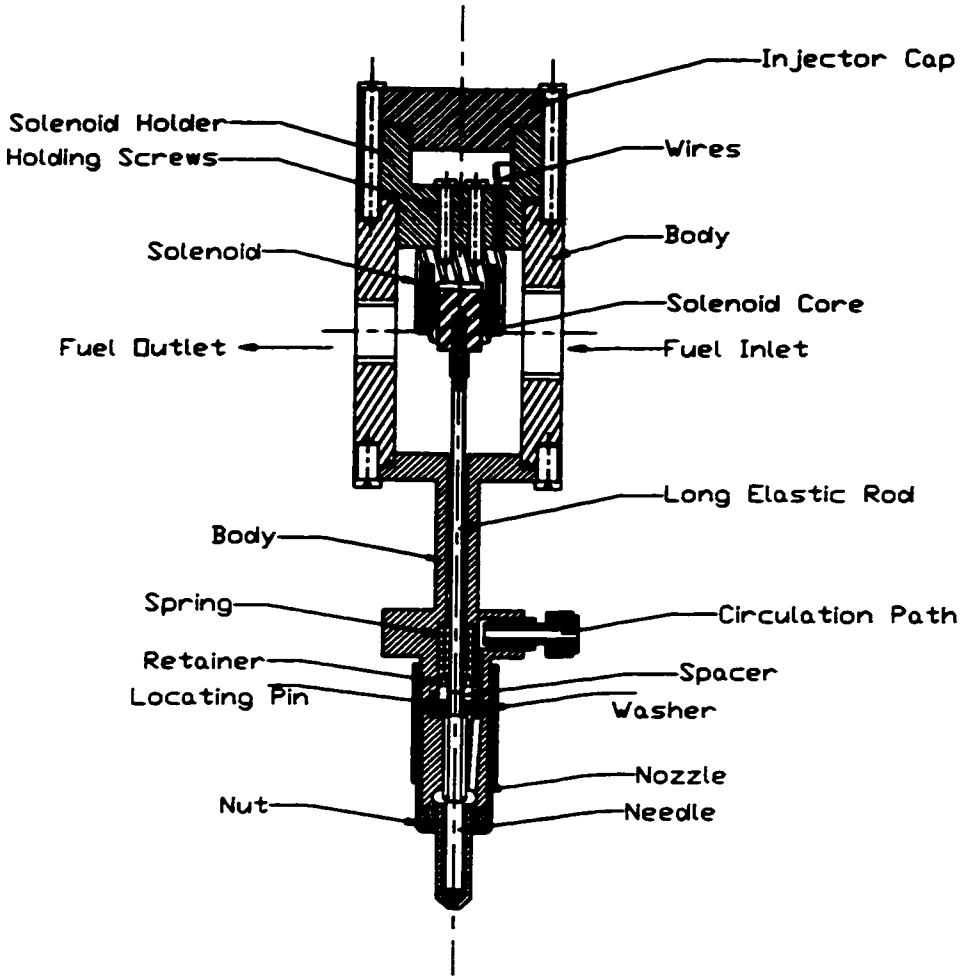

Quantity: 1	Material:	Filename: Thesis Drawings	
Designed by: BABAK TORAB	Approved by - date: DR. KREPEC & DR. HONG - JAN 1998	Date: APRIL/1999	Scale: 1:1
CONCORDIA UNIVERSITY DEPARTMENT OF MECHANICAL ENGINEERING	INJECTOR ASSEMBLY DRAWING_NUMBER	Edition	Sheet

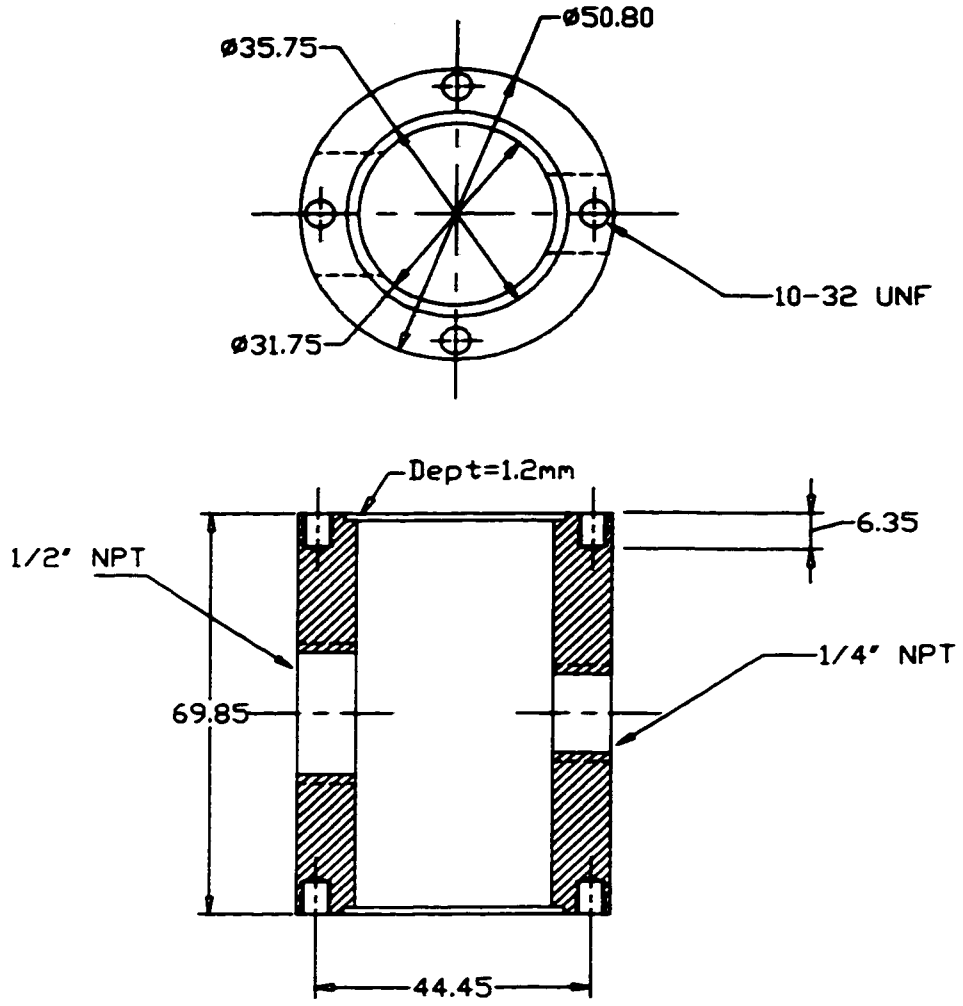

Quantity: 1	Material: Stainless Steel	Filename: Thesis Drawings	
Designed by: BABAK TORAB	Approved by - date: DR. KREPEC & DR. HONG - JAN 1998	Date: APRIL/1999	Scale: 1:1
CONCORDIA UNIVERSITY	BODY		
DEPARTMENT OF MECHANICAL ENGINEERING	DRAWING_NUMBER	Edition	Sheet

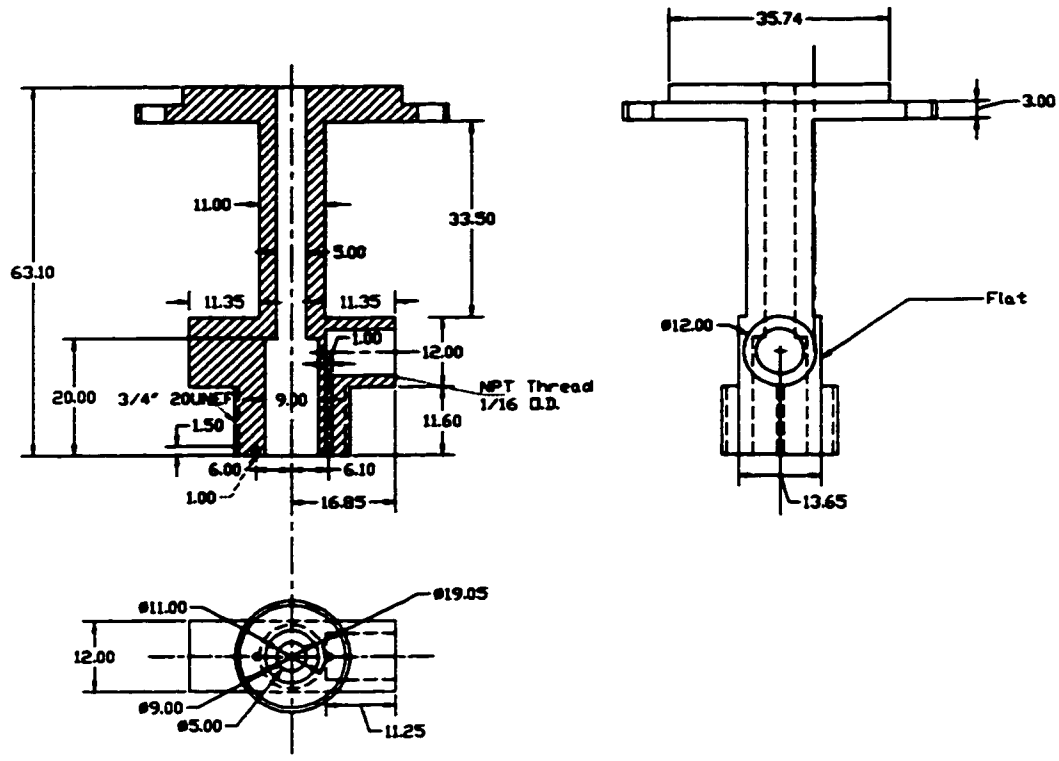

Quantity: 1	Material: Stainless Steel	Filename: Thesis Drawings	
Designed by: BABAK TORAB	Approved by - date: DR. KREPEC & DR. HONG - JAN 1998	Date: APRIL/1999	Scale: 1:1
CONCORDIA UNIVERSITY DEPARTMENT OF MECHANICAL ENGINEERING	BODY		
	DRAWING_NUMBER	Edition	Sheet

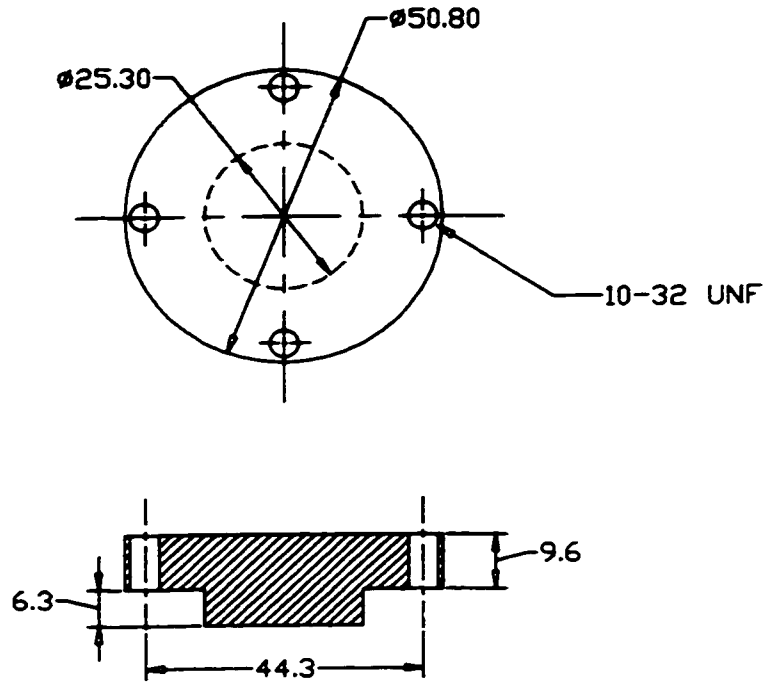

Quantity: 1	Material: Stainless Steel	Filename: Thesis Drawings	
Designed by: BABAK TORAB	Approved by - date: DR. KREPEC & DR. HONG - JAN 1998	Date: APRIL/1999	Scale: 1:1
CONCORDIA UNIVERSITY DEPARTMENT OF MECHANICAL ENGINEERING	CAP		
	DRAWING_NUMBER	Edition	Sheet

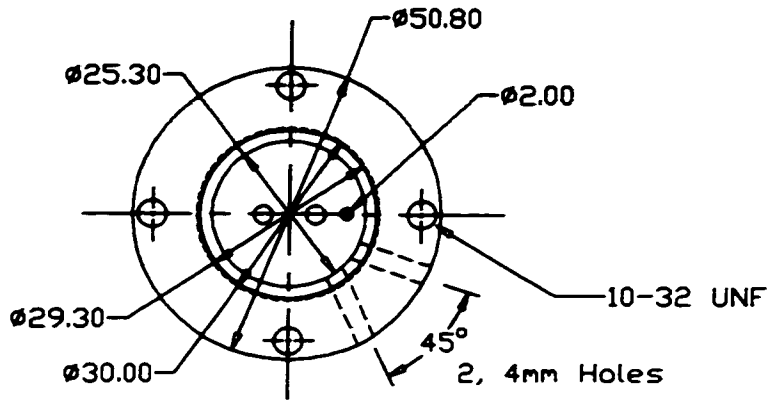

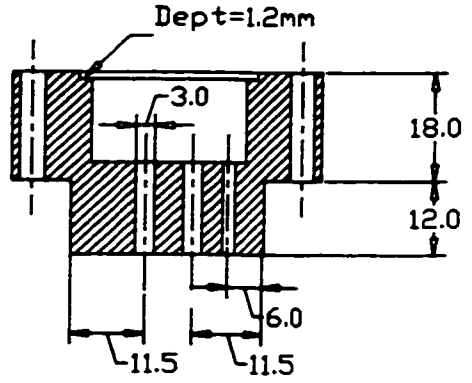

Quantity: 1	Material: Stainless Steel	Filename: Thesis Drawings	
Designed by: BABAK TORAB	Approved by - date: DR. KREPEC & DR. HONG - JAN 1998	Date: APRIL/1999	Scale: 1:1
CONCORDIA UNIVERSITY DEPARTMENT OF MECHANICAL ENGINEERING	SOLENOID HOLDER		
	DRAWING_NUMBER	Edition	Sheet

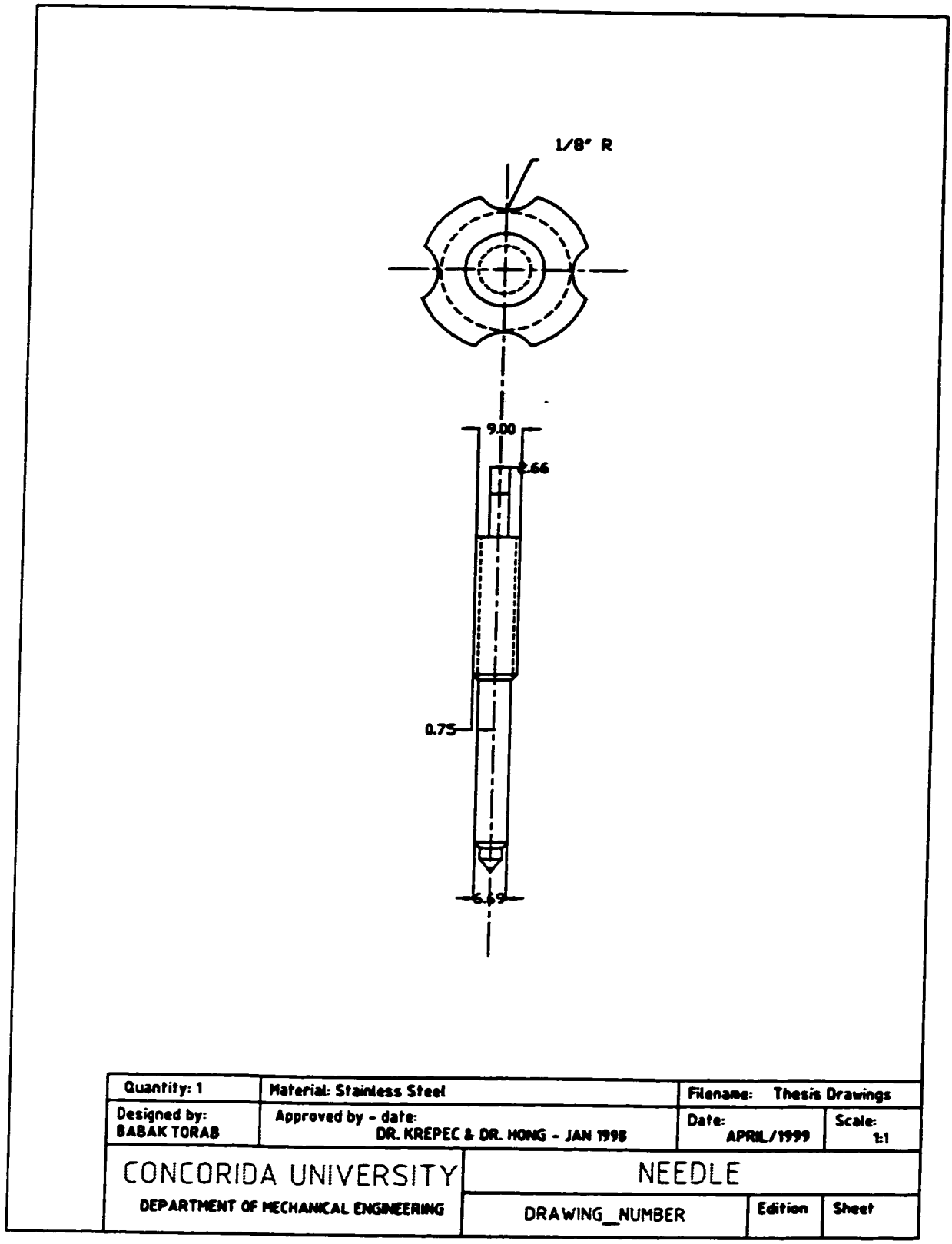

Quantity: 1	Material: Stainless Steel	Filename: Thesis Drawings	
Designed by: BABAK TORAB	Approved by - date: DR. KREPEC & DR. HONG - JAN 1998	Date: APRIL/1999	Scale: 1:1
CONCORIDA UNIVERSITY	NEEDLE		
DEPARTMENT OF MECHANICAL ENGINEERING	DRAWING_NUMBER	Edition	Sheet

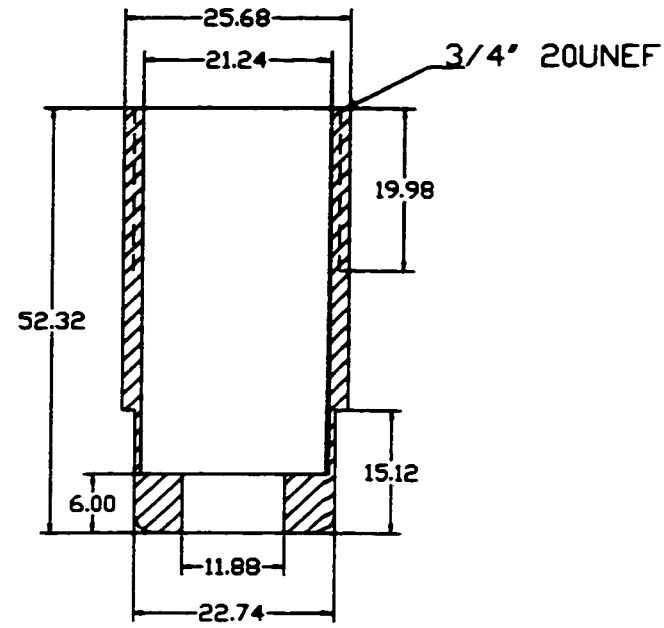

Quantity: 1	Material: Steel	Filename: Thesis Drawings	
Designed by: BABAK TORAB	Approved by – date: DR. KREPEC & DR. HONG – JAN 1998	Date: APRIL/1999	Scale: 1:1
CONCORDIA UNIVERSITY	NUT		
DEPARTMENT OF MECHANICAL ENGINEERING	DRAWING_NUMBER	Edition	Sheet

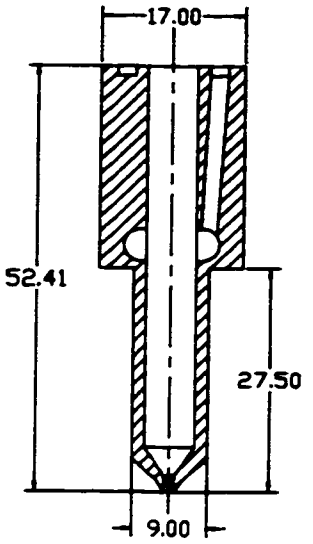

Quantity: 1	Material: Stainless Steel	Filename: Thesis Drawings	
Designed by: BABAK TORAB	Approved by - date: DR. KREPEC & DR. HONG - JAN 1998	Date: APRIL/1999	Scale: 1:1
CONCORDIA UNIVERSITY DEPARTMENT OF MECHANICAL ENGINEERING	NOZZLE		
	DRAWING_NUMBER	Edition	Sheet

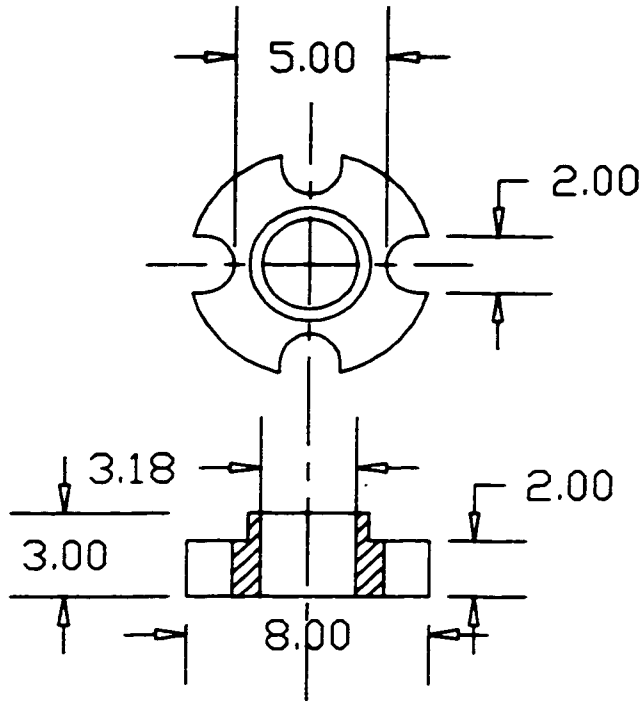

Quantity: 1	Material: Aluminum		Filename: Thesis Drawings	
Designed by: BABAK TORAB	Approved by - date: DR. KREPEC & DR. HONG - JAN 1998		Date: APRIL/1999	Scale: 1:1
CONCORDIA UNIVERSITY DEPARTMENT OF MECHANICAL ENGINEERING	RETAINER			
	DRAWING_NUMBER		Edition	Sheet

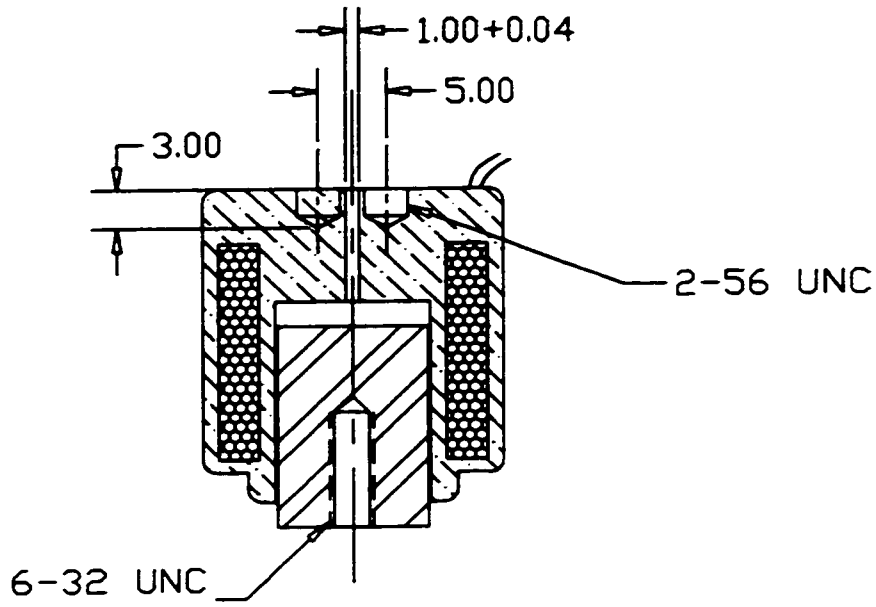

Quantity: 1	Material:	Filename: Thesis Drawings	
Designed by: BABAK TORAB	Approved by - date: DR. KREPEC & DR. HONG - JAN 1998	Date: APRIL/1999	Scale: 1:1
CONCORDIA UNIVERSITY	SOLENOID		
DEPARTMENT OF MECHANICAL ENGINEERING	DRAWING_NUMBER	Edition	Sheet

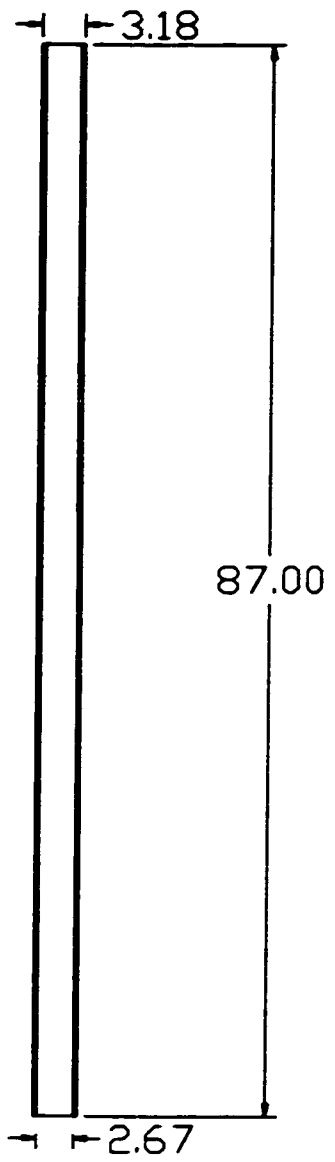

Quantity: 1	Material: Stainless Steel	Filename: Thesis Drawings	
Designed by: BABAK TORAB	Approved by - date: DR. KREPEC & DR. HONG - JAN 1998	Date: APRIL/1999	Scale: 1:1
CONCORDIA UNIVERSITY DEPARTMENT OF MECHANICAL ENGINEERING	ROD		
	DRAWING_NUMBER	Edition	Sheet

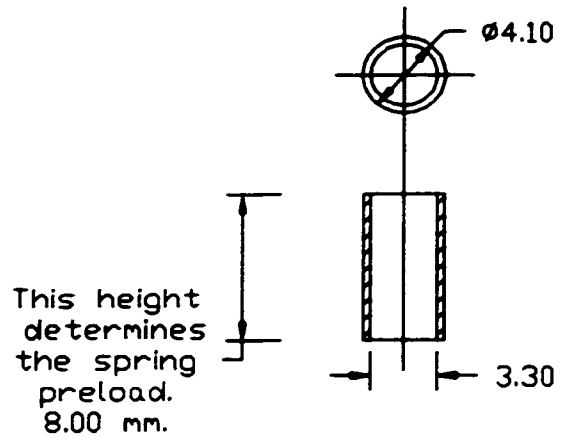

Quantity: 1	Material: Stainless Steel	Filename: Thesis Drawings	
Designed by: BABAK TORAB	Approved by - date: DR. KREPEC & DR. HONG - JAN 1998	Date: APRIL/1999	Scale: 1:1
CONCORDIA UNIVERSITY	SPACER		
DEPARTMENT OF MECHANICAL ENGINEERING	DRAWING_NUMBER	Edition	Sheet

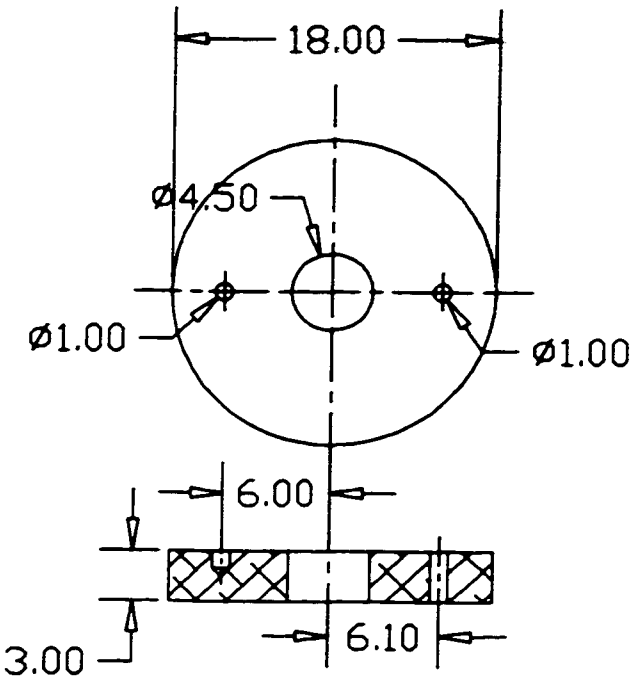

Quantity: 1	Material: Cupper	Filename: Thesis Drawings	
Designed by: BABAK TORAB	Approved by - date: DR. KREPEC & DR. HONG - JAN 1998	Date: APRIL/1999	Scale: 1:1
CONCORDIA UNIVERSITY DEPARTMENT OF MECHANICAL ENGINEERING	WASHER		
	DRAWING_NUMBER	Edition	Sheet

APPENDIX B

Calculations

Appendix B.1; Stress analysis on square tube

From the material handbook, the available square tube was chosen to be Annealed Stainless Steel 316, with rb= 25.4 mm (One inches) and ra= 22.4 mm which gives a thickness of 3 mm. The maximum tensile strength given in the nominal mechanical properties of AISI Stainless Steel is 552 Mpa.

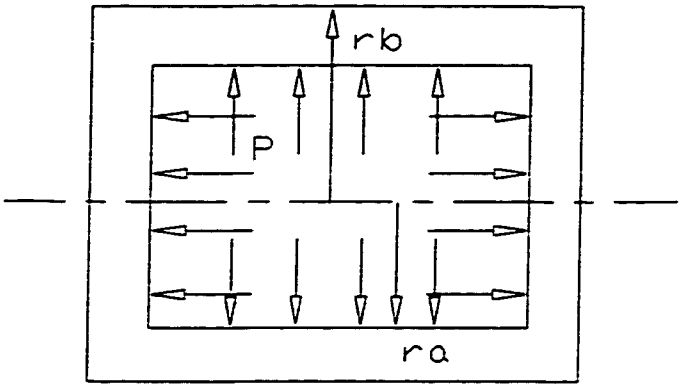

In order to calculate the maximum Longitudinal and Hoop stresses acting on the square tube, the following formulas is been used, knowing the pressure inside the tube is 200 bars.

$$\sigma_L = P\,(ra^2)/(rb^2-ra^2)$$

and $$\sigma_{hmax} = P\,(rb^2+ra^2)/(rb^2-ra^2)$$

By calculating σ_L and σ_{hmax}, and comparing the result with the maximum tensile strength given, safety factor of 3 is been achieved.

APPENDIX C

Coefficients

Approximate values for the spring and material damping coefficients of the seat, k_t and d_t, and stop, k_p and d_p, and rod, k_r and d_r and the core and needle mass in equations (6.2),(6.3) and (6.4) are presented in the following table for different rods.

Spring Stiffness, Material Damping, Core and Needle mass	Solid Stainless Steel Rod	Hollow Stainless Steel Rod	Hollow Aluminum Rod
K_t (kN/mm)	25.0	17.0	11.0
d_t (kg/s)	170.0	160.0	150.0
K_p (kN/mm)	20.0	20.0	20.0
d_p (kg/s)	170.0	170.0	170.0
K_r (kN/mm)	17.5	5.3	1.8
d_r (kg/s)	100.0	100.0	100.0
M_n (kg)	0.012	0.0105	0.009
m_c (kg)	0.016	0.0145	0.013

The mass values were measured, while the spring constant and the material damping values were estimated by observing and matching the oscilloscope traces of the needle displacements with the simulation results.

APPENDIX D

Description and Calibration of Piezo-Cell Force Transducer & the LVDT

A piezo-electric load cell was used to measure the acting force on the nozzle seat. This load cell is produced by KISTLER , type 9001, and its specifications are:

Range	: from 0 to 7.5 KN
Sensitivity	: 4.3 PC/N or 19 PC/lb
Threshold	: 0.01 N
Operating Pressure Range	: -196 to 200°C

A Dual Mode Amplifier, produced by KISTKER, Model 5004 was used as a converter. In the calibration of the force transducer, dead weights were applied to the load cell under compression and the electrical output from the cell was recorded. Figure D.1. plots the calibration cure for the transducer.

The static gain of the force transducer was found to be:

$$K_f = 14.8 \text{ N/V}$$

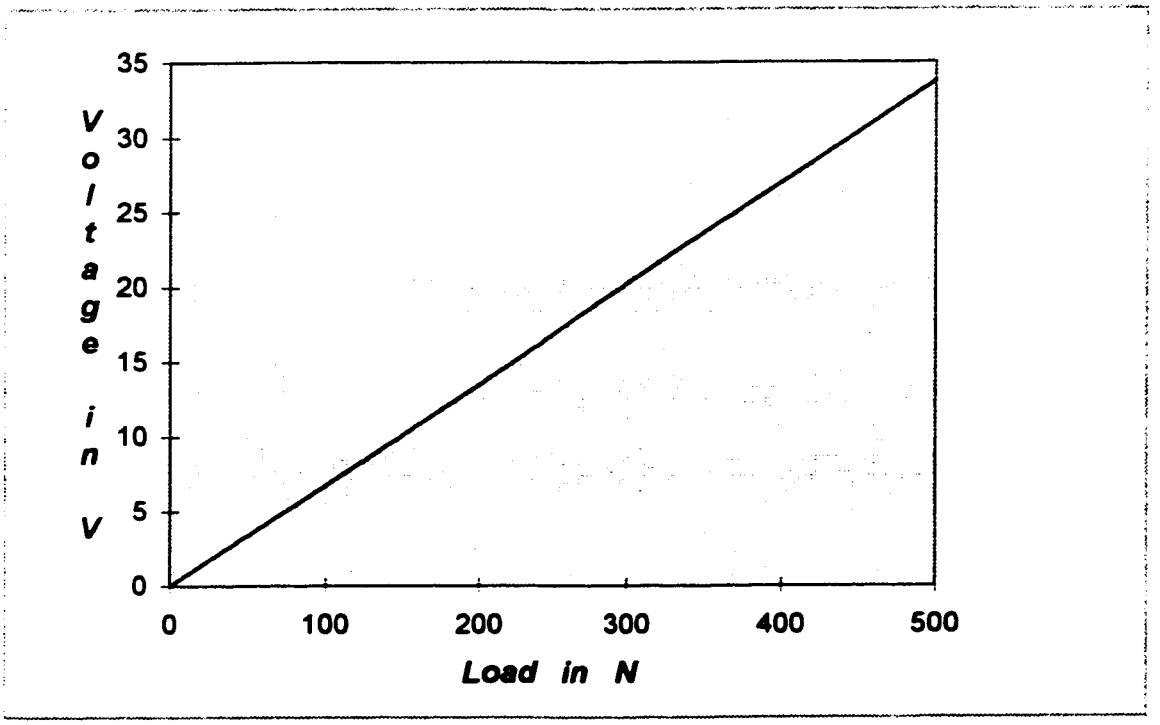

Figure D.1. Force Transducer Calibration Curve

The linear variable differential transformer (LVDT), was used to measure the displacement of the solenoid core. An AVL Type 3075-A02 Carrier Amplifier was used to convert the core movement to an electrical output. It was calibrated by measuring the maximum displacement of the injector needle movement after assembly of the injector. The calibration curve for LVDT is shown in Figure D.2.

The static gain of the LVDT was found to be:

$$K_m = 0.32 \text{ mm/V}$$

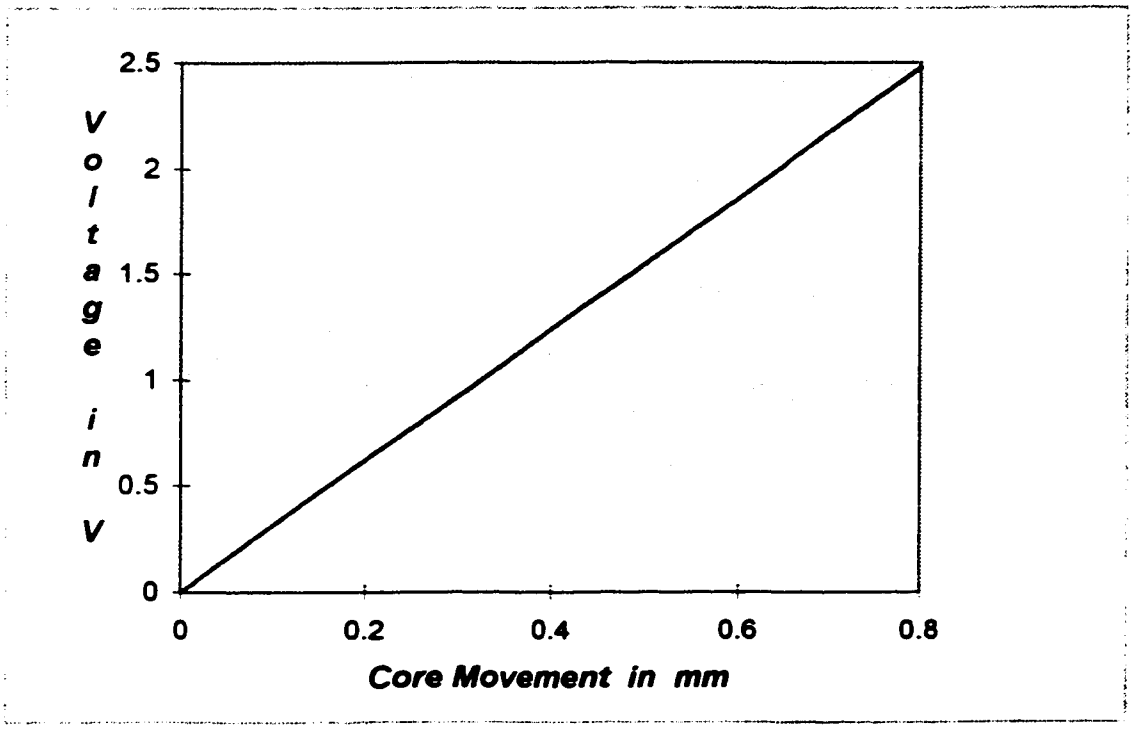

Figure D.2. LVDT Calibration Curve